JAAVSO

Volume 37
Number 2
2009

The Journal of the American Association of Variable Star Observers

The Superoutburst Period of KV Dra

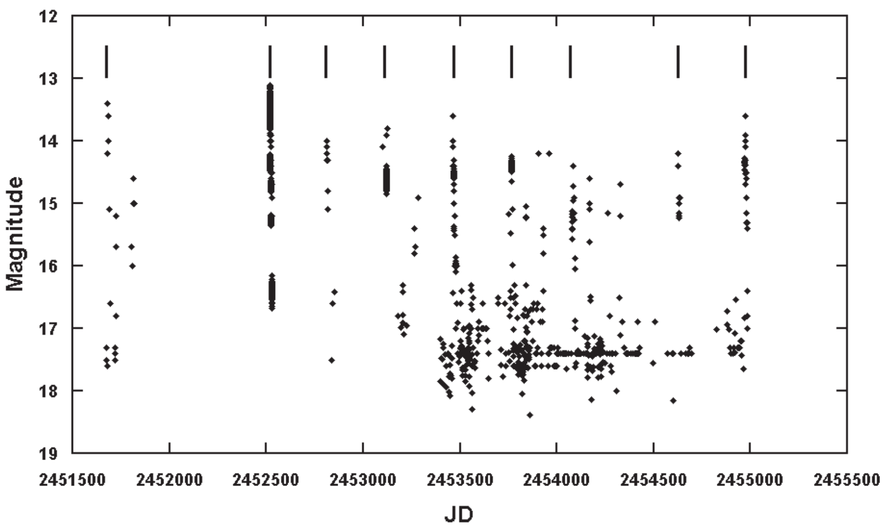

Observations of KV Dra. Superoutbursts are indicated by a bar.

Also in this issue...

- Evidence for Cyclic Activity in an Orion Irregular
- CX Lyrae 2008 Observing Campaign
- Quantifying Irregularity in Pulsating Red Giants

Complete table of contents inside...

49 Bay State Road
Cambridge, MA 02138
U. S. A.

The Journal of the American Association of Variable Star Observers

Editor
John R. Percy
University of Toronto
Toronto, Ontario, Canada

Associate Editor
Elizabeth O. Waagen

Assistant Editor
Matthew Templeton

Production Editor
Michael Saladyga

Editorial Board
Priscilla J. Benson
Wellesley College
Wellesley, Massachusetts

Douglas S. Hall
Vanderbilt University
Nashville, Tennessee

David B. Williams
Indianapolis, Indiana

Thomas R. Williams
Houston, Texas

The Council of the American Association of Variable Star Observers 2008–2009

Director	Arne A. Henden
President	Paula Szkody
Past President	David B. Williams
1st Vice President	Jaime Ruben Garcia
2nd Vice President	Michael A. Simonsen
Secretary	Gary Walker
Treasurer	Gary W. Billings
Clerk	Arne A. Henden

Councilors

Barry B. Beaman
James Bedient
Pamela Gay
Edward F. Guinan
Katherine Hutton
Michael Koppelman
Arlo U. Landolt
Christopher Watson

ISSN 0271-9053

JAAVSO

The Journal of The American Association of Variable Star Observers

Volume 37
Number 2
2009

49 Bay State Road
Cambridge, MA 02138
U. S. A.

ISSN 0271-9053

The *Journal of the American Association of Variable Star Observers* is a refereed scientific journal published by the American Association of Variable Star Observers, 49 Bay State Road, Cambridge, Massachusetts 02138, USA. The *Journal* is made available to all AAVSO members and subscribers.

In order to speed the dissemination of scientific results, selected papers that have been refereed and accepted for publication in the *Journal* will be posted on the internet at the *eJAAVSO* website as soon as they have been typeset and edited. These electronic representations of the *JAAVSO* articles are automatically indexed and included in the NASA Astrophysics Data System (ADS). *eJAAVSO* papers may be referenced as *J. Amer. Assoc. Var. Star Obs., in press,* until they appear in the concatonated electronic issue of *JAAVSO*. The *Journal* cannot supply reprints of papers.

Page Charges

Unsolicited papers by non-Members will be assessed a charge of $15 per page.

Instructions for Submissions

The *Journal* welcomes papers from all persons concerned with the study of variable stars and topics specifically related to variability. All manuscripts should be written in a style designed to provide clear expositions of the topic. Contributors are strongly encouraged to submit digitized text in LATEX+POSTSCRIPT, MS WORD, or plain-text format. Manuscripts may be mailed electronically to journal@aavso.org or submitted by postal mail to *JAAVSO*, 49 Bay State Road, Cambridge, MA 02138, USA.

Manuscripts must be submitted according to the following guidelines, or they will be returned to the author for correction:

Manuscripts must be:
1) original, unpublished material;
2) written in English;
3) accompanied by an abstract of no more than 100 words.
4) not more than 2,500–3,000 words in length (10–12 pages double-spaced).

Figures for publication must:
1) be camera-ready or in a high-contrast, high-resolution, standard digitized image format;
2) have all coordinates labeled with division marks on all four sides;
3) be accompanied by a caption that clearly explains all symbols and significance, so that the reader can understand the figure without reference to the text.

Maximum published figure space is 4.5" by 7". When submitting original figures, be sure to allow for reduction in size by making all symbols and letters sufficiently large.

Photographs and halftone images will be considered for publication if they directly illustrate the text.

Tables should be:
1) provided separate from the main body of the text;
2) numbered sequentially and referred to by Arabic number in the text, e.g., Table 1.

References:
1) References should relate directly to the text.
2) References should be keyed into the text with the author's last name and the year of publication, e.g., (Smith 1974; Jones 1974) or Smith (1974) and Jones (1974).
3) In the case of three or more joint authors, the text reference should be written as follows: (Smith *et al.* 1976).
4) All references must be listed at the end of the text in alphabetical order by the author's last name and the year of publication, according to the following format:
   Brown, J., and Green, E. B. 1974, *Astrophys. J.*, **200**, 765.
   Thomas, K. 1982, *Phys. Report*, **33**, 96.
5) Abbreviations used in references should be based on recent issues of the Journal or the listing provided at the beginning of *Astronomy and Astrophysics Abstracts* (Springer-Verlag).

Miscellaneous:
1) Equations should be written on a separate line and given a sequential Arabic number in parentheses near the right-hand margin. Equations should be referred to in the text as, e.g., equation (1).
2) Magnitude will be assumed to be visual unless otherwise specified.
3) Manuscripts may be submitted to referees for review without obligation of publication.

© 2009 The American Association of Variable Star Observers. All rights reserved.

Journal of the American Association of Variable Star Observers
Volume 37, Number 2, 2009

Table of Contents continued on following pages

Table of Contents continued on following pages

Table of Contents continued on following pages

Quantifying Irregularity in Pulsating Red Giants

John R. Percy
Samantha Esteves
Alfred Lin
Christopher Menezes
Sophia Wu
Department of Astronomy and Astrophysics, University of Toronto, Toronto, ON Canada M5S 3H4

Based on a paper presented at the 98th Spring Meeting of the AAVSO, Big Bear Lake, CA, May 19–21, 2009

Received July 20, 2009; revised August 9, 2009; accepted August 17, 2009

Abstract Hundreds of red giant variable stars are classified as "type L," which the *General Catalogue of Variable Stars* (GCVS) defines as "slow irregular variables of late spectral type...which show no evidence of periodicity, or any periodicity present is very poorly defined...." Self-correlation (Percy and Muhammed 2004) is a simple form of time-series analysis which determines the cycle-to-cycle behavior of a star, averaged over all the available data. It is well suited for analyzing stars which are not strictly periodic. Even for non-periodic stars, it provides a "profile" of the variability, including the average "characteristic time" of variability. We have applied this method to twenty-three L-type variables which have been measured extensively by AAVSO visual observers. We find a continuous spectrum of behavior, from irregular to semiregular.

1. Introduction

Cool red giants are all variable in brightness; there are a dozen excellent essays on Mira and Red Semiregular variables in the "Variable Star of the Season" archive on the AAVSO website. The basic cause of the variability is pulsation. On average, the period and the amplitude increase with decreasing temperature (and increasing size, since the stars are evolving up the giant branch or asymptotic giant branch in the H-R diagram). The coolest (late M spectral type) red giants have visual amplitudes greater than 2.5 and are classified as Mira variables. Less-cool red giants, with visual amplitudes less than 2.5, are placed in one of two classes in the *General Catalogue of Variable Stars*, or GCVS (Kholopov *et al.* 1985): semiregular (SR), or irregular (L).

These types are defined thus:

- SR: "... giants or supergiants of intermediate and late spectral types showing noticeable periodicity in their light changes, accompanied or sometimes interrupted by various irregularities...."

- L: "Slow irregular variables. The light variations of these stars show no evidence of periodicity, or any periodicity present is very poorly defined, and appears only occasionally...."

Clearly these definitions are qualitative at best; is there a boundary between these two classes? Classification is generally made from light curves, often with limited data.

Kiss *et al.* (1999) have carried out a comprehensive time-series analysis of AAVSO visual observations of a large sample of SR variables; most have one period, some have two periods, and a few have three periods. Their sample included five L-type variables: AA Cas, DM Cep, TZ Cyg, V930 Cyg, and CT Del. They found a period of 367 days for DM Cep (possibly an artifact), 247 days for V930 Cyg, and 138 and 79 days for TZ Cyg, and apparently no periods for the other two stars.

We have found that, for stars with appreciable irregularity, self-correlation (Percy and Mohammed 2004 and references therein) is a useful method of time-series analysis. The purpose of the present paper is to apply this method to the study of L-type pulsating red giants.

2. Sources of data

Visual measurements of the twenty-three L stars listed in Table 1 came from the AAVSO International Database, spanning up to a century. There are dozens of L-type red giant variables in the database but, for most of them, the data are sparse. We have chosen stars which had at least 100 observations available. The precision of visual measurements is known to be about 0.2 to 0.3 magnitude. The intercept on the vertical axis of the self-correlation diagram is a measure of the average precision of the measurements, and is consistent with the estimate above (Figures 1–5: intercepts 0.21 to 0.28 magnitude).

3. Analysis of the stars by self-correlation

Self-correlation is a simple method of time-series analysis that determines the characteristic time scale and amplitude of the variability, averaged over the dataset. For a discussion of its nature, strengths, and weaknesses, see Percy and Mohammed (2004) and references therein. Our self-correlation software is available at: http://www.astro.utoronto.ca/~percy/index.html, and a manual for its use is available at: http://www.astro.utoronto.ca/~percy/manual.pdf.

If a star has any periodic behavior, it will show up as a series of minima in the self-correlation diagram, at multiples of the period. The number of minima is a measure of the coherence of the period. If there are no minima, then the star is considered irregular. If there are a large number of minima, the period is regular or coherent. So the number of minima is a quantitative measure of the irregularity or semiregularity of the star.

In constructing self-correlation diagrams, one needs to choose Δt (max), the maximum value of Δt (the minimum is always zero), and the number of bins. The stars in our sample are believed to vary on time scales of tens to thousands of days, so that range was used in selecting values for Δt (max). The number of bins should be chosen so that there are ten or more points in each bin, because of the statistical nature of the method.

4. Results

The results are summarized in Table 1. The columns give: the star name, the spectral type (generally from SIMBAD), the approximate total range (from the light curve), the period(s) if any, the number of minima (which is a measure of the coherence of the period), the amplitude, the number of data points, and the total timespan of the data. The stars show a wide spectrum of behavior.

V Aps, PY Cas, TT Leo, GN Her, TY Oph, and WW Cas show no repeating minima in their self-correlation diagrams; they simply rise to a plateau. We consider these stars to be irregular. TY Oph shows one minimum at 200 days, so it may be marginally periodic. Its amplitude is less than 0.05 magnitude.

Most of the other stars show at least two minima, at integral multiples of the period. The number of minima is a measure of the coherence of the period. Stars such as U Ant and X Lyr, with only two minima, can barely be considered as regular. Stars such as AT Dra, with a dozen or more minima, are much more coherent.

U Ant, AT Dra, X Lyr, EX Ori, and τ^4 Ser show a second period, an order of magnitude longer than the first, which would be considered to be a "long secondary period" (LSP). About a third of pulsating red giants show such an LSP; the nature and cause of these LSPs is not known (Wood *et al.* 2004).

For UX Cam and CP Tau especially, it is not clear whether the single period is an LSP (without a primary period) or whether the single period is simply a long primary period.

Self-correlation diagrams are shown for three representative stars: τ^4 Ser (Figure 1) shows a sequence of minima at multiples of 100 days, and also of 1,200 days, the "long secondary period"; OP Her (Figure 2) shows a series of minima, indicating a reasonably coherent period of 75 days; TY Oph (Figure 3) shows no repeating minima, though there is slight evidence for a time scale of about 200 days—maxima at 100 and 300 days, and a minimum at 200 days.

5. Discussion and conclusions

In the course of this research, we have encountered some of the inherent limitations of the self-correlation method.

We occasionally encounter stars, such as UW Dra (Figure 4), which show a very low-amplitude signal at a period of 365.25 days. Apparently, this is a spurious effect that arises because of the way that visual observations are made. JRP first heard of this effect from the late Dr. Janet A. Mattei. It is called the Ceraski effect, and is briefly described by Buchheim (2007) and by Gunther and Schweitzer (undated). The magnitude difference between two stars is perceived differently, depending on whether their orientation is parallel to or perpendicular to the line between the observer's eyes. This may occur because the orientation of the finding chart changes, depending on whether the observations are made in the evening sky or morning sky. The effect (only 0.01 to 0.02 magnitude) is much smaller than the error of the observations, but can be detected by time-series analysis because it is strictly periodic. Its occurrence may depend on the position of the star in the sky, and the orientation of the chart used. It may occur in many stars, but its small size may be swamped by the actual variability of the star, or by the random errors of observation, or by the different circumstances of different observers.

It is obviously not possible to study the behavior of the star on time scales longer than the time span of the data. In fact: as Δt approaches the total time span of the data, there are fewer and fewer pairs of observations with this value of Δt, and the method breaks down because of the statistical need to have several Δ magnitudes in each bin (CP Tau: Figure 5).

If there are large gaps in the data, there may be ranges of Δt with no pairs of observations. For WW Cas, there were no values of Δ magnitude for Δt between 4,000 and 5,500 days.

It is possible that some stars in our sample are multiperiodic, having two or more radial or non-radial periods. Self-correlation is not very effective if stars have two or more periods which are relatively close—i.e., of the same order of magnitude. We plan to use Fourier analysis to study a few of these stars.

Even for stars which show no minima, it is possible to define a characteristic time scale, on the basis of how fast the self-correlation diagram rises to its plateau, i.e., by comparing the rise to plateau with the rise to first maximum in a star that is periodic. To a first approximation, the time scale would be twice the value of Δt at which the diagram reached the plateau.

We have found a continuous spectrum of behavior in the twenty-one stars that we have studied, from irregular, to marginally coherent, to quite coherent. This indicates that the classification scheme for pulsating red giants is arbitrary; there is no distinct boundary between L and SR types. We found a similar situation for low-mass pulsating yellow supergiants: there is a smooth spectrum from periodic W Virginis stars, through RV Tauri stars, to semiregular (SRd) variables (e.g., Percy and Mohammed 2004). In that case, the temperature of the star might be the astrophysical parameter that varies along the spectrum.

In the case of the pulsating red giants, the situation might be more complicated. Our sample stars vary in temperature, but also in composition type—oxygen-rich or carbon-rich—so there may be at least two controlling parameters. A more detailed study of a larger sample of stars, using both Fourier and self-correlation analysis, would be astrophysically interesting.

6. The University of Toronto Mentorship Program

Authors SE, AL, CM, and SW were participants in the University of Toronto Mentorship Program (UTMP), which enables outstanding senior high school students to undertake research at the university. This program has been described by Percy *et al.* (2008). The present paper was presented as a poster at the 2009 Spring Meeting of the AAVSO and the 2009 conference of the Canadian Astronomical Society, as well as at the 2009 UTMP Research Fair.

7. Acknowledgements

We thank the organizers of the University of Toronto Mentorship Program (especially Farheen Hasan); the Natural Sciences and Engineering Research Council of Canada, and the AAVSO observers and headquarters staff, without whose efforts this project would not be possible. Authors SE, AL, CM, and SW thank their schools: Vaughan Secondary School, Lawrence Park Collegiate, Neil McNeil Secondary School, and the Bishop Strachan School, respectively. This research has made use of the SIMBAD database, operated at CDS, Strasbourg, France.

References

Buchheim, R. K. 2007, *The Sky Is Your Laboratory*, Springer Praxis, Berlin, 89.

Gunther, J., and Schweitzer (undated), http://cdsweb.u-strasbg.fr/afoev/var/edeb.htx

Kholopov, P. N., *et al.* 1985, *General Catalogue of Variable Stars*, 4th ed., Moscow.

Kiss, L. L., Szatmary, K., Cadmus, R. R., Jr., and Mattei, J. A. 1999, *Astron. Astrophys.*, **346**, 542.

Percy, J. R. and Mohammed, F. 2004, *J. Amer. Assoc. Var. Star Obs.*, **32**, 9.

Percy, J. R., Favaro, E., Glasheen, J., Ho, B., and Sato, H. 2008, *J. Amer. Assoc. Var. Star Obs.*, **36**, 145.

Wood, P. R., Olivier, A. E., and Kawaler, S. D. 2004, in *Variable Stars in the Local Group*, eds. D. W. Kurtz and K. R. Pollard, Astron. Soc. Pacific Conf. Proc. Vol. 310, San Francisco, 322.

Table 1. Self-correlation Analysis of L-type Variables.

Star	*Spectrum*	*Range*	*Period*	*Minima*	Δm	*N*	Δt
U Ant	C5,3(NB)	4.5–7.0	350, 2000	2	0.25	555	23307
V Aps	MB	9.0–11.0	irregular	—	—	142	27414
VW Aql	M5III:D	9.5–12.0	800	6	0.15	2986	25399
UX Cam	M6	7.6–9.5	1000	6+	0.05	1012	13789
AA Cas	M6III: D	7.5–9.5	75	6	0.02	4682	14677
PY Cas	M5III: D	9.5–12.0	irregular	—	—	517	14584
WW Cas	C5,5(N1)	9.5–11.5	irregular	—	—	299	12297
ST Cep	M3Iab:C	7.5–9.0	300-400	4	0.03	1306	26999
AT Dra	M4IIID	5.0–6.6	333, 4000	12, 2	0.03, 0.02	3379	14349
UW Dra	K5pvC	7.0–8.5	360 (?)	3	0.02	3653	33216
GN Her	M4IIID	8.0–11.0	irregular	—	—	237	15172
OP Her	M5II-IIIC	5.5–7.5	75, 650	8, 2	0.04, 0.04	4127	19742
TT Leo	M7D	10.0–12.0	irregular	—	—	419	14663
HK Lyr	C6,4(N4)	7.0–9.5	250	5	0.20	1260	19684
T Lyr	C6,5(R6)	7.2–10.0	400	4	0.04	2667	25348
TU Lyr	M6	9.2–11.5	150	7	0.06	6798	26079
X Lyr	M3.5III:D	7.5–10.5	200, 6500	2	0.03	1573	35004
TY Oph	C5,5(N)	9.0–11.0	irregular	—	—	575	19293
EX Ori	M7III	9.0–11.5	100, 500	4, 10	0.05, 0.60	247	20802
ST Psc	M5D	9.0–11.0	700	3	0.20	843	15013
τ^4 Ser	M5II-III	5.9–7.5	100, 1200	5, 3	0.02, 0.04	5970	19813
CP Tau	C5,4(N)	9.0–11.0	1250	9	0.10	1749	14993
X Tra	C5,5(NB)	5.2–7.2	500	3	0.06	2107	23308

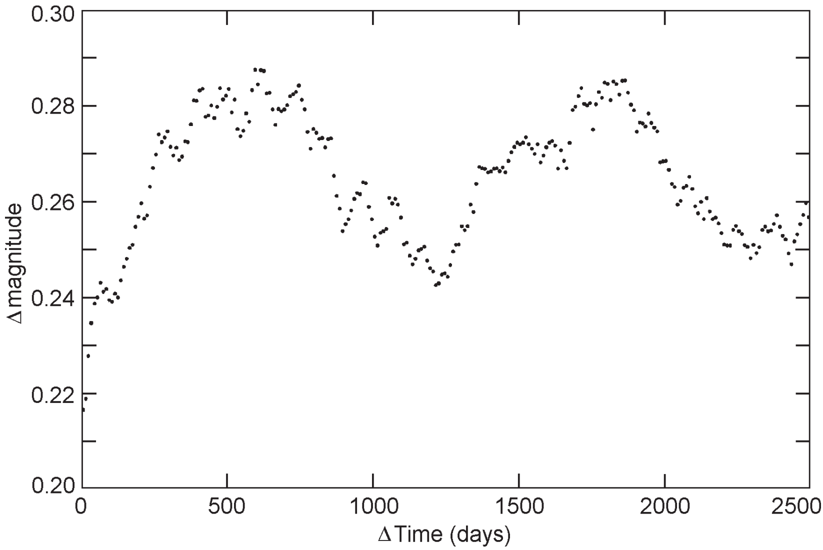

Figure 1. Self-correlation diagram for τ^4 Ser. There are minima at multiples of 100 days, and also of 1,200 days. The former is the primary pulsation period. The latter is an example of a "long secondary period"; its nature and cause are unknown.

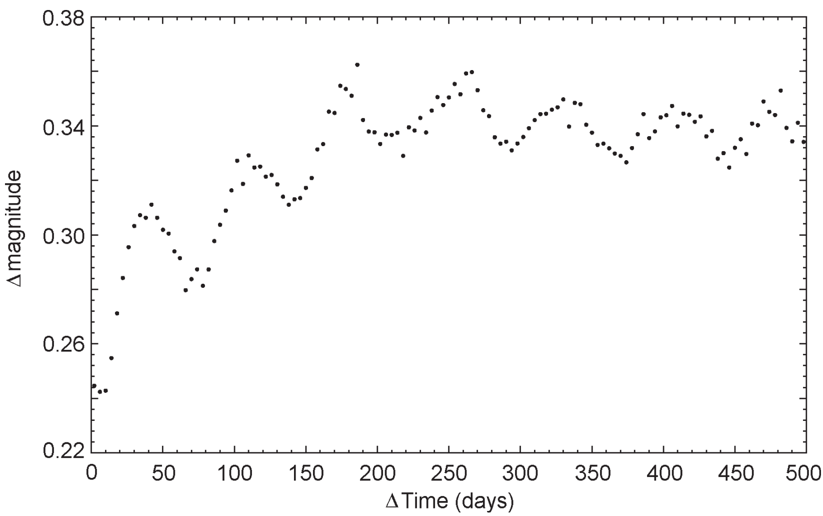

Figure 2. Self-correlation diagram for OP Her. Note the minima at multiples of 75 days. This is a good example of an L star with appreciable periodicity.

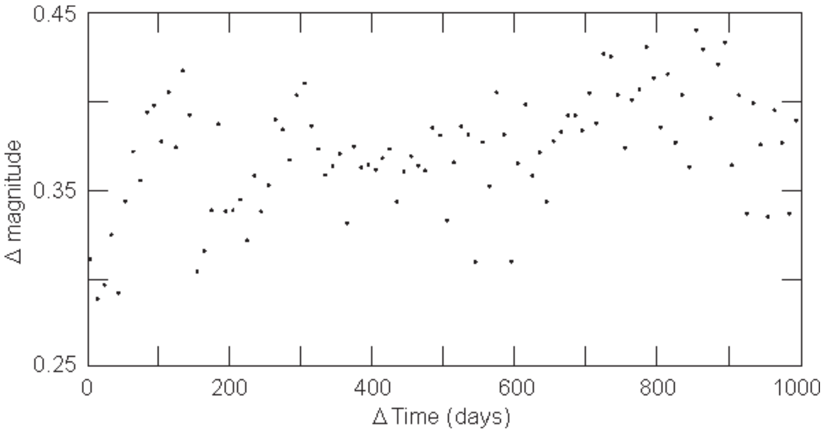

Figure 3. Self-correlation diagram for TY Oph. There are no repeating minima, though the complex structure between Δt = 0 and 400 days could be caused by one or more low-amplitude periods.

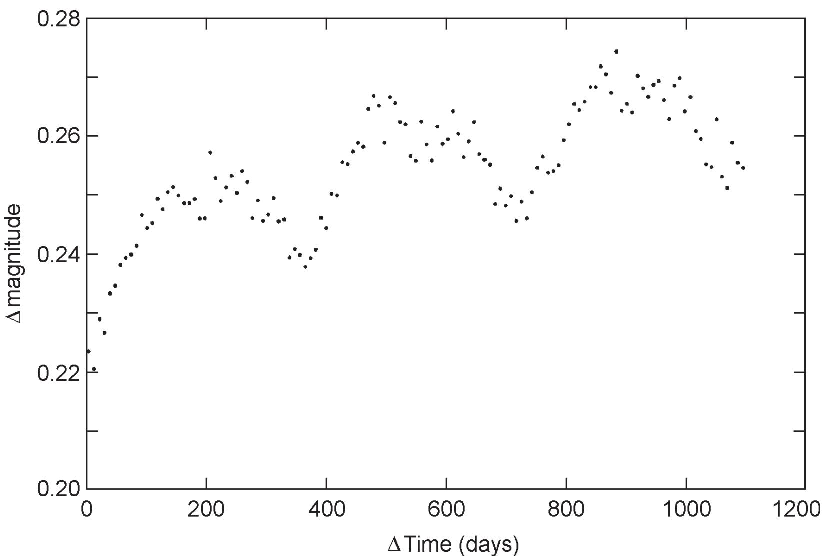

Figure 4. Self-correlation diagram for UW Dra. There are minima at multiples of 365 days, with an amplitude of 0.02 magnitude. These are almost certainly an artifact caused by the visual observing method; see text.

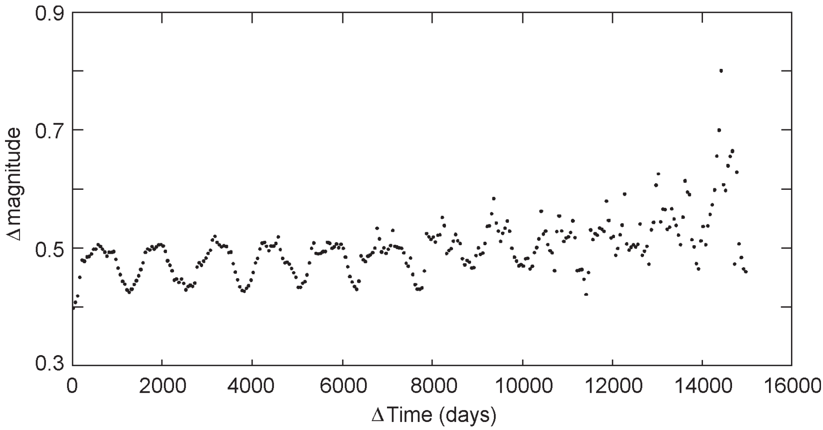

Figure 5. Self-correlation diagram for CP Tau. Note the minima at multiples of 1,250 days—the period. As Δt approaches 15,000 days, the scatter increases, because there are fewer and fewer pairs of measurements, with such large Δt, in each bin.

The Superoutburst Period of KV Draconis

Jeremy Shears
"Pemberton," School Lane, Bunbury, Tarporley, Cheshire CW6 9NR, England

Received April 27, 2009; revised June 5, 2009; accepted June 5, 2009

Abstract Analysis of observations of KV Dra between May 2000 and June 2009 has revealed nine superoutbursts. Assuming a linear ephemeris, the superoutburst period is 301 days, with a standard deviation of 28 days.

1. Introduction

KV Dra (= RXJ1450.5+6403 and HS 1449+6415) is an SU UMa-type dwarf nova having an orbital period, P_{orb} = 0.05898 day. The first known superoutburst of this system was observed in May 2000 and was intensively studied (Vanmunster *et al.* 2000; Nogami *et al.* 2000). The current paper reports the analysis of observations of KV Dra, mainly from the AAVSO International Database, with the aim of determining the interval between superoutbursts, often referred to as the superoutburst period or supercycle.

2. Observations of KV Dra

The AAVSO International Database contains more than 3,200 observations of KV Dra between May 2000 and June 2009. These observations, supplemented with data from Nogami *et al.* (2000), the BAA Variable Star Section's Recurrent Objects Programme (Poyner 1996), and VSNET, are shown in Figure 1, where negative ("fainter than") observations have been omitted for clarity. It is apparent from this plot that the number of observations of KV Dra has increased with time as more observers began to monitor the star. Moreover, the detection limit has improved as more CCD observations are contributed. If we assume that any observation where the magnitude was 17 or fainter is during quiescence, then the average magnitude of KV Dra at minimum is 17.5. At it is brightest it reaches 13.1, which suggests an outburst amplitude of 4.4 magnitudes.

3. Analysis of superoutbursts

In order to identify possible outbursts in the data, we noted when the star was brighter than 16.0. Table 1 shows that twenty-two such possible outbursts have been recorded. It is clear from the outburst durations listed that there are two categories of outburst exhibited by KV Dra. Thirteen of the outbursts were short, lasting less than five days. The remaining nine were longer, lasting more than seven days. Literature references and time-resolved photometry from the AAVSO International Database confirm that six of these longer outbursts showed superhumps, modulations in the light curve that are diagnostic of superoutbursts (unfortunately, time-resolved photometry for the remaining three long outbursts is not available). Thus we interpret the category of short outbursts as "normal" outbursts and the longer outbursts as superoutbursts. The superoutbursts typically last twelve to thirteen days and the normal outbursts are typically less than four days.

The intervals, ΔT, between each of the nine superoutbursts are shown in Table 2. The mean outburst interval is 411 days and the median 330 days. Two of the outburst intervals were considerably longer than the median (545 and 838 days) suggesting that they may be multiples of the superoutburst period. It is entirely possible that further superoutbursts have been missed due to incomplete coverage. Kato *et al.* (2003) suggested a possible superoutburst period of 840 days based on the interval between the 2000 and 2002 outbursts, which corresponds to our 838-day interval. A preliminary superoutburst cycle number was assigned to each observed superoutburst, assuming the ΔT = 545-day interval contains two supercycles and ΔT = 838 days contains three supercycles. A linear ephemeris was calculated from the superoutburst times:

$$JD_{max} = 2451641(18) + 301(8) \times E \qquad (1)$$

This suggests a superoutburst period of 301 ± 8 days. The corresponding O–C diagram is shown in Figure 2. The O–C residuals range over about ± 38 days, or about 13% of the proposed superoutburst period. The standard deviation of the residuals is 28 days and this value probably gives a more realistic idea of when a superoutburst might be seen, rather than the formal error on the superoutburst period (Shears *et al.* 2009). Thus the adopted superoutburst period is 301 ± 28 days.

In another approach to investigate the potential superoutburst periods, the Date Compensated Discrete Fourier Transform (DCDFT) power spectrum of the positive observations of KV Dra was constructed using the PERANSO software (Vanmunster 2007) and is shown in Figure 3. The strongest signal lies at 302 ± 28 days, which is consistent with the superoutburst period determined from the linear analysis of superoutburst times.

4. Discussion

The linear analysis of the superoutbursts, described above, suggests that three superoutbursts may have been missed: two between May 2000 and August 2002 and one between December 2006 and June 2008. During the first interval there are 255 separate observations in the AAVSO International Database, but the gaps between observations are sufficiently large that superoutbursts could have been missed. The longest gap is 54 days, but there are twenty-seven instances of gaps of more than 7 days. By contrast, the later interval corresponds to a period when there were much more frequent observations. In the period covering two standard deviations either side of the superoutburst time predicted by the linear ephemeris (Equation 1) there were 109 observations. The longest gap was 7 days, but the median and mean were both 1 day. One outburst was detected during this period. The relative faintness ($V = 14.7$) and short duration (< 7 days) suggests it was not a superoutburst, although this cannot be ruled out. Had it been a superoutburst, it occurred only 25 days before the time predicted by Equation 1. Thus, although we cannot completely rule out a superoutburst during this interval, we consider such an event unlikely.

Superoutbursts are thought to be triggered by normal outbursts when sufficient mass transfer of material from the secondary star into the accretion disc has occurred to expand the outer part of the disc into a region where it becomes unstable (Hellier 2001). At this point, the disc then becomes elliptical and starts to precess, resulting in superhumps in the light curve. Normally the mass-transfer rate in SU UMa systems is thought to be constant, resulting in regular spacing of superoutbursts (Hellier 2001). Thus our observation that a superoutburst of KV Dra may actually be "missing" is surprising. Further close monitoring of this object should continue to improve the statistics on the superoutburst period and show whether KV Dra does in fact "miss" some superoutbursts.

We have tried to compare the superoutburst period of KV Dra with that of other SU UMa stars of similar P_{orb} listed in Kato *et al.* (2003). However, this is complicated by that fact two sub-types of SU UMa systems with extreme superoutburst behavior have similar P_{orb} values. The WZ Sge stars have exceptionally long superoutburst periods measured in years; WZ Sge itself has $P_{orb} = 0.057$ day and a superoutburst period of around 30 years. By contrast, the ER UMa stars have exceptionally short superoutburst periods of a few days or weeks, e.g., RZ LMi has $P_{orb} = 0.059$ day and a superoutburst period of 19 days. The more conventional SU UMa system PU CMa has $P_{orb} = 0.058$ day and a superoutburst period of 362 to 391 days.

5. Conclusion

Examination of observations of KV Dra between May 2000 and June 2009 has revealed nine likely superoutbursts, although gaps in the data mean that further superoutbursts could have been missed. Analysis of the superoutburst times, assuming a linear ephemeris and allowing for possible missed outbursts, results in a superoutburst period of 301 days, with a standard deviation of 28 days. Further observations are required to refine the ephemeris and to confirm whether some superoutbursts predicted by the ephemeris were not in fact triggered. All observers are encouraged to monitor this star regularly.

6. Acknowledgements

The author gratefully acknowledges the use in this research of observations from the AAVSO International Database contributed by observers worldwide, as well as observations contributed to VSNET relating to the "missing" outburst in 2007 (kindly highlighted to the author by Wolfgang Renz) and to the BAA Variable Star Section's Recurrent Objects Programme, which were provided by the programme co-ordinator, Gary Poyner.

References

Hellier, C. 2001, *Cataclysmic Variable Stars: How and Why They Vary*, Springer-Verlag, New York.

Kato, T., Nogami, D., Moilanen, M., and Yamaoka, H. 2003, *Publ. Astron. Soc. Japan*, **55**, 989.

Kato, T., *et al.* 2009, *Publ. Astron. Soc. Japan*, submitted, pre-print available at http://arxiv.org/abs/0905.1757

Kato, T. 2009, vsnet-alert 11249, http://ooruri.kusastro.kyoto- u.ac.jp/pipermail/vsnet-alert/2009-May/002855.html

Nogami, D., Engels, D., Gänsicke, B. T., Pavlenko, E. P., Novak, R., and Reinsch, K. 2000, *Astron. Astrophys.*, **364**, 701.

Poyner, G. 1996, *J. Brit. Astron. Assoc.*, **106**, 155.

Shears, J., *et al.* 2009, *J. Brit. Astron. Assoc.*, **119**, 31.

Vanmunster, T., Skillman, D. R., Fried, R. E., Kemp, J., and Novak, R. 2000, *Inf. Bull. Var. Stars*, No. 4940.

Vanmunster, T. 2007, PERANSO period analysis software, http://www.peranso.com

Table 1. Outbursts of KV Dra between May 2000 and June 2009.

Detection date	*JD*	*Magnitude at maximum*[a]	*Outburst duration (d)*[b]	*Superhumps detected?*
2000 May 14	2451679.4	13.4v	14 *	Y 1
2000 Jun 25	2451721.3	15.2R	3	
2000 Sep 17	2451805.3	15.7v	<3	
2000 Sep 25	2451813.3	14.6v	<5	
2002 Aug 31	2452517.6	13.1C	13 *	Y 2, 3
2003 Jun 20	2452811.4	14.1V	>7 *	
2004 Apr 4	2453100.4	14.1v	<4	
2004 Apr 22	2453118.4	13.9v	>5 *	Y 2, 3
2004 Sep 14	2453263.3	15.4v	<3	
2005 Apr 2	2453462.5	13.6v	>10 *	Y 3
2005 Apr 18	2453479.4	15.9C	<4	
2006 Jan 17	2453752.8	15.2C	<4	
2006 Jan 26	2453762.4	14.3C	12 *	Y 2
2006 Apr 14	2453840.4	15.0C	<3	
2006 Jun 19	2453905.6	14.2v	<3	
2006 Jul 13	2453930.4	15.4v	<3	
2006 Dec 9	2454079.4	14.4C	12 *	
2007 Mar 9	2454168.8	14.6v	<3	
2007 Jun 11	2454262.6	15.2V	<3	
2007 Aug 12	2454325.4	14.7v	<3	
2008 Jun 7	2454624.7	14.2V	13 *	
2009 May 18	2454970.3	13.6v	13 *	Y 4

[a] *v = visual, R = CCD + Johnson* R *filter, C = unfiltered CCD, V = CCD + Johnson* V *filter.*

1 Vanmunster et al. *(2000) and Nogami* et al. *(2000); 2 AAVSO International Database; 3 Kato* et al. *(2009); 4 Kato (2009).*

[b] Probable superoutbursts are marked with an asterisk.

Table 2. Superoutbursts of KV Dra.

Detection date	*JD*	*ΔT (d)*
2000 May 14	2451679.4	
2002 Aug 31	2452517.6	838.2
2003 Jun 20	2452811.4	293.8
2004 Apr 22	2453118.4	307.0
2005 Apr 2	2453462.5	344.1
2006 Jan 27	2453762.4	299.9
2006 Dec 9	2454079.4	317.0
2008 Jun 7	2454624.7	545.3
2009 May 18	2454970.3	345.6

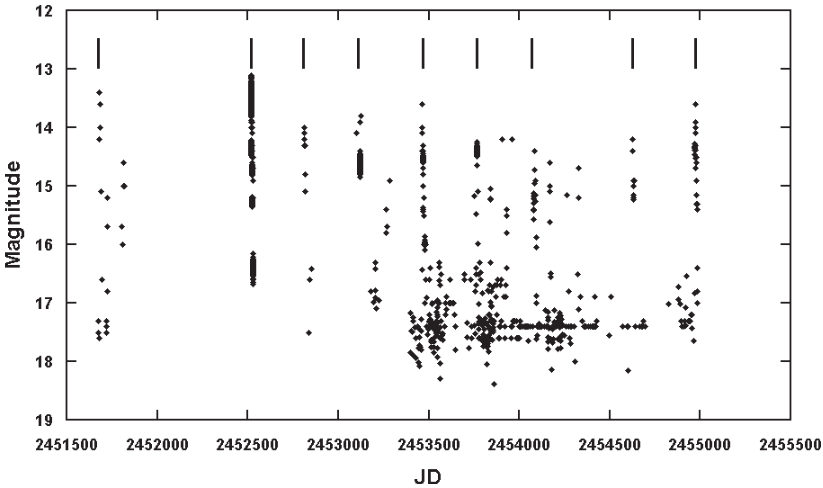

Figure 1. Observations of KV Dra. Superoutbursts are indicated by a bar.

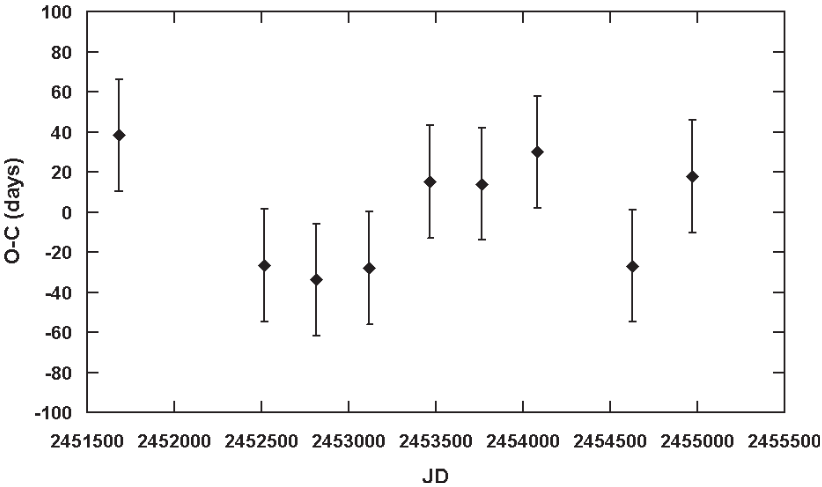

Figure 2. O–C diagram of superoutbursts of KV Dra. Error bars represent the standard deviation of the O–C residuals (28 days).

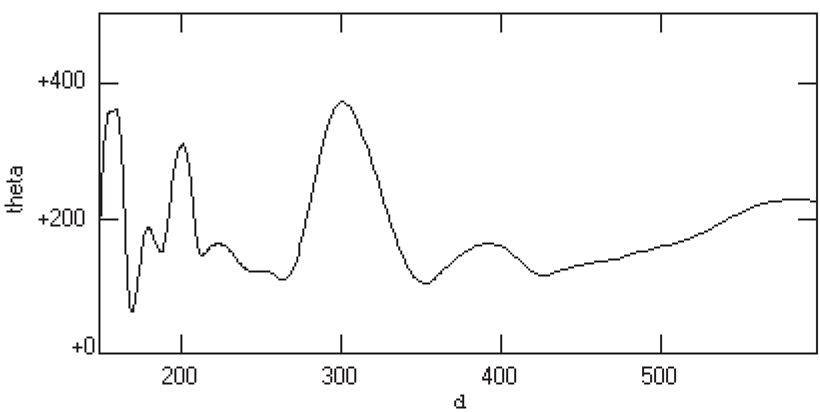

Figure 3. DCDFT power spectrum of the positive observations of KV Dra.

BH Crucis: Period, Magnitude, and Color Changes

W. S. G. Walker
Wharemaru Observatory, P. O. Box 173, Awanui, 0451, New Zealand

Received June 28, 2009; revised September 2, 2009; accepted September 2, 2009

Abstract The period changes of the dual maxima Mira star BH Cru and the associated color changes are discussed. *UBV* measures before the change in period began are compared with those after the star had stabilized at the new, longer, period and those made during the twelve cycles of lengthening period are summarized. A 30% increase in mean *V* brightness is noted, as is a distinctly redder color in *B–V*. The apparent single maximum that has now appeared can be explained by a relative brightening of the second maximum with the first maximum now somewhat hidden by it.

1. Introduction

BH Crucis was discovered in October 1969 by Ronald G. Welch of Auckland, New Zealand, during a photographic search for new variables. His request to the Auckland Observatory for confirmation resulted in its being added to the *UBV* observing program. Since then 417 *UBV* measures have been made: 366 at Auckland Observatory, 38 at the Milton Road Observatory in Auckland, and 13 at the Wharemaru Observatory near Awanui. These ceased in 1996. The first 181 measures, during which the period was stable at 421 days, are shown in Figure 1.

The *B–V* and *U–B* color measures provide information about the temperature changes in the star and have not previously been discussed. Over this long time scale the stability of the measuring system comes into question so this is described. During the period 1970–1990 all measures were made at the Auckland Observatory using either of two EMI 9502 photomultiplier tubes. Both were calibrated using the E Region standards (Cousins and Stoy 1962). Two adjacent stars were selected as comparison and check and values determined:

HD 106475	$V = 7.29$	$B–V = 1.33$	$U–B = 1.33$	Comparison
HD 106202	$V = 8.17$	$B–V = 0.32$	$U–B = 0.15$	Check

No indication of variability has been found in either star. All photomultiplier tubes used have S11 photocathodes with a similar wavelength response, but the Aukland Observatory measures used the 14-stage, EMI 9502 photomultiplier tube, while the Milton Road and Wharemaru observatories used the less sensitive, but less costly, 11-stage version.These were calibrated in the same manner. Transformations were checked several times each year.

Error values for these observations are not available, but for both *V* and *B–V* are <0.02, probably <0.005 at the brighter levels. The *U–B* for such a red star is not as good due to faintness in the *U* filter but would usually be within 0.05 to 0.10. In all the figures the zero phase is that of the deeper minimum, which is not normal for Mira stars, but adds clarity and is similar to the policy with RV Tauri stars, which objects BH Cru resembles in some ways with dual maxima and strong color changes during each cycle (Kholopov 1985). It is redder, however, with a much longer period than an RV Tau star. As noted in the text the period has changed noticeably over the forty years since discovery.

At the time of discovery only R Cen and R Nor were considered to be members of the unusual group of Mira stars with double maxima. Some time later NSV 4721, now V415 Vel, was noted as another such object by Williams (1980). These stars are characterized by a wide double-peaked maximum, with a steep rise to the first maximum and a sharp drop to minimum from the second. As a consequence, the minima are quite sharp.

How these stars differ from a number of other variables which show bumps on the light curves, or which sometimes appear almost double peaked, is not clear. Many of these are amongst the semiregular stars and the amplitude of BH Cru is, at times, close to the minimum for a Mira star. Even more confusing is that both R Cen and BH Cru have recently evolved in such a manner that they now show strongly single maxima. In the case of R Cen there is now a well-defined hump on the falling light curve. In contrast, BH Cru shows only a small hump on the rise to maximum.

A number of other stars have been ascribed to this group at times but the closest to the symmetrical light curve characteristics appear to be BX Car and perhaps TT Cen. Others such as DH Cyg (Templeton *et al.* 2005) and several mentioned by Campbell (1955) appear to be Miras of half the quoted periods, but with frequently irregular erratic maxima and minima**.** Some unambiguous method of identifying objects of this group is needed.

2. Period changes

This small group of variables is unusual in that two of the stars have shown dramatic changes of period. The period of R Cen is slowly becoming shorter, with the second peak becoming much smaller and now lacking the dramatic fall in brightness. The period of BH Cru, on the other hand, increased by 104 days, or 25%, in a mere twelve cycles. This is shown in Figure 2.

There is a suggestion of earlier period changes in Ziljstra *et al.* (2004) but as the observations come from random sky surveys this is uncertain. When classifying this star, Walker *et al.* (1972) drew attention to some of these early measures and the difficulty of determining any useful periods due to the variety of film types and the paucity of the data. If BH Cru did have a longer period prior to 1970 the star becomes even more puzzling.

The exact length of the present period is uncertain. Ziljstra *et al.* determined 540 days using a wavelets analysis, the epochs of minimum show 525 days, and the later PEP and CCD measures are best fitted by a 530-day period, as are some of the visual measures.

3. Color photometry

Figure 3 shows *B–V* colors of BH Cru during the first five cycles observed, then the first three cycles of the 530-day period. All of these were made by the Auckland Photoelectric Observers' Group (APOG) using PEP. One final color cycle was made by G. di Scala using CCD photometry.

This figure appears to confirm a cooling of BH Cru, expected if its radius has increased as deduced from the change in period.

Figure 4 presents *V*, *B–V*, and *U–B* measures since JD 2448997. There are inadequate measures during the intervals where the period was changing (155 measures over thirteen cycles) to allow determination of any periods suitable for data plotting. But the salient features are presented in Table 1. For cycles 19–21, by which time the period had stabilized, there are fifty-one measures; and di Scala made twenty-one in cycle 29, and two in cycle 30, as shown in the AAVSO International Database. He did not measure in U so there are no *U–B* values for the last two cycles. Cycles are shown as filled diamonds, 530/1; open squares, 530/2; square crosses, 530/3; and complex crosses, 530/10 and 530/11. It should be remembered that the period derived from the photoelectric measures differs slightly from that of the visual period. One noticeable feature is that there is a pronounced difference between the *B–V* colors in cycle 530/1 and the subsequent cycles.

4. Mean brightness of BH Cru

Has BH Cru changed in average brightness as a result of these changes in period and color? Figures 5a and 5b show mean *V* light curves in 1970–1975 and 1993–2009. The mean magnitudes at intervals of 0.05 cycle have been determined by phasing and averaging the *V*-measures—221 in the first interval, 74 in the second. From these, intensities were derived and a mean intensity during each cycle, which was then reconverted to mean magnitudes.

Visual measures were made from 1969 onward, but those up to 1985 have not been published in detail. Those used in Figure 7 were provided by Bedding (2009). ASAS3 untransformed V measures (Pojmański 2002), in view of the large *B–V* changes, were considered incompatible in this context. The latter, however, have been used in determining the minima of Figure 2.

While the star was pulsating with a period of 421 days, the mean magnitude was 8.047, but now the period is 530 days with a mean magnitude of 7.762. This represents an increase in *V*-brightness of exactly 30%, in spite of the decreased temperature.

5. Evolution and changes in the light curves

In Figure 6 the separate *V* light curves are superimposed. The result shows that the changes are almost all associated with the region between phases 0.35 to 0.65. The original first maximum has now become the hump on the rise, and the dip prior to the second, brighter maximum has been replaced by a feature which turns the light curve into a relatively normal Mira light curve.

Various ideas have been put forward for the double maxima phenomenon. The more generally accepted one involves double mode pulsation, with the ratio being almost exactly 2:1. Other possibilities include atmospheric filtering (Templeton *et al.* 2005), perhaps even other mechanisms.

The question which is posed by Figures 6 and 7 is why the change in period and shape of the light curve should result in increased brightness in BH Cru. This argues for some other discrete cause rather than the normally quoted helium ignition events. In stars such as R Aql and R Hya the consequences of the helium event are relatively long lasting with a much slower rate of period change. Little information is available about possible brightness changes for those two stars.

There are twelve cycles between the two graphs in Figures 5a and 5b and fourteen between the two curves of Figure 6. These are summarized in Table 1. During this interval BH Cru was unstable in period, the nature of the maxima changed and the maximum became brighter toward the end of the interval.

It can be seen that the double maxima continued until JD 2446132, although the previous rather bright maximum perhaps indicated a change was imminent.

The change in period was relatively smooth but there were some partial reversions to a shorter period. In summary, the light curve shape changed significantly at JD 2445500 with a single reversion to the previous double maxima. This was much in line with the changing brightness.

The single maximum appears to have replaced the second maximum but occurs about 5% earlier in each cycle. The first maximum is still present, but shows only as a hump on the light curve at the same phase as previously. This has not affected the deeper minimum, but the shallow secondary minimum has been hidden by the greater brightness and width of the second, and now clearly, primary maximum.

6. Conclusion

Since its discovery in 1969 BH Cru has evolved in a unique manner. Its period has changed by 25% over a mere twelve cycles, its color has reddened by 0.5 magnitudes in *B–V*, and the amplitude of the color change in *B–V* during each cycle has increased by a similar amount of 0.5 magnitudes. Its mean brightness has increased by 30%, at the same time as it changed from a double maxima Mira star to a more normal looking Mira with a noticeable hump on the rise. As shown by the photoelectric measures, this hump is at exactly the same magnitude and phase as the initial first maximum of the 1970s and 1980s.

The *B–V* colors indicate a cooler temperature as expected from the longer period. But the increase in brightness is unexpected and implies a rather larger radius change than that calculated by Zijlstra *et al.* (2004). All indications are that some other event occurred around 1983 to 1986. In R CrB stars, abrupt changes in brightness can be caused by obscuring dust clouds, but Whitelock *et al.* (2000) argue that the mass loss rate from BH Cru is unusually low, which precludes any suggestion that an obscuring cloud around the star is now less opaque.

7. Acknowledgements

The *UBV* measures used were made by a variety of Auckland Astronomical Society members using the Edith Winstone Blackwell telescope and equipment at the Auckland Observatory. Later measures came from the Milton Road Observatory of Harry Williams and the author's observatory at Wharemaru. *BVRI* measures by Giorgio di Scala were obtained from the AAVSO International Database (AAVSO 2009).

References

AAVSO 2009, observations from the AAVSO International Database (www.aavso.org).
Bedding, T. 2009, private communication.
Campbell, L. 1955, *Studies of Long Period Variables*, AAVSO, Cambridge, MA.
Cousins, A. W. J., and Stoy, R. H. 1962, *Roy. Obs. Bull.*, **49**, 3.
Kholopov, P. N. 1985, *General Catalogue of Variable Stars*, 4th ed., Moscow.
Pojmański, G. 2002, *Acta Astron.*, **52**, 397.
Templeton, M. R., Mattei, J. A., and Willson, L. A. 2005, *Astron. J.*, **130**, 776.
Walker, W. S. G., Marino, B. F., and Welch, R. G. 1972, *Circ. Var. Star Sec. Roy. Astron. Soc. New Zealand*, No. 188.
Whitelock, P., Marang, F., and Feast, M. 2000, *Mon. Not. Roy. Astron. Soc.*, **319**, 728.
Williams, P. F. 1980, private communication.
Zijlstra, A. A., *et al.* 2004, *Mon. Not. Roy. Astron. Soc.*, **352**, 325.

Table 1. BH Cru: sparsely observed cycles in interval of period change.

Cycle No.	*No. of Obs.*	*Epoch of Max (JD)*	*Max V mag.*	*Comments*
6	22	2442831	7.354	Double maximum
7	11	2443304	7.404	Double maximum
8	11	2443725	7.580?	Double maximum
9	10			First maximum only observed
10	20	2444683	7.525	Double maximum
11	16	2445152	7.234	First maximum only observed
12	15	2445574	7.141	Brighter than normal, hump at first maximum position
13	26	2446132	7.512	Double maximum
14	8	2446562	7.154	Single maximum only
15	8	2447023	7.190	Probable single maximum
17	18	2448045	7.069	Probable single maximum

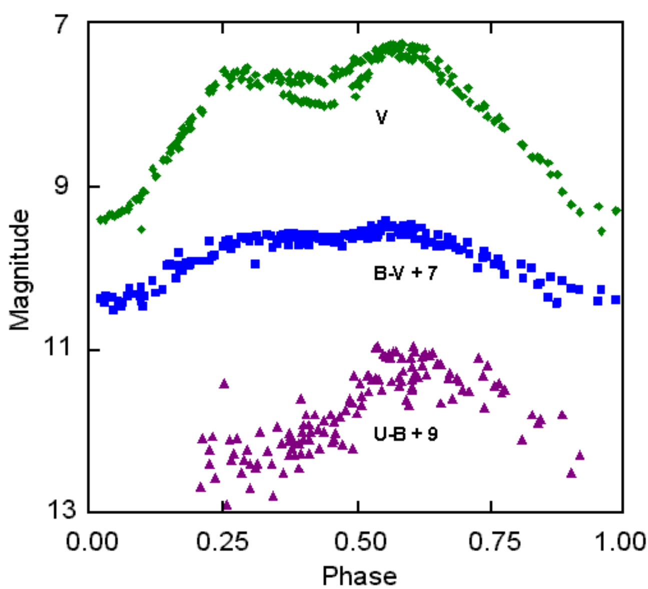

Figure 1. Phase diagram for BH Cru showing *V, B–V*, and *U–B* colors during the interval JD 2440862–2442544 phased to the light elements of the deep minimum, JD 2440645+421E. The *B–V* has been offset by adding 7, *U–B* by adding 9. The scales are identical otherwise. *U–B* colors up to phase 0.20 were very poor due to the faintness of BH Crucis in *U*—magnitude 15–16 at those phases. However, these still show the remarkable difference between the *U–B* color of the two maxima.

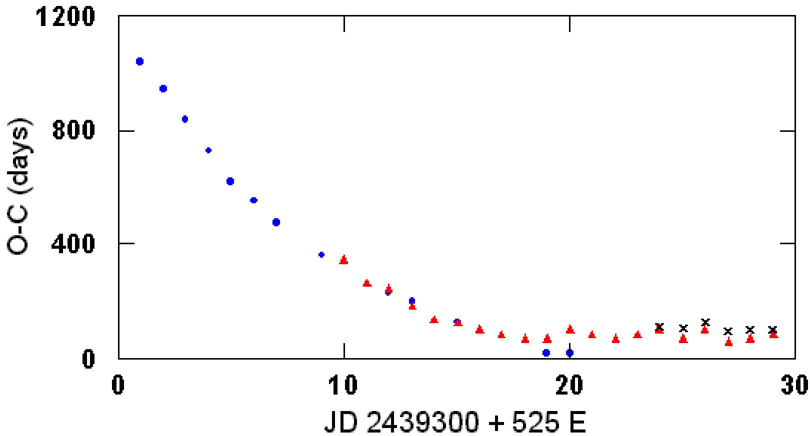

Figure 2. Due to the changing shape of the light curve it is preferable with BH Cru to determine epochs using minima. This O–C plot shows the first five minima with a stable period of 421 days; the next twelve show a gradual increase in period—with some deviations—then the present visually-based period of 525 days. Circles represent Auckland Photoelectric Observers' Group (APOG) data; triangles, AAVSO data; crosses, ASAS3 data.

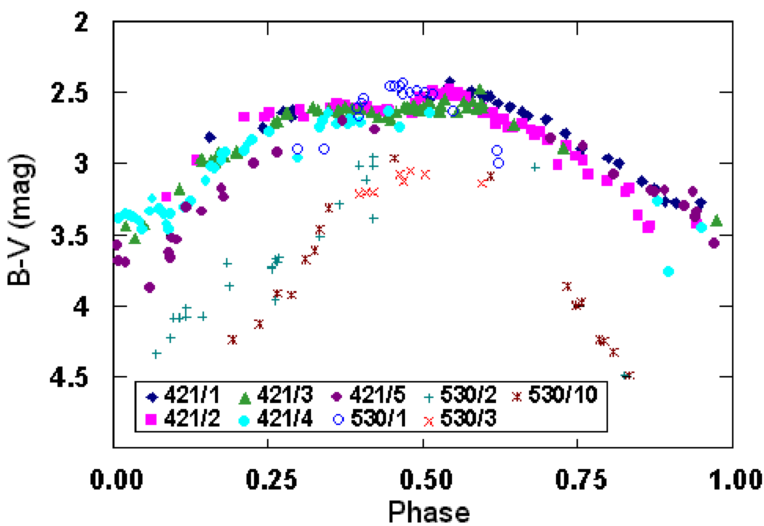

Figure 3. Phase diagram for BH Cru showing *B–V* colors during the two stable periods shown in Figure 2. The earlier cycles are denoted by solid colors, more recent ones by unfilled circles or crosses of various kinds. There is a noticeable change in the *B–V* amplitude, from 1.0 magnitude in the 1970s to 1.5 magnitudes in the 1990s and 2000s.

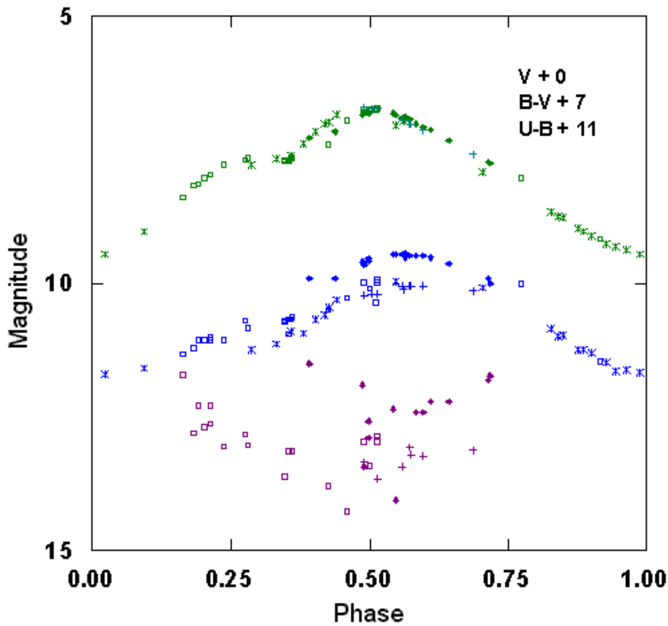

Figure 4. Recent phase diagrams for BH Cru in *V*, *B–V*, and *U–B*. The *V*-curve shows a marked hump on the rising branch, but is certainly not double peaked as it was on discovery. Peak brightness seems to occur slightly earlier than previously, although there are not enough measures and too few cycles to be certain. Cycle 530/1 is rather brighter in *B–V* than the remainder, although this does not show in the *V* brightness. The *U–B* measures appear quite different from those of Figure 1, but the detectors used were less sensitive and the data are noisy.

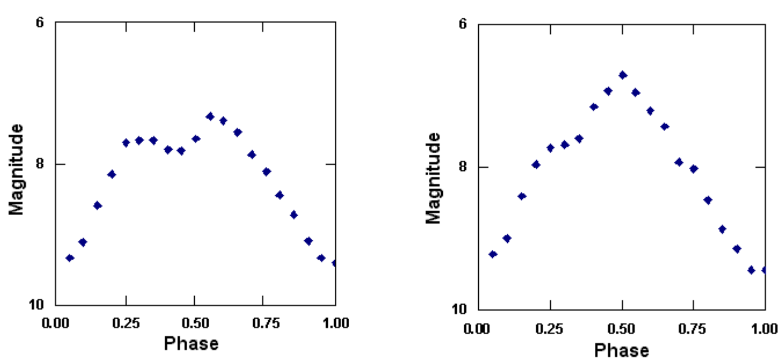

Figure 5a, 5b. Mean phase diagrams for BH Cru, determined in the manner described in the text. These appear to show an increase in mean brightness in *V* of 30% over the ~20-year interval.

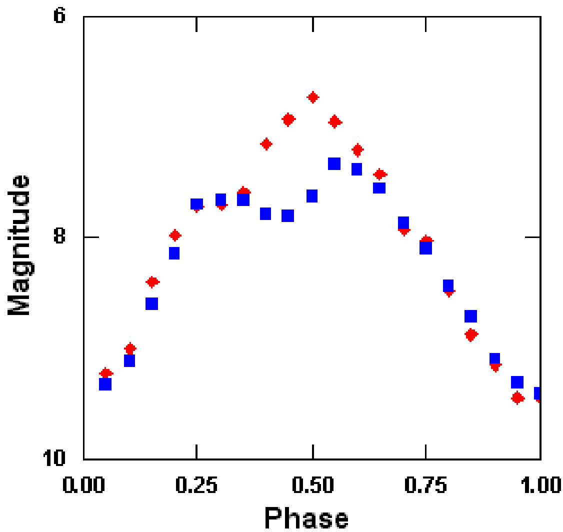

Figure 6. BH Cru: the *V* phase diagrams of Figure 5 superimposed to show the continued presence of the first maximum, as well as the increase in brightness from phase 0.35 to 0.65.

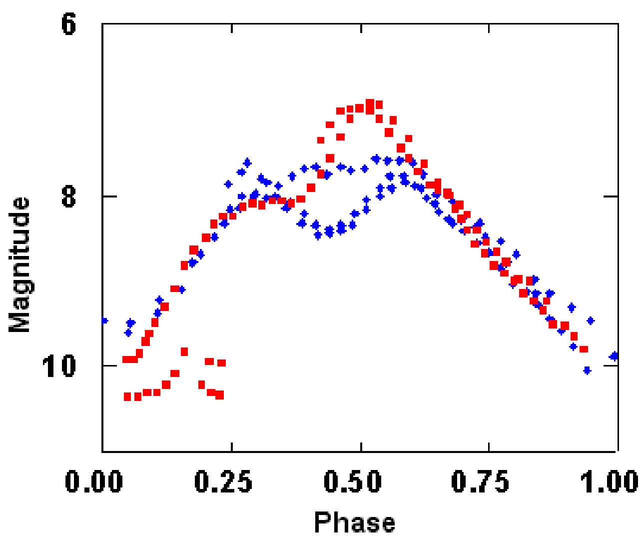

Figure 7. Visual observations of BH Cru made by members of the RASNZ. Cycles 1–4 are shown as diamonds, with cycles 18–22 shown as squares. A five-point running mean has been applied to the data.The visual observations seem more divergent as to amplitude than the photoelectric measures but, in general, are similar to Figure 6.

The 2009 Eclipse of EE Cephei

Gerard Samolyk
P.O. Box 20939, Greenfield, WI 53220

Rudy Poklar
14084 N. Willow Bend Drive, Tucson, AZ 85737

Received May 22, 2009; revised June 22, 2009; accepted July 13, 2009

Abstract An eclipse of the long period system EE Cephei occurred in 2009. CCD observations of this eclipse show a significantly different shape than the previous eclipse in 2003.

1. Background

The variability of EE Cephei was first identified by Romano (1956). His initial analysis indicated that this star was an R CrB type variable. However, this was later changed to an eclipsing binary type by Romano and Perissinotto (1966). The eclipsing nature was confirmed by Meinunger (1973).

Campaigns to observe the two eclipses in the 1990s were lead by Halbach (1992 and 1999). A study by Graczyk *et al.* (2003) evaluated eclipse data through epoch 8. This study proposed a disk model for the system. A CCD campaign in 2003 by Samolyk and Dvorak (2004) showed the eclipse to be highly asymmetrical, supporting the Graczyk *et al.* model.

The light elements from the *General Catalogue of Variable Stars* (GCVS; Kholopov *et al.* 1985) were used to predict these eclipses (no error values available). These are given in equation 1:

$$JD_{min} = 2434346.0 + 2049.53\,E \quad (1)$$

2. Observations

Observations were made with telescopes of 20- to 30-cm aperture. ST9E or ST9XE CCD imagers were used by all observers. Observations were made in Arizona, Texas, and Wisconsin. Observations from three different sites increased the number of clear nights available and helped us obtain a complete light curve. A Johnson *V* filter was used for all observations.

Field photometry of the following stars, provided by Brian Skiff (2003), was used for the comparison and check stars.

	GSC Nr.	Mag. *V*	*B–V*
Comparison Star	3973 1177	10.386	0.396
Check Star	3973 2150	11.248	0.109
Alternate check Star	3973 1103	11.232	0.410

These are the same comparison stars used for the 2003 eclipse (Samolyk and Dvorak 2004) so the light curves can be directly compared. Images by Simmons (2009) and Poklar were processed using AIP4WIN software. Images by Gerner (2009) and Samolyk were processed using MIRA software. Occasional simultaneous data between observers showed a correlation of 0.01 magnitude or better. All observations from this project are available in the AAVSO International Database.

3. Analysis

The model proposed by Graczyk *et al.* (2003) consists of an optically thick disk surrounded by a semi-transparent layer at the periphery. In addition to the contacts observed in a conventional eclipse, additional contacts occur at the beginning and end of the transit of the semi-transparent portion of the disk.

The duration of the 2009 eclipse (E = 10) caused by the optically thick disk (time between the first and fourth contact) was 37 days. The duration of the entire eclipse, including the semi-transparent layer, is estimated at 90 days. With a minimum magnitude of 11.25 *V*, this was among the shallowest eclipses on record. Other shallow eclipses include 1969 (E = 3) (Graczyk *et al.* 2003) and 2003 (E = 9) (Samolyk and Dvorak 2004). Graczyk *et al.* (2003) suggested that there was an inverse linear relationship between eclipse depth and duration. The 2009 eclipse is a decent fit to the Graczyk plot and supports this hypothesis.

With the exception of irregularities in the descending leg, the 2009 eclipse was much more symmetrical than the typical EE Cep eclipse. This indicates that axis of the disk has rotated significantly from its orientation during the 2003 eclipse. The irregular shape of the descending portion of the eclipse may have been caused by one or more anomalies in the disc structure revealed by the current disc orientation.

The time of mid-eclipse for the 2009 eclipse (E = 10) was determined to be HJD 2454842.1. The available times of minimum from eclipses are listed in Table 1. The Cycle and O–C are calculated using Equation (1).

All observations obtained for this study are available in the AAVSO International Database located at http://www.aavso.org.

4. The next eclipse

The next mid-eclipse of EE Cephei will occur during in July 2014. Observations for a four-month time period are planned to record all contacts of the eclipse.

5. Acknowledgements

The authors would like to thank Henry Gerner and Neil Simmons for contributing CCD observations to this project.

References

Gerner, H. 2009, private communication.

Graczyk, D., Mikołajewski, M., Tomov, T., Kilev, D., and Iliev, I. 2003, *Astron. Astrophys.*, **403**, 1089.

Halbach, E. A. 1992, *J. Amer. Assoc. Var. Star Obs.*, **21**, 129.

Halbach, E. A. 1999, *J. Amer. Assoc. Var. Star Obs.*, **27**, 35.

Kholopov, P. N., *et al.* 1985, *General Catalogue of Variable Stars*, 4th ed., Moscow.

Meinunger, L. 1973, *Mitt. Veränderliche Sterne*, **6**, 89.

Romano, G. 1956, *Doc. Obs. Circ.*, Nr. 9.

Romano, G., and Perissinotto, M. 1966, *Mem. Soc. Astr. Ital.*, **37**, 255.

Samolyk, G., and Dvorak, S. 2004, *J. Amer. Assoc. Var. Star Obs.*, **33**, 42.

Skiff, B. 2003, private communication.

Simmons, N. 2009, private communication.

Table 1. Available times of minimum from eclipses of EE Cep.

JD(min) Heliocentric 2400000+	*Cycle*	*O–C*	*Method*	*Observers*
32297	–1	0.5	photographic	Weber
34346	0	0.0	photographic	Romano
36399	1	3.5	photographic	Romano, Perissinotto
38440	2	–5.1	photographic	Romano, Perissinotto
40493	3	–1.6	photographic	Baldinelli, Ghedini, Tubertini
42543.3	4	–0.8	visual	Bauer, Braue, Klebert
42543.7	4	–0.4	PEP	Locher
42544	4	–0.1	photographic	Baldinelli, Ghedini, Tubertini
42544	4	–0.1	visual	Duruy, Thouet, Vedrenne, Verdenet
42544.1	4	0.0	PEP	Rossiger, Pfau, Uhlig
42544.2	4	0.1	visual	Peter
42544.2	4	0.1	photographic	Sharof, Perova
42545.48	4	1.4	PEP, photo	Bahyl
44594.1	5	0.4	PEP, photo	Baldinelli, Ferri, Ghedini
46643	6	–0.2	visual	AAVSO Data
48691.0	7	–1.7	visual	Halbach
48691.0	7	–1.7	CCD	Borovicka
48692.5	7	–0.2	visual	Baldwin
48693.0	7	0.3	visual	Samolyk
50743.8	8	1.6	visual	Samolyk
50743.9	8	1.7	CCD	Cook
50744.0	8	1.8	visual	Berg
52795.0	9	3.2	CCD	Samolyk, Dvorak
54842.5	10	1.2	CCD	Samolyk, Poklar

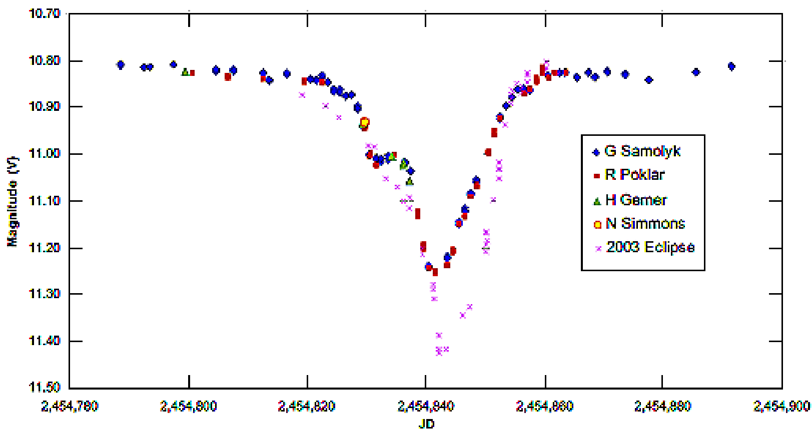

Figure 1. Observations of the 2009 eclipse of EE Cep. The 2003 eclipse (x-symbol) is shown for comparison. Observers are: Samolyk (diamond); Poklar (solid square); Gerner (triangle); Simmons (open square).

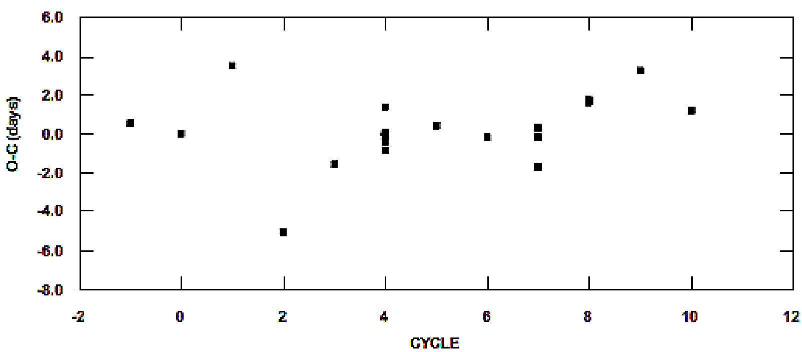

Figure 2. Times of minimum of EE Cep listed in Table 2. The O–C values were calculated using Equation (1).

Photometry of Z Tauri to Minimum

Walter R. Cooney, Jr.
Blackberry Observatory, 1927 Fairview Drive, Port Allen, LA 70767

Arne A. Henden
AAVSO, 49 Bay State Road, Cambridge, MA 02138

John Gross
Sonoita Research Observatory, Sonoita, AZ

Dirk Terrell
Southwest Research Institute, 1050 Walnut Street #400, Boulder, CO 80302

Received July 6, 2009; revised September 3, 2009; accepted September 7, 2009

Abstract The long period Mira variable, Z Tauri, was followed to near minimum magnitude in late 2006 and early 2007. Z Tau reached a minimum *V* magnitude of 18.0, well below the minimum of about 14 as found in the archival AAVSO data. Photometry from previous minima at the USNO confirm similar minima in previous cycles. The presence of a close companion star resulted in the erroneous minima derived from the visual data. A preliminary phased light curve of a field star located near Z Tau that was found to be variable is also presented.

1. Introduction

Z Tau (R.A. = 05^h 52^m 24.855^s, Dec. = +15° 47' 43.81", J2000.0) = BD+15 962a = GSC 01312-02344 = 2MASS J05522485+1547438 is a Mira-type long period variable star. It has been an AAVSO program star since December of 1909 when C. J. Hudson of Amherst College estimated it to be of magnitude 9.7. Since that first AAVSO observation, more than 3,500 observations have been submitted to the AAVSO by dozens of dedicated observers. Their data show that Z Tau reaches a minimum of about 14th magnitude and stays there for some weeks or months until it begins to brighten again. A case of mistaken identity has hidden the real behavior of Z Tau at minimum light. This paper discusses observations of Z Tau as it approached minimum in late 2006 and early 2007 that show it dropped to a minimum of 18.0. Supporting observations from the U.S. Naval Observatory are presented where Z Tau was below 17th magnitude during previous minima.

2. Background

In March 2006 AAVSO member Erwin van Ballegoij posted a note to the AAVSO discussion group that observers should take care when estimating Z Tau at its current minimum. He noted the wide flat bottom of the AAVSO light curve and that there were also reports of it being below magnitude 16. He pointed out that there was a companion star to Z Tau that could easily be mistaken for Z Tau when at minimum. Richard Huziak responded that the chart team had added a note on charts about this issue.

This AAVSO email discussion sparked the interest of the first author. A long-studied Mira with a minimum that had been mostly hidden from a century of observers was worth investigating. An observation of Z Tau from the first author's Blackberry Observatory showed an elongated image of the three involved stars. Z Tau appeared to be at between magnitude 14.5 and 15 through a *V* filter based on estimating the height of its peak relative to the brighter of the companions. It was clear that Z Tau's behavior at minimum had long been disguised by the close companion.

Further research found that Merrill (1956) had suspected that there was an unseen companion to Z Tau based on its long flat minimum. Price and Klingenberg (2005) also pointed out that a companion star could be responsible for the apparent long flat minimum. Indeed, in December 2001 Arne Henden sent photometry of the offending companion and another fainter companion to Mike Simonsen. Simonsen included it in draft updated AAVSO charts and noted in an AAVSO discussion list email in 2003 that "Revised and new charts for Z Tau are also in the 2Bchecked folder. This is a Mira with a troublesome close companion."

3. Observations

The observations reported here were made at the U. S. Naval Observatory Flagstaff Station (NOFS), and at the Sonoita Research Observatory (SRO). Both the 1.0-m and 1.55-m telescopes were used at NOFS, with either a SITe/Tektronix thinned, backside illuminated 1024×1024 or 2048×2048 CCD. SRO is a collaborative effort between John Gross, Walt Cooney, Dirk Terrell, and the AAVSO. This observatory in Sonoita, Arizona, houses a 0.35m Schmidt Cassegrain with an SBIG STL-1001E CCD camera and *BVRI* filters on a Software Bisque Paramount ME robotic telescope mount. The telescope resides in an automated Technical Innovations HomeDome and is run by the collaborators remotely over the internet using ACP observatory control, planning, and scheduling software from DC3 Dreams.

Z Tau reached maximum brightness during the summer of 2006 and then started heading back down. In order to find out how deep the minimum of Z Tau really was, monitoring of Z Tau started in November of 2006. A pair of images in both *V* and *I* were recorded on almost every clear night. Exposures were three minutes in *V* and had to be brought down to five seconds in *I* to keep from saturating this Mira.

IRAF was used to do Point Spread Function photometry of the *V* images of Z Tau as well as the two companions and a check star. Although the Landolt (1983) standard star, GD71, was in the field of view, it was not used as a comparison star since it is rather blue with a *B–V* color index of –0.249 while a Mira like Z Tau is quite red. Instead, GSC 1312-2620 was used as a comparison star for the *V*-band PSF photometry. We had previously calibrated the Z Tau field in $UBVR_cI_c$. Per that calibration, GSC 1312-2620 has a *B–V* color index of 0.548. Our $UBVR_cI_c$ calibrated magnitudes for this star are listed in Table 1 and a finder chart for GSC 1312-2620 is shown in Figure 1.

Point Spread Function photometry was not used for the SRO *I*-band photometry since the companion stars were very faint relative to Z Tau in *I*. Instead, aperture photometry was performed with a six-star ensemble and the two companion stars were subtracted using Lew Cook's "Nemesis" spreadsheet (http://www.geocities.com/lcoo/nemesis.htm) to give the resulting I_c magnitude of Z Tau.

The *V* data from SRO are presented in Figure 2. The figure illustrates that over many cycles, the AAVSO visual observations cut off as Z Tau approached 14th magnitude while the SRO data show that Z Tau reached a minimum of approximately 18.0 during the minimum of early 2007.

Our $UBVR_cI_c$ data obtained with the NOFS 1.0-m and 1.55-m telescopes confirm that similar minima have been reached in previous cycles. The NOFS *V* data are shown in Figure 2 with the AAVSO and SRO data. AAVSO members A. Corlan (CUA) and R. Corlan (CXR) submitted *V*-filter data for Z Tau in September 2003 (JD 2452903 and 2452910). Their data are confirmed by the NOFS observations and correctly measured only the magnitude of Z Tau although it was well below 15th magnitude.

The full transformed SRO data set in *V* and *I* for Z Tau is presented in Figure 3. Pairs of measurements for each night were averaged to a single value to improve signal-to-noise. The interference of the Sun prevented SRO from monitoring through minimum and the rise back to maximum light but the shape of the curve does indicate that SRO was able to monitor at least to very close to or just past the minimum of this cycle.

As is expected for a Mira, the color index shows that this very red star continues to redden as its light diminishes reaching a $(V–I_c)$ color index of 8 near minimum.

Our complete NOFS $UBVR_cI_c$ data set and the SRO *V* and I_c dataset have been entered into the AAVSO database and can be accessed via the AAVSO website, *http://www.aavso.org*.

4. The companions

The companion stars to Z Tau are shown clearly in the *V*-band image of the Z Tau field taken with the NOFS 1.55-m reflector shown in Figure 4. The brighter companion, star A, is 4.79 arc seconds NNE from Z Tau and the fainter, star B, is 5.84 arc seconds south of Z Tau. Our all-sky calibration using the NOFS 1.0-m and 1.55-m telescopes and PSF fitting to separate the components is presented in Table 2. These are transformed magnitudes.

The untransformed SRO photometry of the companion stars is shown in Figure 5. These stars served as check stars for the PSF photometry. Pairs of data points for each night are not averaged in this figure. The SRO companion star photometry was not transformed because aperture photometry performed on the *I*-band images was not suitable for providing measured magnitudes for these stars.

5. Field variable

A field star was discovered to be variable over the course of the SRO work. The new variable is USNO-B1.0 1057-0097388 at R.A. 05^h 52^m 55.56^s, Dec. +15° 42' 07.8", J2000. The star is identified in the Z Tau field shown in Figure 1. At brightest the star is $V=15.7$ with an amplitude in *V* of approximately 0.38 magnitude. A possible phasing with a period of 9.3576 ± 0.001 hours is presented in Figure 6. The shape, period, and amplitude of the curve are consistent with that of a W UMa eclipsing binary although the identification would not be considered definitive based on the data presented here. The authors have submitted the light curve for this star to the AAVSO International Variable Star Index and the star is now designated as VSX J055255.5+154207. The data have also been submitted to the AAVSO database and are available through the organization's web page at *http://www.aavso.org*.

References

Landolt, A. U. 1983, *Astron. J.*, **88**, 439.
Merrill, P. 1956, *Publ. Astron. Soc. Pacific*, **68**, 162.
Price, A., and Klingenberg, G. 2005, *J. Amer. Assoc. Var. Star Obs.*, **34**, 23.

Table 1. NOFS calibration of GSC 1312-2620.

U	*B*	*V*	R_c	I_c
13.263±0.015	13.216±0.011	12.668±0.029	12.33±0.013	12.008±0.019

Table 2. NOFS astrometry and all-sky photometry of Z Tau and companion field stars.

	R. A. (2000) *h m s*	*Dec. (2000)* ° ′ ″	*V*	*B–V*	*V–R*$_c$	*R*$_c$*–I*$_c$
Z Tau	05 52 24.855	+15 47 43.81 ±30mas	—	—	—	—
Star A	05 52 25.079	+15 47 47.99	13.707 ±0.027	0.380 ±0.012	0.223 ±0.020	0.210 ±0.020
Star B	05 52 24.785	+15 47 37.63	16.672 ±0.040	0.731 ±0.010	0.562 ±0.080	

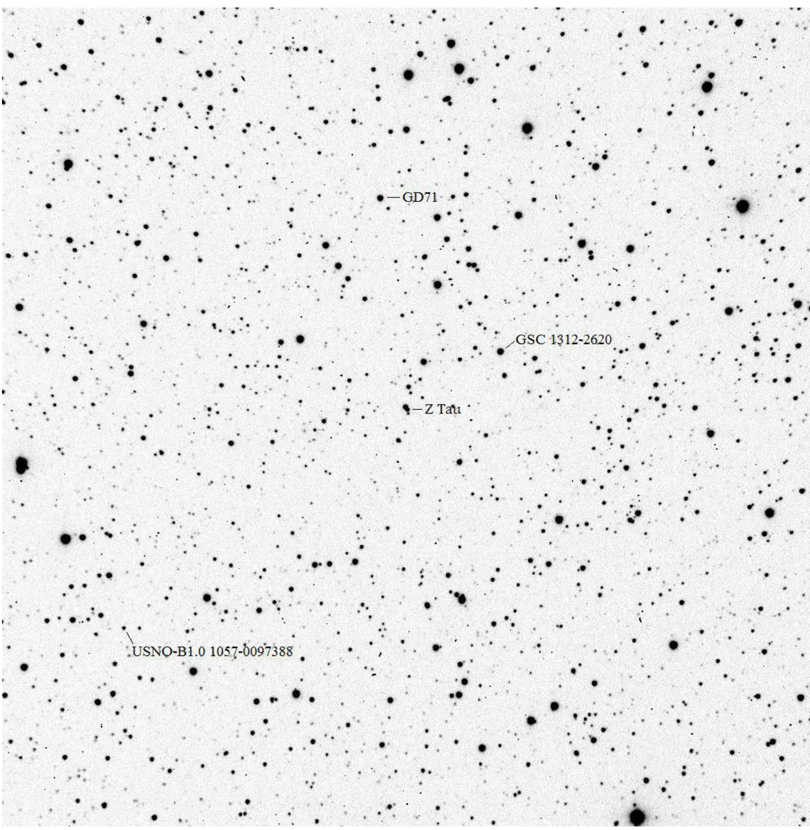

Figure 1. Z Tau and the comparison star used for V-band photometry. The field variable star, USNO-B1.0 1057-0097388, discussed in Section 5 is also identified. North up, east to the left. 21 arc minute wide field. SRO image.

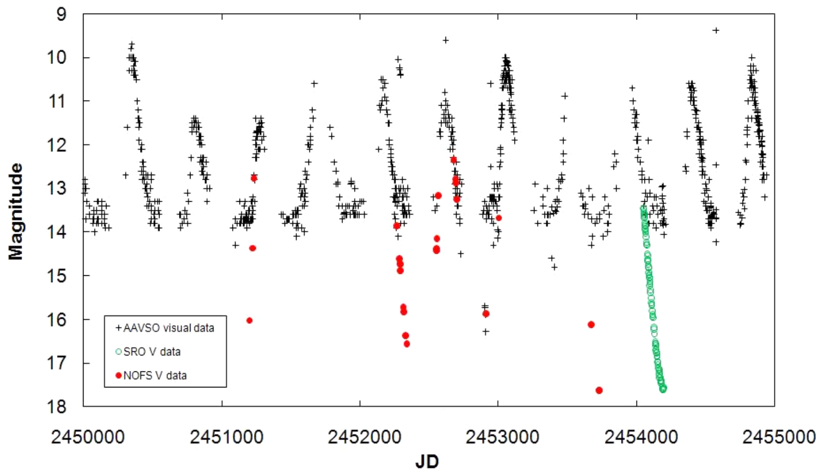

Figure 2. AAVSO, SRO, and NOFS *V* data for Z Tau.

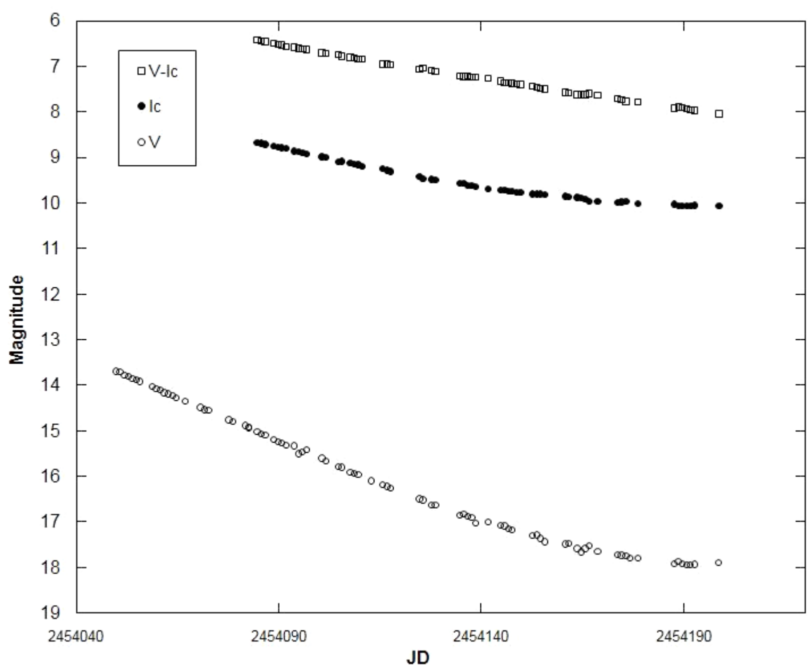

Figure 3. Transformed SRO photometry for Z Tau in *V* and I_c.

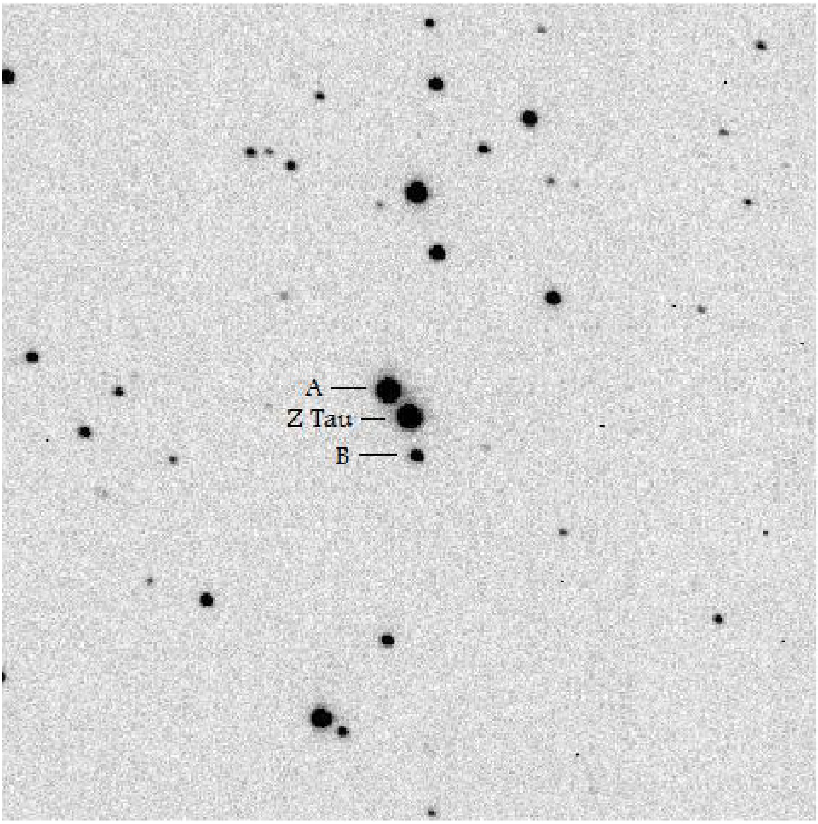

Figure 4. *Z* Tau and companion field stars. North up, east to the left. 2 arc minute wide field. USNO image.

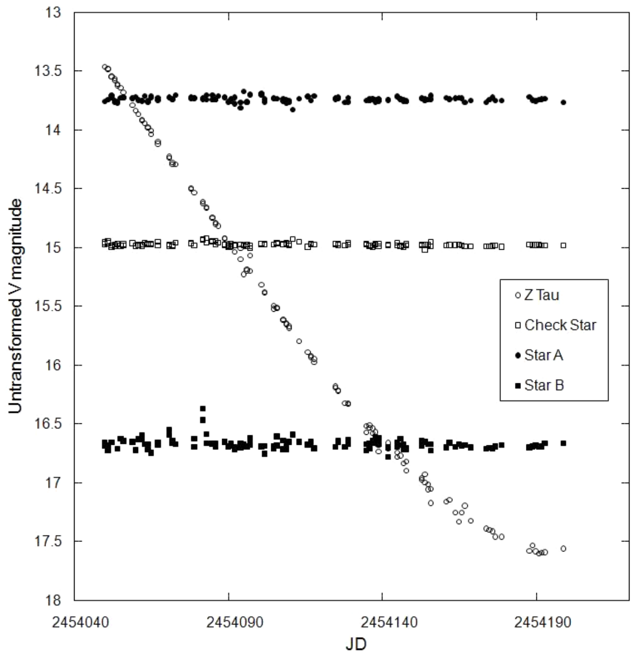

Figure 5. Untransformed SRO photometry of Z Tau, companion stars, and check star.

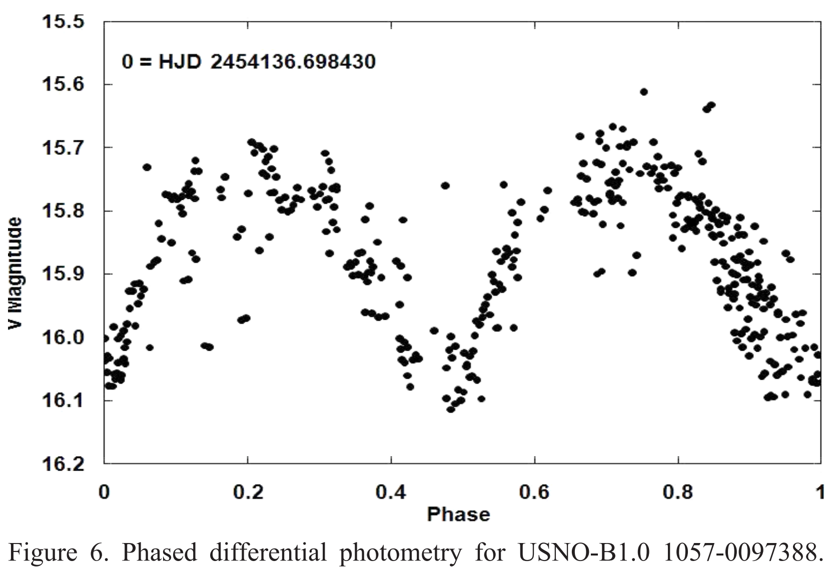

Figure 6. Phased differential photometry for USNO-B1.0 1057-0097388. Period = 9.3576 hours.

BS Tauri—Evidence for Cyclic Activity in an Orion Irregular

Lawrence Krumenaker
1890-C Briarcliff Circle, Atlanta, GA 30329

Received April 30, 2009; revised June 9, 2009; accepted June 9, 2009

Abstract The irregular variable star BS Tauri (type Inbs?) is found to have not only H-α emission and an irregular brightness variation but also an underlying six-year periodicity in brightness. BS Tau should actually be classified as a classical T Tauri star (Int, CTTS), but whether the cyclicity is caused by starspots, a companion, or a circumstellar disk is not certain. Tests to determine the origin of variation are listed.

1. Introduction

Off the east edge of the Taurus T-association, northeast of Aldebaran, lies the variable star BS Tauri (R.A. 04^h 58^m 51^s Dec. +28° 31' 24" (2000)), discovered by Hoffleit (1935) and originally classified as "L"—a possible slow irregular with no known period—and with no known emission spectrum. Fadeev (1972) (sometimes spelled as "Fedeyev") reported slow irregular variations, but with superimposed rapid changes in brightness of up to 2.5 magnitudes over a couple of days. The brightness range was stated as "14.4 to 17.0 photographic." In his article was a chart without marked comparison stars. BS Tau on Palomar plates (POSS) appeared yellow to him, and it lies near a noticeable group of dark clouds. The present author, as an undergraduate student, discovered BS Tau to be an emission-line star on two 1974 H-α sensitive objective prism plates (Bidelman 1976).

The star was included in an unpublished 1978 study by the author in which variability was researched using Harvard College Observatory photographic plates. At that time, magnitudes for the field stars were estimated from the Palomar POSS-blue charts using the relation of image size to magnitude by Liller and Liller (1975). The average error in any *B* magnitude estimate was determined to be ±0.2 magnitude by estimating the brightness of stars in the Landolt (1967) standard star fields in Taurus. The 1978 light curve, based on estimates made from plates at the Harvard Observatory Plate Stacks, showed a waviness indicating a periodicity of around six years in more than thirty years of magnitude estimations but no further work was done on the investigation.

Recently a more extensive article by Fedeev (1973) came to the writer's attention. In it Fedeev classified the star as "Insb?" based on several nights of extensive photographic studies, and this time a finder chart with a fine net of comparison stars was included. To check the old periodicity finding, we revisited the Harvard Plate Stacks early in 2009 and re-measured BS Tau using the original magnitude framework and Fedeev's. Only one star was common to both the Fedeev and Krumenaker systems and its magnitudes differed by 0.4 magnitude. The averaged magnitudes for BS Tau in the two systems differed by 0.36 magnitude and a comparison of the estimates of individual plates consistently differed by 0.33 on average. This new study indicated the two scales gave consistent results but averaging one-third of a magnitude different. Also, the star estimates in the author's system rarely differed over the intervening thirty years. In the 2009 study, a field star was chosen as a check and data were added from the 1960s and 1970s. The finer Fedeev-comparison-star derived values will be used in this analysis.

2. Observations

Table 1 lists, and Figure 1 plots, the *B* magnitudes for BS Tau derived from the 2009 visit to the Harvard Plate Stacks. The bulk of these magnitudes, from observations between 1922 and 1951, are plotted versus Julian date in Figure 1. Two very early observations from 1899 and 1903, and eight from 1969 to 1978, are not plotted.

The study yields a mean *B* magnitude of 14.9 with a standard deviation of 0.5. Known *V*-magnitude values, including some photoelectric observations taken in 1980, are in Table 2. The arithmatic *V*-magnitude average is 14.1, causing BS Tau to have an approximate *B–V* value of 0.8, comparable to a yellowish G-type star, confirming the POSS coloration. No MK classification for BS Tau is known to us.

3. Analysis

Visually noting some waviness to observations plotted in Figure 1, the 1920–1950s data was inserted into a period-finding program called AVE, yielding a periodogram (Figure 2) that shows the strongest period to be 2,176 days (5.96 years), confirming our 1979 observation of a six-year-long periodicity. Using all 79 years of estimates provides an uncertainty of 100 days; the few very early and very recent observations act as overly influential outliers in the statistical analysis. The plateau beginning around 4,000 days also shows up in the non-variable field star and thus signifies a technological origin and not a stellar one. All others are regarded as aliases or low-number statistics noise.

To be sure, a False Alarm Probability (FAP) was calculated using the formulations of Horne and Baliunas (1986). The high peak has an FAP of 1.4%, the next highest peak, around 1500 days, is about 99%. The plateau came in at an FAP of 88%. A phase diagram (Figure 3) was then made using the 2,176-day period with the time origin five cycles before our earliest brightest observation so all 79 years of observations could be included.

Very clearly, the irregular light variations have an underlying cyclicity, causing times when the brightness can be higher or lower than usual. Note that the range of the irregular variation is generally unchanged throughout the whole cycle, with only extremes a bit accentuated or, conversely, the mean varying cyclicly. Such long-term variations are not unknown in T Tauri-type and other related variables. T Tauri itself has a 2,200-day period (Melnikov and Grankin 2005), DI Cep has a cycle varying between 14 and 19 years (Kolotilov *et al.* 2004), and PZ Mon has one of 50 years' length (Alekseev and Bondar 2006).

4. Discussion

If this periodicity is due to a non-visible but obscuring companion star, then one can estimate the companion's orbital distance with a simple application of this period into Kepler's Third Law. T Tauri stars are generally considered to be around one solar mass (Petrov 2003). Estimating the combined mass to be at least 2 solar masses gives us a minimum distance of around 4 AU. Assuming its position near the T-Tauri association clouds indicates BS Tau is at a distance of 140 parsecs, the binary separation is well under 100 mas, far too close for any telescope to separate. Possibly speckle interferometry or an infrared survey might be able to split it, as was done for T Tau itself, at 700 mas and 100 AU separation (Melnikov and Grankin 2005; Appenzeller and Mundt 1989). An occultation might also resolve this binary but faintness of the star likely precludes this as a viable method of observation.

Ismailov (2005) suggests there are five kinds of T Tauri light curves which all depend on external factors such as companion stars, adding to the natural rapid variations. His Type III is defined by the mean brightness changing but not the amplitude of the rapid, irregular variations, which he says requires a companion of equal brightness plus cool starspots. These two requirements would cause variation in brightness but not much in color. Ismailov's Type IV has both mean magnitude and rapid variation amplitude changing over time and caused by a combination of chromospheric activities and eclipses, though by what he does not specify. He puts T Tau in this class.

The BS Tau 30-year light curve would seem very close to his Type IV, as the amplitude in brightness varies from small to several magnitudes, but this could be because of our small number of observations. However, Ismailov did not examine phase diagrams for those stars he studied that had long-term variations. If one examines BS Tau's phase diagram, the rapid variation amplitude does not change with phase, just the mean. This result would make BS Tau more likely a Type III. Since at least 42% of all T Tauri's may have companions (Petrov 2003), and with BS Tau's minimum centered at phase 0.1–0.2 and maximum centered around 0.70–0.80, a companion star eclipse could be possible.

Another possible explanation for this long-term variation is a Schwabe-like sunspot cycle. The irregular variations in T Tauri stars are caused either as cool ("cold") starspots or hot spots. For the cool type, as the spot count goes up and surface area is more covered with cooler areas, the magnitude may be slightly fainter than normal. Halfway through the cycle, there may be less than normal coverage and the star slightly brighter. Not all peaks and valleys would be identical in intensity. Our own Sun's Schwabe sunspot cycle varies slightly, ranging from ten to twelve years and with varying peaks. An examination of the BS Tau phase diagram shows that at the extremes, the star gains and loses about a magnitude over the general range of the general rapid variation.

Starspots have been indicated for other pre-main sequence and T Tauri variables, with coverage up to 50%; cold spots causing variations maximizing at up to a one-third of a magnitude (Alekseev 2006), whereas hot spots due to accretion from a circumstellar disk can cause long-lived spots that change the brightness by 1–3 magnitudes (Petrov 2003). The late-type flare star PZ Mon at its minimum brightness can have a variation in magnitude up to 1.0 magnitude over a 50–60-year cycle (Alekeev and Bondar 2006). Starspot periodicities would be most easily viewed in periodically changing colors, particularly in the *U–B* or *B–V* color ranges (Kolotilov *et al.* 2004), such as those seen in DI Cep. Alekseev (2006) reports spots can also be detected using molecular band spectrophotometry over time. Although some spotted stars have cycles measuring into the decades, most starspot-suspected cycles are measured in mere days.

A better explanation for the periodicity might be a circumstellar disk that periodically and partially occults the star. Such disks can cause up to a three-magnitude decrease in minimum brightness, and it is more common in the earlier spectral types such as that of BS Tau (Petrov 2003). Pinte and Menard's (2004) model of the classical T Tauri star AA Tau indicates that eclipses by the disk can skip a period and the magnitude changes can range up to 1.4 magnitudes. (A classical T Tauri star, or CTTS, as summarized by Appenzeller and Mundt (1989), has a central star surrounded by a disk, showing spectral lines in emission, as opposed to weak T Tauri's that do not have emission.) If the disk is not uniform, it could explain the variations from one cycle to another.

To test the hypotheses of companion star, sunspot cycle, and circumstellar disk, there is the need to measure BS Tau's polarization in infrared and its color, particularly the blue or ultraviolet spectral regimes, at minimum and maximum. Specifically:

- to test for a companion, monitor color during entire cycle; there should be no color or polarization changes;

- to test for a sunspot cycle, monitor color (*U–B* or *B–V*) for changes over the cycle; also, changes in spots can be detected with molecular band spectrophotometry (Alekseev 2006);

• to test for a circumstellar disk, observe linear polarization at minimum and maximum of cycle; the linear polarization should increase at minimum.

5. Conclusions

On the basis of our light curve, the classification for BS Tau should be changed from "Orion Insb" type to "T Tauri (Int)" and falling into the Classical T Tauri (CTTS) regime. BS Tau's brightness over time has an underlying cyclical nature with an period of 5.96 years that could be caused either by a Schwabe-type variation in spot coverage or a partially eclipsing circumstellar disk or companion. The most recent maximum should have been around 2006, the next maximum should be centered around 2012, with BS Tau currently in a minimum period centered around this year, 2009. This would be a good time to begin checking BS Tau's light for polarization and color changes over the cycle to determine characteristics that would depend the cause of the long-term variation.

6. Acknowledgements

The writer wishes to thank: Dr. W. P. Bidelman for guiding the original undergraduate work, the late Dr. Martha Hazen who gave access and instruction to the plate stacks in 1979, and Ms. Alison Doane for allowing me the privilege thirty years later, R. Levrault for photoelectric observations, the Pisgah Astronomy Research Institute for giving access to the Case Western Reserve objective prism plates, and Dr. Amy Lovell and Dr. Rick Williamon for valuable discussions.

References

Alekseev, I. 2006, *Astrophys.*, **49**, 259.
Alekseev, I., and Bondar, N. 2006, *Astron. Astrophys. Trans.*, **25**, 247.
Appenzeller, I., and Mundt, R. 1989, *Astron. Astrophys. Rev.*, **1**, 291.
Bidelman, W. P. 1976, *Bull. Amer. Astron. Soc.*, **8**, 268.
Fadeev, Yu. A. 1972, *Astron. Tsirk.*, **714**, 8.
Fadeev, Yu. A. 1973, *Perem. Zvezdy, Prilozh.*, **1**, 411.
Hoffliet, D. 1935, *Bull. Harvard Coll. Obs.*, **901**, 20.
Horne, J. H., and Baliunas, S. L. 1986, *Astrophys. J.*, **302**, 757.
Ismailov, N. Z. 2005, *Astron. Rep.*, **49**, 309.
Kohoutek, L., and Wehmeyer, R. 1997, *Abh. Hamb. Sternw.*, **11**, 2.
Kolotilov, E. A., Metlov, V. G., Metlova, N. V., and Petrov, P. P. 2004, *Astron. Astrophys. Trans.*, **23**, 185.
Landolt, A. U. 1967, *Astron. J.*, **72**, 1012.

Lasker, B. M., Russel, J. L., Jenkner, H., Sturch, C. R., McLean, B. J., and Shara, M. M. 1996, *The HST Guide Star Catalog Version 1.1*, The Association of Universities for Research in Astronomy, Inc.
Liller, M. H., and Liller, W. 1975, *Astrophys. J., Lett. Ed.*, **199**, L133.
Melnikov, S. Yu., and Grankin, K. N. 2005, *Astron. Lett.*, **31**, 109.
Petrov, P. P. 2003, *Astrophys.*, **46**, 506.
Pinte, C., and Menard, F. 2004, in *The Search for Other Worlds: Fourteenth Astrophysics Conference*, AIP Conference Proceedings, Vol. 713, S. S. Holt, and D. Deming, eds., Melville, NY, American Institute of Physics, p. 123.

Table 1. *B* Magnitude Observations of BS Tau.

Date	*Plate*	*B**	*Date*	*Plate*	*B**
1899 12 9	I 24204	14.4	1937 10 30	RH 7831	15.7
1903 11 28	I 31216	14.4	1937 11 3	BM 696	15.4
1922 11 13	MC 19241	14.9	1937 11 30	RH 7899	15.4
1923 10 17	MC 20151	14.4	1937 12 1	RH 7906	15.8
1924 10 30	MC 21098	14.2	1938 1 6	B 62728	14.4
1926 11 5	MC 22195	15.3	1938 1 20	RH 8044	15.2
1926 12 29	MC 22300	14.7	1938 2 20	B 62845	15
1927 9 29	MC 22725	14	1938 10 25	RH 8542	15.5
1928 2 13	MC 23184	15.4	1938 11 1	RH 8541	15.5
1928 10 14	MA 2321	15.5	1938 11 20	RH 8594	15.5
1928 10 20	MC 23739	15.4	1938 11 25	RH 8608	14.7
1928 11 9	MC 23805	15.3	1938 12 13	RH 8650	15.6
1928 12 5	MC 23862	14.7	1938 12 15	BM 1067	15.3
1929 2 12	MC 24078	15.3	1938 12 22	RH 8667	14.7
1929 10 13	MC 24558	15.5	1939 10 15	RH 9199	15.5
1931 11 4	MC 25729	15.4	1939 11 8	RH 9288	15.2
1932 11 27	RH 4731	14.7	1939 11 15	BM 1739	15.1
1933 12 11	RH 5598	14.2	1939 12 12	RH 9369	14.5
1934 2 6	RH 5738	14.4	1940 1 1	RH 9422	15.4
1935 1 24	RH 6413	13.9	1940 1 2	RH 9425	14.5
1935 2 28	RH 6463	13.8	1940 1 9	B 65049	14.9
1935 10 2	B 60296	14.4	1940 1 29	MC 30768	15.4
1936 2 18	RH 7044	14.2	1940 2 4	BM 2096	14.4
1936 2 23	RH 7063	14.6	1940 2 9	BM 2114	14.3
1936 11 10	RL 1097	15	1940 11 25	MC 31203	14.8
1937 1 16	RL 1184	14.4	1940 12 3	IR 4391	15.3
1937 1 16	RL 1185	14.5	1940 12 31	IR 4501	15.5
1937 2 2	B 61629	16.3	1941 8 25	B 67047	14.8
1937 9 12	B 62515	14.7	1941 11 23	B 67271	14.8

(Table 1 continued on following page)

Table 1. *B* Magnitude Observations of BS Tau, continued.

Date	*Plate*	*B**	*Date*	*Plate*	*B**
1942 8 12	B 67925	15.2	1948 11 7	RH 14835	14.4
1942 9 15	B 68025	14.7	1948 11 27	B 74314	14.7
1942 10 12	IR 6218	15.5	1948 11 29	RH 14850	14.9
1942 10 15	B 68105	14.6	1948 12 28	RH 14882	14.6
1944 8 24	B 69839	15.2	1949 2 18	B 74452	14.3
1944 10 17	IR 7451	15.2	1949 8 29	B 75043	14.9
1944 10 23	IR 7486	15.6	1949 10 19	RH 15170	15.4
1944 12 18	B 70052	14.7	1949 10 20	RH 15173	16.3
1945 2 5	RH 12888	14.9	1949 11 23	B 75162	14.4
1945 10 5	B 71257	15.7	1950 1 14	RH 15238	15.4
1946 10 3	RH 14079	14.7	1950 10 13	RH 15467	14.9
1946 10 5	RH 14086	15.1	1950 11 13	RH 15513	14.4
1946 10 23	B 72119	15.5	1951 1 29	B 75706	15.7
1946 10 29	B 72306	13.8	1951 9 9	RH 15753	15
1946 11 18	RH 14157	14.9	1951 11 29	RH 15793	14.3
1946 12 24	B 72378	15.2	1967 11 6	DNY 86	15.9
1947 1 22	RH 14210	15	1967 12 1	DNY 88	15.9
1947 8 24	B 73086	14.3	1969 1 15	DNB 238	15.3
1948 1 11	RH 14430	14.8	1969 1 15	DNY 156	15.7
1948 1 30	B 73288	13.8	1969 10 19	DNY 201	15.7
1948 9 2	B 74059	14.4	1974 12 6	DNB 865	14.9
1948 10 26	B 74249	14	1978 11 2	DNB 2183	14.1

** Magnitudes are from blue plates, with comparison star magnitudes in Johnson B.*

Table 2. *V* Magnitudes of BS Tau.

Year	*V*	*Source*
1997	13.5	Kohoutek and Wehmeyer
1996	14.4	Lasker *et al.*
1980	14.0	R. Levrault, photoelectric
1980	14.0	L. Krumenaker, photoelectric

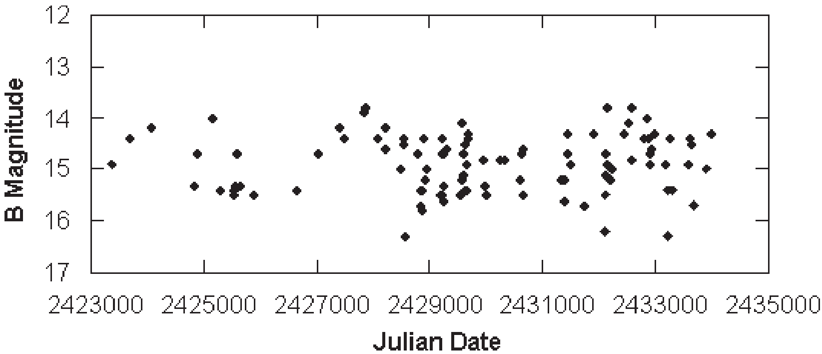

Figure 1. Light curve of BS Tau (1922–1951), using Fedeev comparison stars.

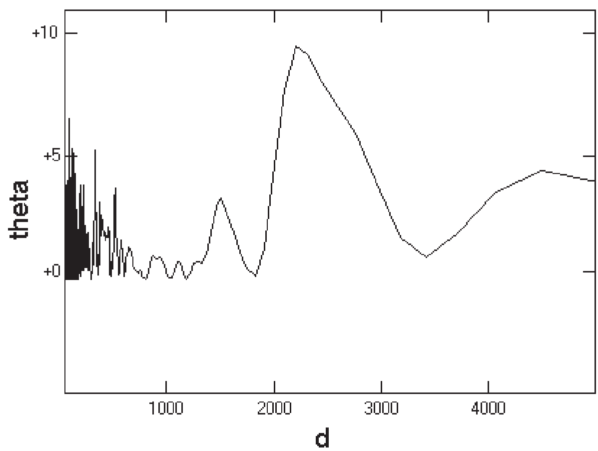

Figure 2. Periodogram created from the 1922–1951observations of BS Tau.

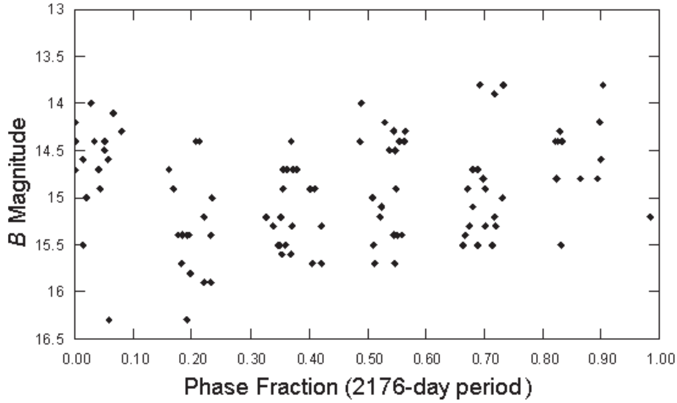

Figure 3. Phase Diagram for BS Tau based on a 2,176-day period.

CX Lyrae 2008 Observing Campaign

Pierre de Ponthière
15 Rue Pre Mathy, Lesve, Profondeville, 5170, Belgium

Jean-François Le Borgne
GEOS (Groupe Européen d'Observations Stellaires), 23 Parc de Levesville, 28300 Bailleau l'Evêque, France

and

Laboratoire d'Astrophysique de Toulouse-Tarbes, Observatoire Midi-Pyrénées (CNRS/UPS), Toulouse, France

F. -J. Hambsch
GEOS (Groupe Européen d'Observations Stellaires), 23 Parc de Levesville, 28300 Bailleau l'Evêque, France

Bundesdeutsche Arbeitsgemeinschaft für Veränderliche Sterne e.V. (BAV), Germany

and

Vereniging Voor Sterrenkunde, Werkgroep Veranderlijke Sterren (VVS), Belgium

Received February 25, 2009; revised May 22, 20009; accepted July 7, 2009

Abstract The Blazhko effect in CX Lyr has been reported for the first time by Le Borgne *et al.* (2007). The authors have pointed out that the Blazhko period was not evaluated accurately due to dataset scarcity. The possible period values announced were 128 or 227 days. A newly conducted four-month observing campaign in 2008 (fifty-nine observation nights) has provided fourteen times of maximum. From a period analysis of measured times of maximum, a Blazhko period of 62 ± 2 days can be suggested. However, the present dataset is still not densely sampled enough to exclude that the measured period is still a modulation of the real Blazhko period. Indeed the shape of the (O–C) curve does not repeat itself exactly during the campaign duration.

1. Introduction

The star CX Lyr is classified in the *General Catalogue of Variable Stars* (GCVS; Samus *et al.* 2008), under number 520124, as an RRab variable star with a period of 0.61664495 day and with minimum and maximum magnitudes of 12.14 and 13.17V. CX Lyr is also identified as GSC 02121-02076 (STScI 2001). According to SIMBAD, CX Lyr is spectral type F4, and the (*B–V*) color index is thus around 0.4.

CX Lyr has been observed sporadically for over one hundred years. In total, fifty-one maxima have been recorded and data are available in the GEOS database (GEOS 2009). From these data, it can be seen that the pulsating period over the last century has decreased at a constant rate. Finally, an apparent Blazhko effect has been reported in CX Lyr for the first time by Le Borgne *et al.* (2007).

2. New CCD observations and data reduction

Hambsch and de Ponthière observed CX Lyr during fifty-nine nights between June 19, 2008 (JD 2454637), and November 12, 2008 (JD2454783). Hambsch's measurements were performed through V and R_c photometric filters with an exposure time of 120 seconds. An ST8 CCD mounted on a C14 at *f*/5.6, located in Hechtel (Belgium), was used for imaging in 3 × 3 binning mode. Image acquisition was done using CCDSOFT software(Software Bisque 2009). After dark and flat field correction the images were analysed with the MUNIWIN software (Motl 2009). The positions and photometric data for the comparison and check stars used are listed in Table 1. The V magnitudes and color indexes were derived from the NOMAD catalogue (Zacharias *et al.* 2009). The color indexes have been obtained as differences between B and V values.

de Ponthière's measurements were performed through a V filter with an exposure time of thirty seconds using a Meade 8-inch LX200GPS at *f*/6.3 and ST7 CCD camera located in Lesve, Belgium. To improve the SNR, groups of four consecutive images were combined using the MAXIMDL software (Diffraction Limited 2004). Aperture photometry was performed using custom software which evaluates the SNR and estimates magnitude errors in accordance with formulae (12) and (13) of Newberry (1991). The variable and comparison star data are listed in Table 2. The V magnitudes of C1 and C2 have been derived from SIMBAD. The color indexes were obtained as differences between B and V values provided in the NOMAD catalogue.

The comparison star C1 was used as magnitude reference, C2 and C3 as check stars. To avoid measurements affected by variable sky conditions, the measurements with an estimated error greater than 0.050 magnitude (SNR < 21) have been discarded.

Hambsch and de Ponthière observed CX Lyr simultaneously on the night of September 1, 2009. From this common observation, it was possible to derive the magnitude offset created by the choice of different comparison stars. This offset has been used to adjust the magnitudes at maximum measured by Hambsch.

The list of measured maxima is provided in Table 3. This table includes an older measurement performed by Maintz (Hübscher, Steinbach, and Walter 2008). Unfortunately, the magnitude at maximum for this measurement cannot be reliably adjusted as a non-standard filter was used for this observation.

3. Period analysis and folded light curve

With the de Ponthière data, a period analysis performed with the ANOVA algorithm of PERANSO (Vanmunster 2007) provided a pulsation period of 0.616703 ± 0.000026 day. The corresponding periodogram is presented in Figure 1a, the small peak at 0.7623 day (1.3107c/d) is a sampling alias. Aliases arise because the interval between measurements and signal period are of the same order. The alias frequency is related to signal one as (f + 1) / 2 = (1.6214 + 1) / 2 = 1.3107, where f = 1 / 0.616703.

The folded light curves of de Ponthière's measurements are presented in Figure 2, with the elements HJD 2454677.5688 + 0.616703 E (i.e., time of first maximum of de Ponthière). This figure clearly shows the existence of a Blazhko effect for this star.

A period analysis with the LOMB-SCARGLE algorithm in PERANSO has revealed side lobes close to the main lobe as shown in Figure 1b. The frequencies of two closer side lobes are, respectively: f1 = 1.606875 and f2 = 1.635417 day^{-1}. An estimation of the Blazhko period can be derived as 2 / (f2 – f1) = 70 days. The ANOVA algorithm reveals also equivalent side lobes but their levels are very weak.

A careful analysis of folded light curves shows that when the maximum is reached with maximal delay in respect to the ephemeris, the magnitude at the preceding minimum is at its lowest value. It was the case for JD 2454758, with a minimum magnitude of 13.37 measured at phase 0.84.

For de Ponthière's measurements, Le Borgne evaluated the times of maxima with a custom algorithm, fitting the measurement curve by a polynomial function whose degree depends on the number and dispersion of points. Hambsch evaluated the maxima from his own observations with the PERANSO program.

A linear regression on all (O–C) values presented in Table 3 provided a new pulsation period of 0.61675 ± 0.000024 day. The (O–C) values were re-evaluated with this new pulsation period. The elements we use for 2008 observations is then:

$$\begin{aligned} HJD = 2454677.5688 &+ 0.61675E \\ \pm 0.0037 &\pm 0.000024E \end{aligned} \qquad (1)$$

The Blazhko period was evaluated by an analysis of the (O–C) value variations with the ANOVA algorithm. The resulting period is 62 ± 2 days. This value is probably more accurate than the value derived previously from the global spectral analysis. Indeed, the spectral analysis did not include the Hambsch observations. For those observations only the times of maxima and their corresponding magnitudes were available. However, it is too soon to announce an accurate Blazhko period for this star. The data cover only 2.5 Blazhko periods with a limited number of observations. It is still possible that the period detected here is a variation superimposed on the previously reported potential Blazhko periods of 227 and 128 days (Le Borgne *et al.* 2007), although the time variations of (O–C) and magnitude at maximum shown in Figure 3 leave little doubt.

The (O–C) values as a function of time are presented in Figure 3. The (O–C) values and magnitudes at maximum as a function of Blazhko phase are presented in Figure 4. The Blazhko phases are calculated with the elements 2454677.5688 + 62.0 E.

The curve of the (O–C) shows a slow change for increasing (O–C) values and an abrupt change for decreasing values. We can see that the periodic variations of (O–C) and magnitude are obviously synchronous and more or less in phase. The (O–C) values and magnitudes reach their minimum at the same time. But the magnitude maximum is reached while the (O–C) values are still increasing.

The Blazhko period can be divided into three sub-periods of more or less equal durations:

- (O–C) value and magnitude increase.
- (O–C) value increases and magnitude decreases.
- (O–C) value decreases abruptly and magnitude decreases.

The behavior for UX Tri as reported by Achtenberg and Husar (2006), presented in Figure 5, is opposite to the present findings. An abrupt variation for increasing (O–C) values and a slow change for decreasing values is the usual behavior of Blazhko (O–C) phase diagrams. The magnitude and (O–C) minima occur at the same phase, but the behavior for three sub-periods (of unequal duration) is as follows

- (O–C) value increases abruptly and magnitude increases.
- (O–C) value decreases and magnitude increases.
- (O–C) value decreases and magnitude decreases.

It is clear that although both CX Lyr and UX Tri have a strong Blazhko effect, they have different characteristics. Both variations of magnitude at maximum are close to sinusoidal and (O–C) are reversed. The behavior of UX Tri is typical of the Blazhko effect.

Further observations are required to be sure that the measured periodic variations are not a simple oscillation superimposed on the main Blazhko variation. With new observations, it will be possible to remove this doubt and obtain a better value of the Blazhko period.

4. Acknowledgements

We would like to thank Jacqueline Vandenbroere (GEOS) for her suggestions at the beginning of this CX Lyr campaign. Thanks to Dieter Husar for authorizing publication of the UX Tri figures. This work has made use of the SIMBAD database, operated at CSD, Strasbourg, Strasbourg, France, and the GEOS RR Lyr database.

References

Achterberg, H., and Husar, D. 2006, *Open European J. Var. Stars*, **41**, 1 (http://arxiv.org/abs/astro-ph/0607503).

Diffraction Limited 2004, MAXIM DL image processing software, http://www.cyanogen.com

Groupe Européen d'Observation Stellaire (GEOS) 2009, GEOS RR Lyr Database, http://rr-lyr.ast.obs-mip.fr/

Hübscher, J., Steinbach, H. -M., Walter, F. 2008, *Inf. Bull. Var. Stars*, No. 5830.

Le Borgne, J. F., *et al.* 2007, *Astron. Astrophys.*, **476**, 307.

Motl, D. 2009, C-MUNIPACK V1.1.24 software, http://sourceforge.net/projects/c-munipack

Newberry, M. 1991, *Publ. Astron. Soc. Pacific*, **103**, 122.

Samus, N. N., *et al.* 2008, *Combined General Catalogue of Variable Stars* (GCVS), http://www.sai.msu.su/groups/cluster/gcvs/gcvs/

Software Bisque 2009, CCDSOFT V5, http://www.bisque.com/products/ccdsoft/

Space Telescope Science Institute (STScI) 2001, *The Guide Star Catalog*, Version 2.2 (VizieR On-line Data Catalog: I/271), STScI, Baltimore.

Vanmunster, T. 2007, PERANSO, period analysis software, http://www.cbabelgium.com and http://www.peranso.com

Zacharias, N., Monet, D., Levine, S., Urban, S., Gaume, R., and Wycoff, G. 2009, The Naval Observatory Merged Astrometric Dataset (NOMAD), http://www.usno.navy.mil/USNO/astrometry/optical-IR-prod/nomad/

Table 1. Comparison star data for CX Lyr (F. -J. Hambsch observations).

	Identification	*R.A. (2000)* h m s	*Dec. (2000)* ° ′ ″	*V*	*B–V*
C1	GSC 2121-1980	18 51 14.24	28 43 37.88	12.74	0.55
C2	GSC 2121-2842	18 51 07.00	28 45 12.88	13.0	0.70

Table 2. Comparison star data for CX Lyr (P. de Ponthière observations).

	Identification	*R.A. (2000)* h m s	*Dec. (2000)* ° ′ ″	*V*	*B–V*
C1	GSC 2121-2818	18 51 51.49	28 49 08.11	10.58	0.58
C2	GSC 2121-2053	18 51 16.38	28 51 16.38	10.48	0.49
C3	GSC 2121-1980	18 51 14.24	28 43 37.88	12.74	0.55

Table 3. List of measured maxima of CX Lyr.

Maximum HJD	*Error*	*O–C (day)*	*E*	*Observer*
2452362.4056	0.0004	–0.0019	–511	G. Maintz
2454637.4929	0.0026	0.0138	–65	F. -J. Hambsch
2454661.5051	0.0020	–0.0278	–26	F. -J. Hambsch
2454677.5688	0.0018	0.0000	0	P. de Ponthière
2454685.5930	0.0020	0.0063	13	P. de Ponthière
2454692.3815	0.0013	0.0104	24	P. de Ponthière
2454708.4197	0.0019	0.0127	50	P. de Ponthière
2454711.5050	0.0040	0.0142	55	P. de Ponthière
2454719.5020	0.0050	–0.0068	68	P. de Ponthière
2454724.4300	0.0040	–0.0129	76	P. de Ponthière
2454729.3630	0.0030	–0.0140	84	P. de Ponthière
2454750.3518	0.0016	0.0048	118	P. de Ponthière
2454758.3736	0.0012	0.0086	131	P. de Ponthière
2454774.4100	0.0030	0.0092	157	P. de Ponthière
2454782.3940	0.0030	–0.0248	170	P. de Ponthière

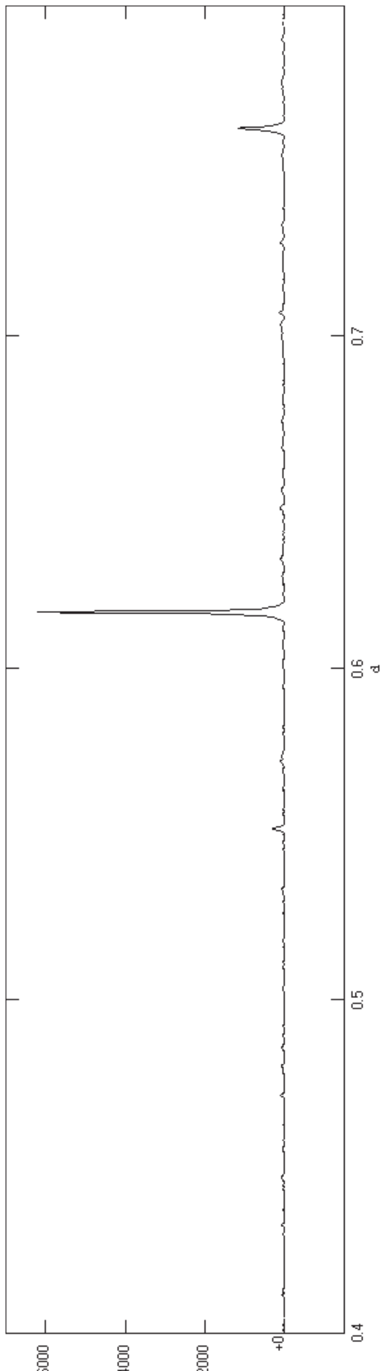

Figure 1a. CX Lyr Periodogram (PERANSO—ANOVA algorithm).

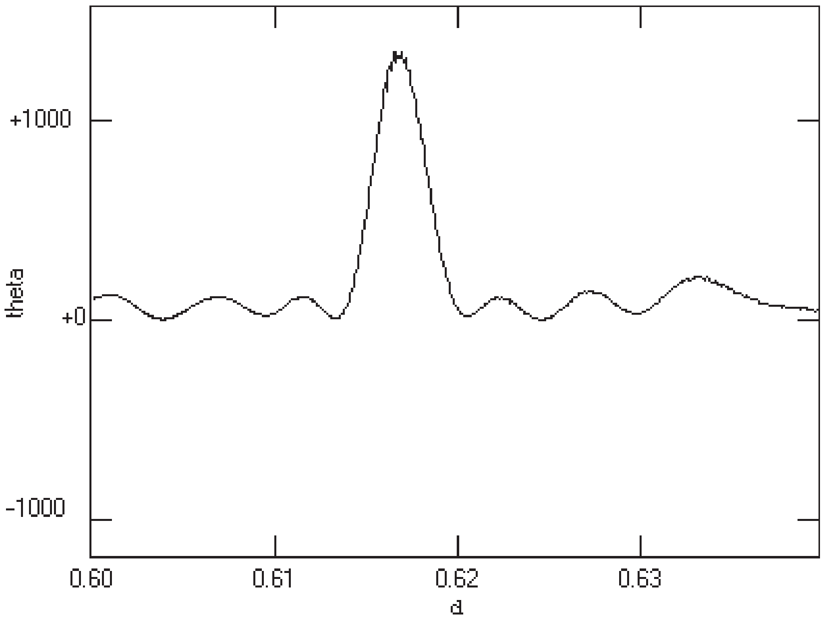

Figure 1b. CX Lyr Periodogram (PERANSO—LOMB-SCARGLE algorithm).

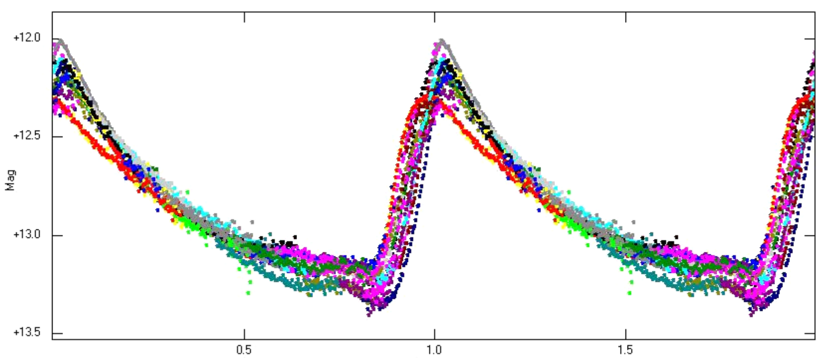

Figure 2. CX Lyr folded light curves (de Ponthière data).

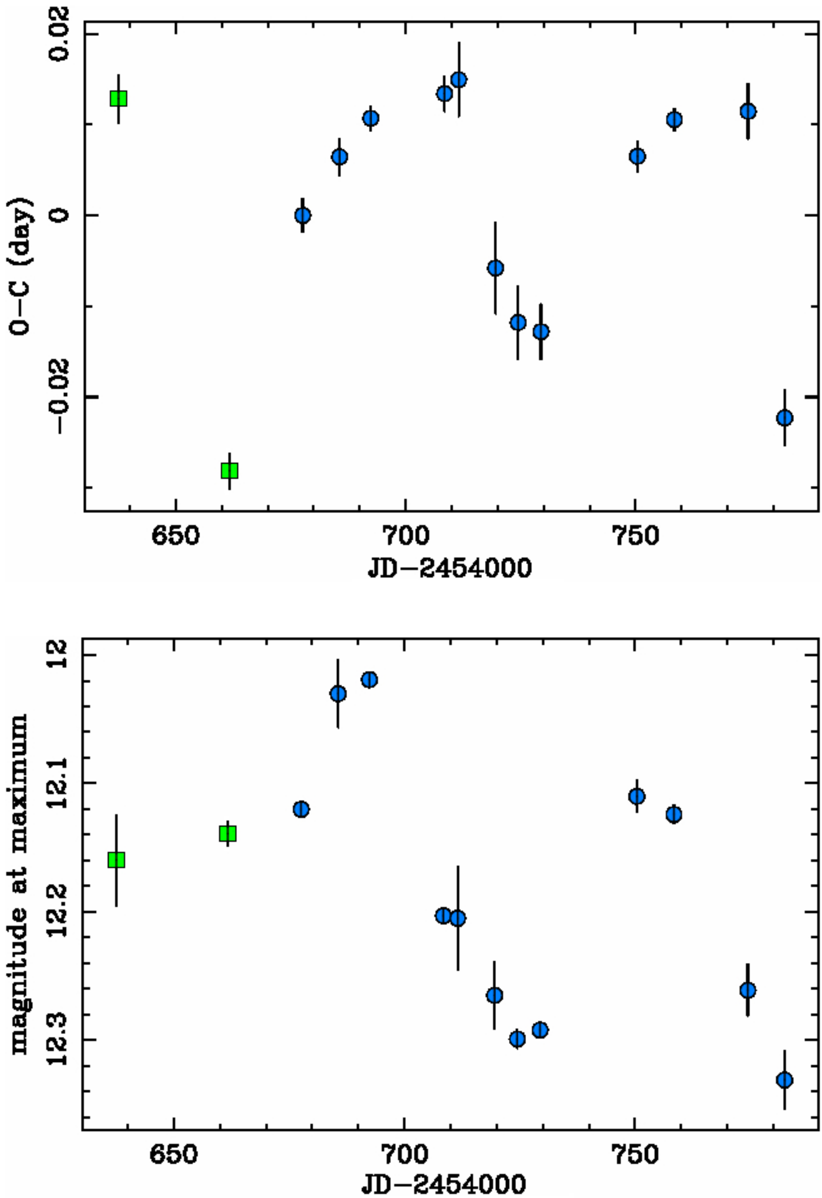

Figure 3a, 3b. CX Lyr (O–C) (top) and magnitude (bottom) at maximum diagram. Symbols correspond to observers: F.-J. Hambsch (squares) and P. de Ponthière (circles).

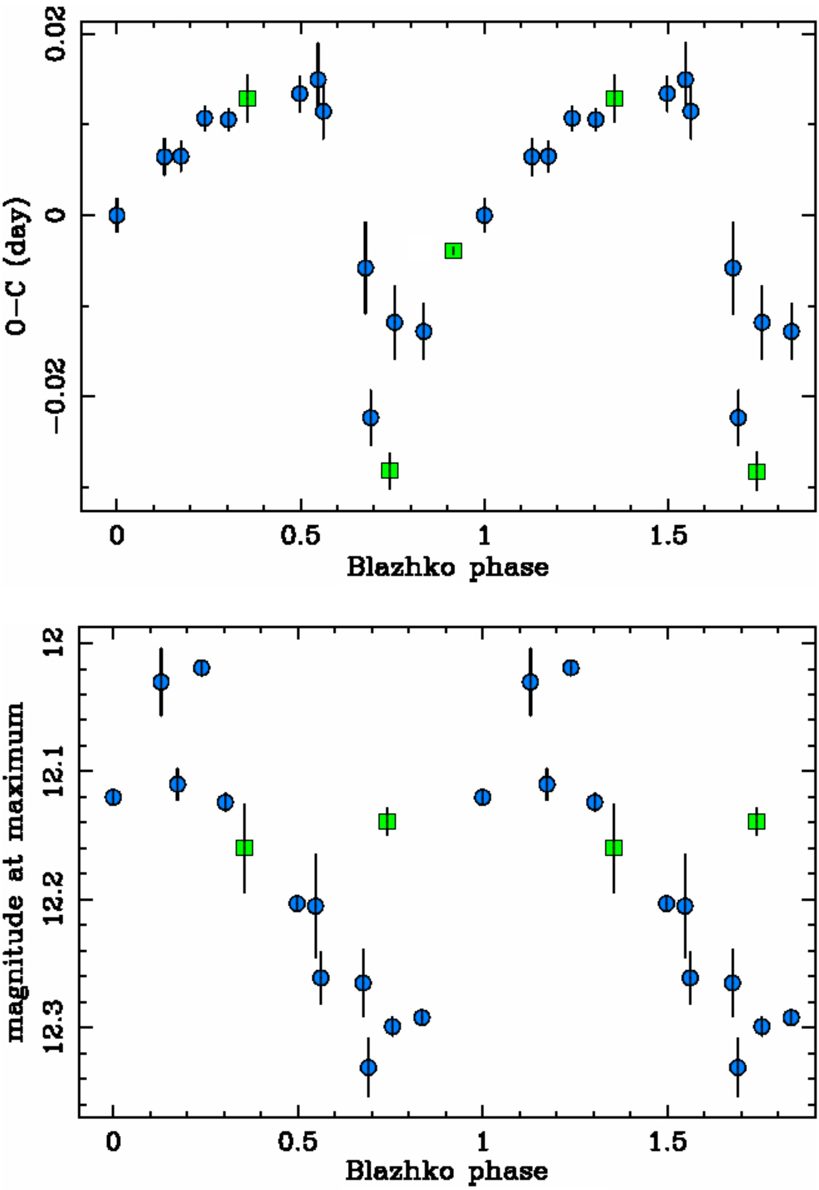

Figure 4a, 4b. CX Lyr (O–C) (top) and magnitude (bottom) at maximum versus Blazhko phase. Symbols correspond to observers: F.-J. Hambsch (squares) and P. de Ponthière (circles).

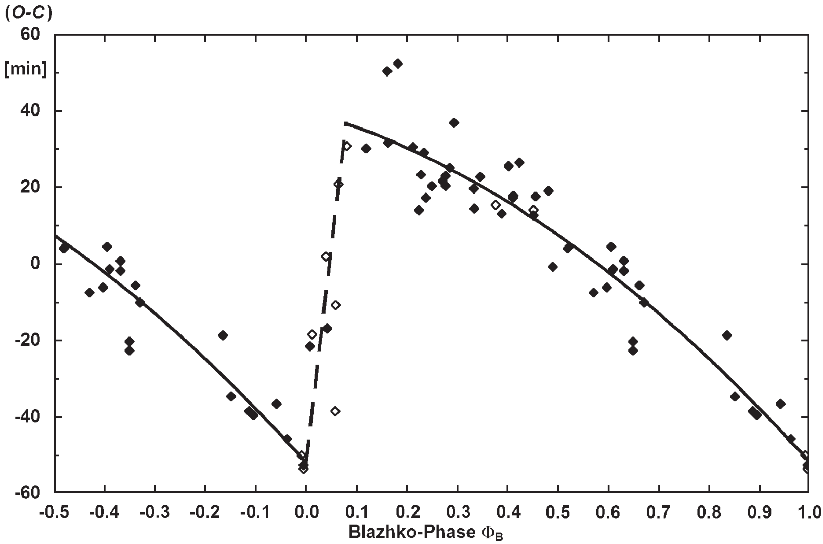

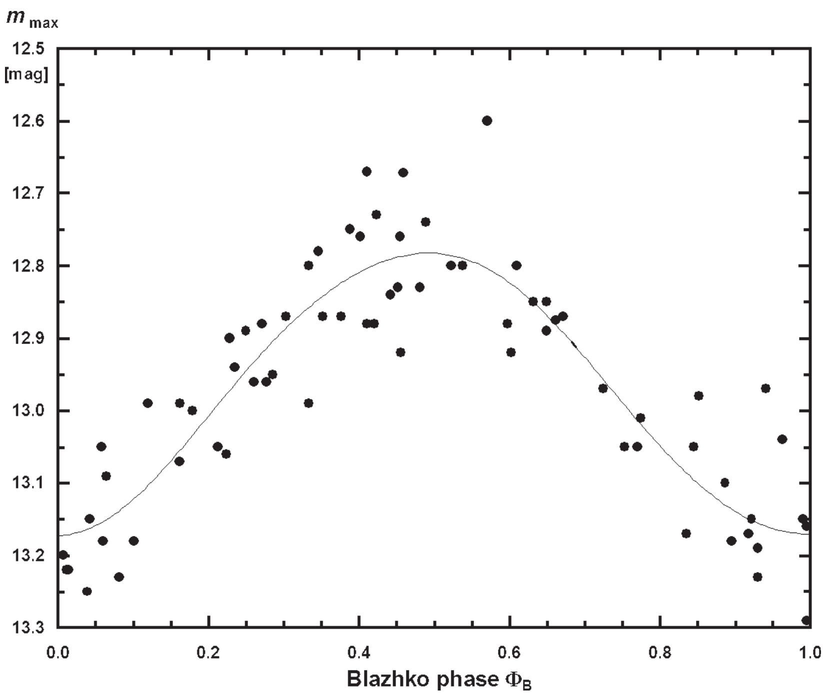

Figure 5a, 5b. UX Tri (O–C) (top) and magnitude (bottom) at maximum versus Blazhko phase.

Deciphering Multiple Observations of V480 Lyrae

Jerry D. Horne
3055 Lynview Drive, San Jose, CA 95148

Based on a paper presented at the joint meeting of the Society for Astronomical Sciences and the American Association of Variable Star Observers, held in Big Bear Lake, CA, May 19–21, 2009

Received June 3, 2009; revised August 18, 2009; accepted September 1, 2009

Abstract Existing and new observations of the variable V480 Lyr are examined and analyzed. This study utilized a 25-cm Schmidt-Cassegrain Telescope (SCT) to observe multiple cycles of the star and obtain new *BVRI*-band photometry. These new observations, when combined with other published observational data, allowed the determination of multiple period values for the variable. From this multi-period behavior, and from an examination of other intrinsic parameters, there is evidence that V480 Lyr could be classified as an RV Tauri type star, which differs from earlier classifications.

1. Introduction

V480 Lyr is listed in the *General Catalogue of Variable Stars* (GCVS; Sternberg Astron. Inst. 2009) as an eclipsing binary (β Lyr type). This designation is based on the initial work of H. Gessner (Gessner 1983), who produced a partial light curve and postulated that the variable was an EB type with a period of approximately 100 days. The Gessner light curve is quite sparse and is shown in Figure 1. The initial demonstration phase of the Robotic Optical Transient Search Experiment (ROTSE 1) from 1998 produced a *V*-band set of data for V480 Lyr that was interpreted as the variable being a Cepheid, with a period of 44.5 days (Akerlof *et al.* 2000). This interpretation has been repeated in several other publications (Samus *et al.* 2003; Schmidt *et al.* 2007). Analysis of subsequent ROTSE data and new observations of this star by the author in 2007 and 2008 called into question the accuracy of this interpretation and period.

2. Observations

All observations by the author were made using a Meade LX200 10-inch (0.25m) telescope, with a Starlight Xpress MX 716 CCD camera, which has a 550 × 720 pixel array. One-minute exposures were taken at an *f*-ratio of 6.3 (for an effective field of view of approximately 12 × 16 arc minutes) with standard *BVRI* photometric filters. Five contiguous one-minute exposures were averaged to produce a single data point during the time-series observations.

Typical seeing conditions for this low-altitude site were between 3.5 and 4.5 arc seconds FWHM for each image. The air mass for observations ranged from 1.01 through 1.45. All exposures were dark current- and bias-subtracted, and also flat-fielded (using twilight sky flats) according to established procedures. The software tool AIP4WIN (Berry and Burnell 2000) was utilized to make photometric measurements.

The *B, V, I,* and *R* photometric data were calibrated with measurements taken from Tycho observations of comparison and field stars (Høg *et al.* 2000) corrected to the Johnson-Cousins system. Zero points were then determined from the comparison star photometry and applied to photometry of V480 Lyr using AIP4WIN, to produce standardized *B–V*, *V–R*, and *V–I* measurements. The calculated photometric error of observations of the variable star was at or below 0.03 magnitude in all bands.

V480 Lyr was observed from JD 2454263.706 to 2454382.608 (2007 June 12 to 2007 October 9) and from JD 2454632.705 to 2454726.632 (2008 June 15 to 2008 September 17).

All exposures of V480 Lyr included two comparison stars, GSC 3130-1721 and GSC 3130-1779, whose *BVRI* magnitudes are shown in Table 1. To ensure that the comparison stars were not variable, the difference between GSC 3130-1721 and GSC 3130-1779 was also measured for each exposure. The standard deviation of the *V*-band magnitude difference of these two comparison stars over all observations was found to be 0.017 magnitude.

The position determined for V480 Lyr was R.A. (2000.0) $18^h\,40^m\,23^s$, Dec. (2000.0) +43° 56' 21", based upon the reference coordinates in the *USNO-A2.0 Catalog.* It very closely matches the position generated from the SIMBAD website (FK5 2000.0 coordinates: R.A. $18^h\,40^m\,23^s$, Dec.+43° 26' 22" or the coordinates in the GCVS.

3. Analysis

Inspection of the 2007 and 2008 observations by the author (Figure 2) shows an alternating pattern of shallow and deep minima for this variable. This pattern is also apparent from an examination of additional data on V480 Lyr from the ROTSE project from JD 2452473 through 2452706 (2002 17 July to 2003 9 March) shown in Figure 3 (available through the Northern Sky Variability Survey, Woźniak 2004). The light curve of V480 Lyr clearly is not that of a typical type 1 Cepheid, nor an eclipsing binary, but the alternating pattern of minima, together with the varying depth of shallow minima, may indicate that V480 Lyr may be a RV Tauri-type star.

There are a number of published papers on RV Tauri stars and their respective behavior. In general, the visual light curves of RV Tauri stars have alternating deep and shallow minima, and have periods between 30 and 150 days (Sterken and Jaschek 1996). Pollard *et al.* (1996) list a number of characteristics for determining a star's inclusion in the RV Tauri class of variable stars. While Pollard *et al.* list a total of nine characteristics, some are only applicable to their comparison of a group of RV Tauri stars. Hence, the applicable characteristics to a single star, and this paper, can be summarized as follows:

a) there are alternating deep and shallow minima in the light and color curves;

b) secondary minima depths are more variable than primary minima depths;

c) a mean phase lag exists between the color index and light curves;

d) during extremely deep pulsations, the photometric colors get very blue; and

e) the shorter period RVa subclass exhibits a constant mean magnitude.

RV Tauri stars are known to be giant and supergiant stars, having masses close to that the Sun, spectral types at maximum ranging from early F to late G or early K, and most have low metal abundances. RV Tauri stars are known to be strong infrared sources, and some observations have shown that RV Tauri stars have substantial amounts of dust surrounding them (Wallerstein 2002).

4. Period determination

Because of the alternating shallow and deep minima of RV Tauri stars, the usual method of determining the period from adjacent minima cannot be used. The established convention for these types of stars places the primary, or deeper minimum at phase 0.0, and the secondary, or more shallow, minimum at phase 0.5. Additionally, the "formal," or double, period is defined to be the time between deep minima and the "fundamental," or single, period is time between successive minima.

A well known explanation for the alternating shallow and deep minima of RV Tauri stars (Takeuti and Petersen 1983) suggests a 2:1 resonance exists between the fundamental mode and the first overtone vibrations of an RV Tauri star.

To examine this hypothesis for V480 Lyr, the 2007 and 2008 *V*-band observations by the author, together with the 2002 and 2003 *V*-band ROTSE data, were entered into the software program PERANSO (Vanmunster 2007). Utilizing the PDM (Phase Dispersion Minimization) period determination tool, two periods were readily apparent. One period is the primary ("formal") period at 104.2 ± 0.6 d and is shown in Figure 4. A second significant period is seen at 52.09 ± 0.2 d and is shown in Figure 5. These two periods have a period ratio consistent with the 2:1 resonance model.

While these two periods were pre-whitened, the PDM tool did not reveal any other significant periods beyond those within the margin of error for each period found earlier.

It is noted that the interval between the two primary minima observed in 2007 and in 2008 (Figure 2) is 312 days, or three times the "formal" period of 104 days.

As an additional check on the two periods determined, a self correlation analysis was conducted (Percy *et al.* 2003). This analysis also revealed the 52- and 104-day periods previously determined.

5. Color index and light curves

Light curves for the *BVRI* photometry are shown in Figure 6. Each curve shows the typical primary and secondary minima and is phased to the 104.2-day period. The differences between maxima and the two minima are listed in Table 2. The deepest primary minima occur in the *B* band (1.48 magnitudes), while the deepest secondary minima occur in the *R* band (0.61 magnitude). The ratio of magnitude change in primary to secondary minima is approximately 3:1 for the *B* and *V* bands, and approximately 2:1 for the *R* and *I* bands.

A comparison of mean *V*-band magnitude was made using the ROTSE 1 data and data from the author. For the available data, the V480 Lyr mean magnitude is remarkably constant at *V* mag = 12.68, varying only 0.17 magnitude from this on one instance (circa JD 2451444.00).

The *B–V*, *V–I*, and *V–R* color indices compared with the *V*-band light curve are shown in Figure 7. Examination of these indices shows alternating deeper and shallow minima similar to the *BVRI* light curves, although not at the same amplitude. Also of note is that the *B–V* phase changes precede the *V*-band phase changes by approximately 0.15 phase. The color curves are typically bluer (smaller numbers) at phases around 0.15 and phase 0.60 (on the rising branch of the light curve), which is not unexpected in an RV Tauri star, possibly due to shock-related features. The colors are reddest (largest numbers) at phase around 0.95–1.0, when V480 Lyr is faintest.

6. Conclusions

New photometry of V480 Lyr has been obtained, and when combined with previously published data, shows that V480 Lyr meets many of the published characteristics of an RV Tauri type star. V480 Lyr shows an alternating pattern of shallow and deep minima, and the two periods (104.2 days and 52.09 days) show the characteristic 2:1 ratio for RV Tauri stars. The color indices show a phase lag with the single color curves, the primary minima is very deep in the blue band, and the mean magnitude of all pulsations is constant, at 12.68 magnitude.

The lack of many shallow minima in the 2002 and 2003 ROTSE 1 data may present a problem in being confident in the conclusion that V480 Lyr is a RV Tauri star, although the ROTSE 1 data are essentially *R*-band photometry, and the depths of alternating minima are not as significant at redder wavelengths. Still, additional *V*-band observations will be necessary to provide such confidence or suggest an alternative classification.

7. Acknowledgements

This research has made use of the SIMBAD database, operated at Centre de Données astronomiques de Strasbourg, and the GCVS databases, operated by the Sternberg Astronomical Institute, Moscow, Russia. This research has also made use of the website and associated material from various "Variable Stars of the Season" articles from the AAVSO.

References

Akerlof, C., *et al.* 2000, *Astron. J.*, **119**, 1901.

Berry, R., and Burnell, J. 2000, "Astronomical Image Processing Software," version 2.1.0, provided with *The Handbook of Astronomical Image Processing*, Willmann-Bell, Richmond, VA.

Gessner, H. 1983, *Mitt. Veränderliche Sterne*, **9**, 115.

Høg, E. *et al.* 2000, *Astron. Astrophys.*, **355**, L27, http://tdc-www.harvard.edu/catalogs/tycho2.html

Percy, J. R., Hosick, J., and Leigh, N. W. C. 2003, *Publ. Astron. Soc. Pacific*, **115**, 59.

Pollard, K. R., Cottrell, P. L., Kilmartin, P. M., and Gilmore, A. C. 1996, *Mon. Not. Roy. Astron. Soc.*, **279**, 949.

Samus, N. N., *et al.* 2003, *Astronomy Letters*, **29**, 468.

Schmidt, E. G, Langan, S., Rogalla D., and Thacker-Lynn, L. 2007, *Astron. J.*, **133**, 665.

Sterken, C., and Jaschek, C. 1996, *Light Curves of Variable Stars, A Pictorial Atlas*, Cambridge University Press, Cambridge, 96–98.

Sternberg Astronomical Institute 2009, *General Catalogue of Variable Stars*, http://www.sai.msu.su/groups/cluster/gcvs/gcvs/

Takeuti, M., and Petersen J. O. 1983, *Astron. Astrophys.*, **117**, 352.

Vanmunster, T. 2007, PERANSO period analysis software, http://www.peranso.com

Wallerstein, G. 2002, *Publ. Astron. Soc. Pacific*, **114**, 689.

Woźniak, P. R., *et al.* 2004, *Astron. J.,* **127**, 2436, (Northern Sky Variability Survey, http://skydot.lanl.gov/nsvs/nsvs.php)

Table 1. The magnitudes of V480 Lyr comparison stars from observations by the author in 2008.

Comparison Stars	*B*	*V*	*R*	*I*
GSC 3130-1721	11.49 ± 0.03	10.95 ± 0.03	10.67 ± 0.03	10.41 ± 0.03
GSC 3130-1779	13.95 ± 0.03	13.09 ± 0.03	12.88 ± 0.03	12.57 ± 0.03

Table 2. The magnitude differences between the maxima and the primary and secondary minima from *BVRI* photometry of V480 Lyr by the author in 2008.

Band	*Max–Min (Primary)*	*Max–Min (Secondary)*
B	1.48	0.42
V	1.41	0.50
R	1.09	0.61
I	0.95	0.57

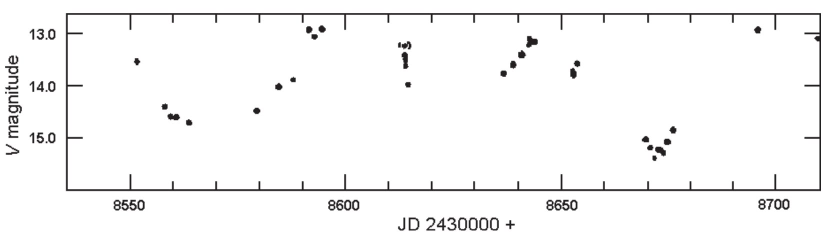

Figure 1. An early light curve for V480 Lyr from Gessner (1983).

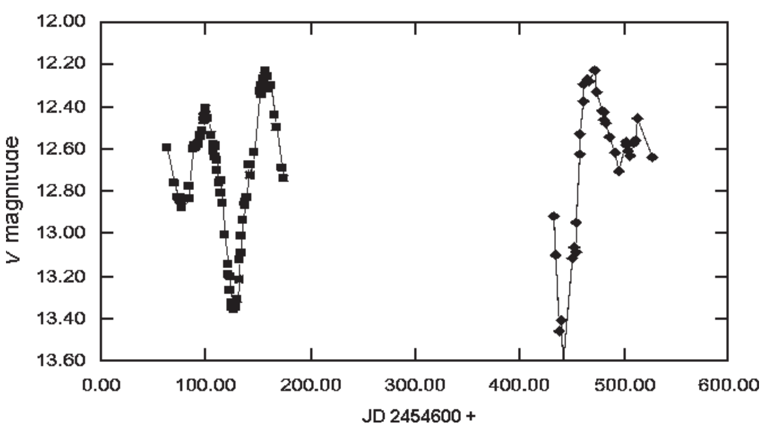

Figure 2. The *V* magnitude of V480 Lyr from observations by the author in 2007 (squares) and 2008 (diamonds).

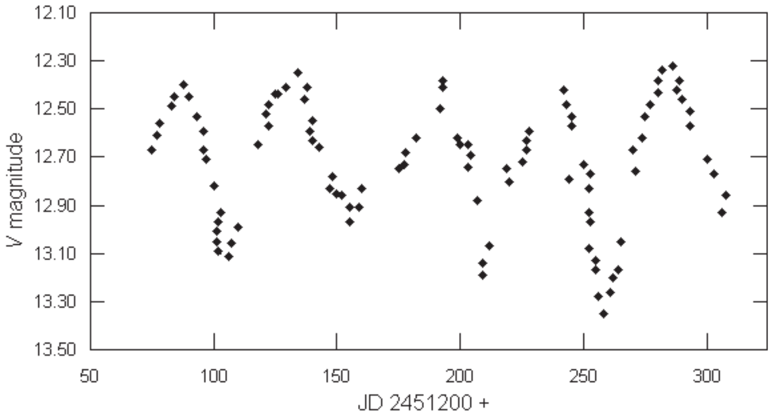

Figure 3. The *V* magnitude of V480 Lyr in 2002 and 2003 from the Northern Sky Variability Survey (Woźniak 2004).

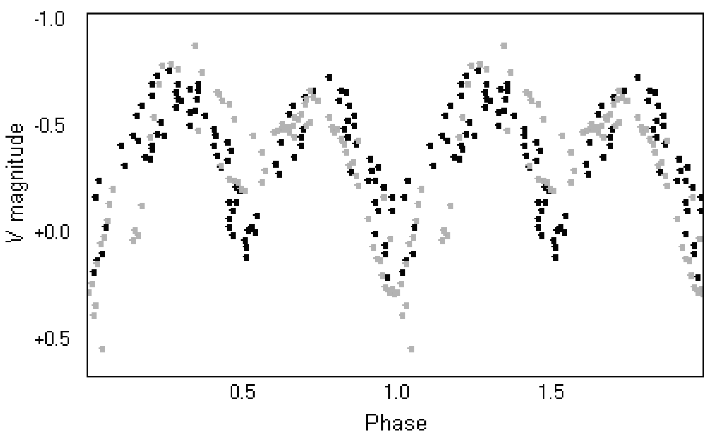

Figure 4: The *V* data for V480 Lyr phased with the primary (formal) 104.2-day period. These data are from observations by the author in 2007 and 2008 (gray dots), and from the Northern Sky Variability Survey in 2002 and 2003 (black dots).

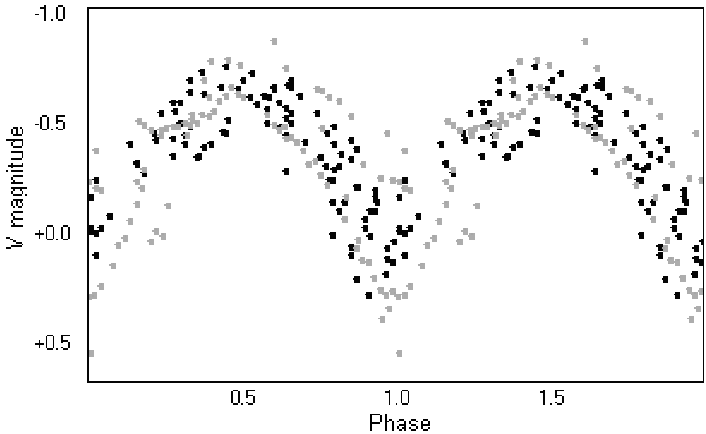

Figure 5: The *V* data for V480 Lyr phased with the second significant period of 52.09 days. These data are from observations by the author in 2007 and 2008 (gray dots), and from the Northern Sky Variability Survey in 2002 and 2003 (black dots).

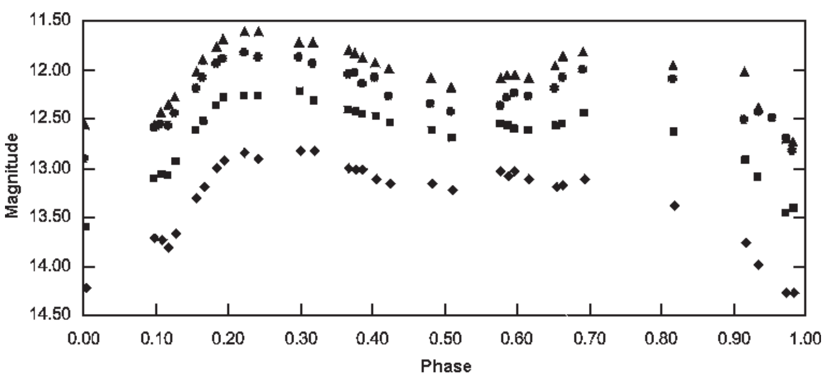

Figure 6. The new photometry of V480 Lyr from observations by the author in 2008: *B* (diamonds), *V* (squares), *R* (dots), and *I* (triangles).

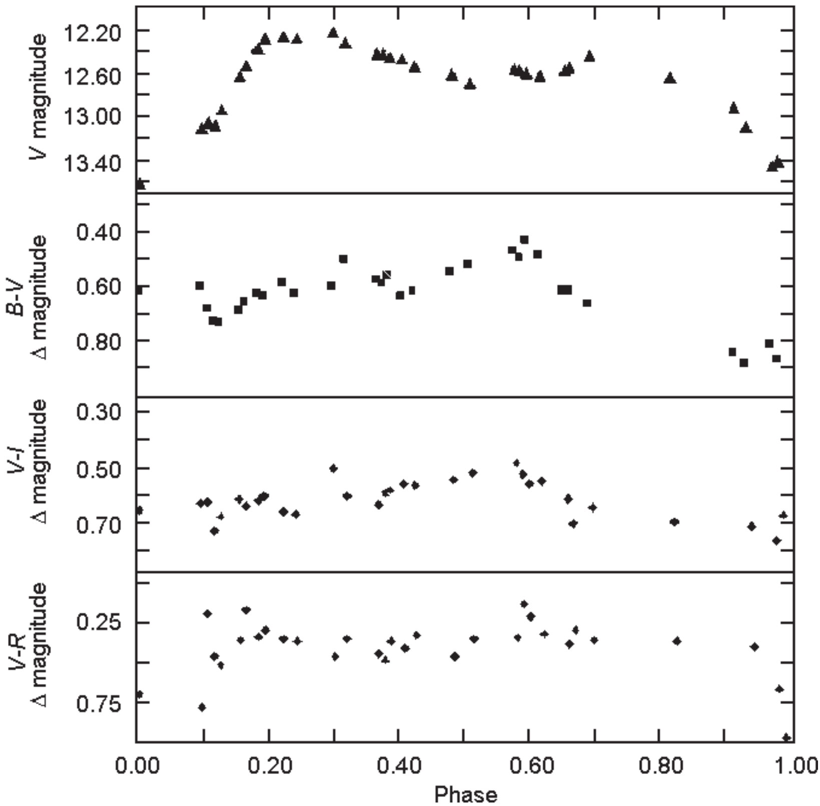

Figure 7. New photometry of V480 Lyr from the author in 2008, comparing the *V* light curve with the *B–V*, *V–I*, and *V–R* color indices.

VZ Librae: an Eclipsing Contact Binary in a Ternary System

Michel Bonnardeau
116 Jonquille Arzelier, 38650 Chateau-Bernard, France

Received July 13, 2009; Revised August 24, 2009; accepted September 3, 2009

Abstract Time series of the eclipsing contact binary VZ Lib are reported and times of minima (ToM) of the eclipses are measured. This system has a third component. From the O–C analysis of the observed ToM and of those in the literature, the orbital parameters of the third body can be derived: the orbital period is 34.8 years and the inclination is 11.5°.

1. Introduction

VZ Librae is an eclipsing contact binary system with a period of 8.6 hours (W UMa type) in a triple system. The third star was observed spectroscopically by Lu *et al.* (2001) with a relative flux of 0.2. Zola *et al.* (2004) fitted the light curve with a relative flux of 0.048 (in *V*), and D'Angelo *et al.* (2006) observed by spectroscopy a flux of about the same value (0.045). Ruciński *et al.* (2007) attempted to resolve the third star with adaptive optics (resolution down to 0.07") but they came up with a negative result.

The parallax of VZ Lib is 4.92±1.96m", as measured by Hipparcos (Perryman *et al.* 1997). The distance is then 203±81pc. According to Szalai *et al.* (2007) the distance is 171±8 pc.

2. Observations

I observed VZ Lib with a 203mm Schmidt-Cassegrain telescope, Johnson *V* and *B* filters, and a SBIG ST7E camera (KAF401E CCD) at my amateur MBCAA Observatory. In 2007, most of the observations were done by observing with the *V* and *B* filters. In 2008–2009, only the *V* filter was used. The exposure durations were 60 seconds for the *V* images and 200 seconds for the *B* images:

- 2007: 4 sessions, 116 *V* images, 62 *B* images;
- 2008: 7 sessions, 799 *V* images;
- 2009: 3 sessions, 363 *V* images.

For the differential photometry, the comparison star used was TYC 6184-1101-1 with *B* = 9.944 and *V* = 9.450 (computed from the Tycho magnitudes owing to Mamajek *et al.* 2002, 2006). All the data are in the AAVSO International Database, observer code BZU. An example of a light curve is given in Figure 1.

The color may be considered as constant, with *B–V* = 0.617 ± 0.022 (transformed).

3. Modeling the eclipsing binary with BINARY MAKER 3

The 2008 measurements were folded with the published period of the contact binary (the 2007 and 2009 measurements were not included as the period seems to vary, see below). I fit the resulting phase plot with BINARY MAKER 3, a software program for the study of binary stars (Bradstreet and Steelman 2004).

With the parameters of Zola *et al.* (2004), I achieved a good fit to my data (and also those from the ROTSE-1 (Woźniak *et al.* 2004) and ASAS-3 (Pojmański 2002) surveys, see below). The phase plot with the synthetic light curve is in Figure 2. With the parameters of Szalai *et al.* (2007) I also achieved a good fit although they are somewhat different of those of Zola *et al.* (2004), e.g. third light (as a fraction of the system light flux) of 0.2 instead of 0.043, mass ratio of 0.33 instead of 0.255.

I observed eight minima and I timed them by fitting with the synthetic light curve. These times of minima are, along with twenty-five others from the literature, listed in Table 1.

The ROTSE-I/NSVS survey observed VZ Lib in 1999 and 2000. These measurements were folded with the derived period and two phase plots were obtained for the two seasons. I fitted them by hand with the BINARY MAKER 3 synthetic light curve and I obtain two times of minima. These ToM are then not determined from the observation of individual minima, but each of them is rather an average over the season. Figure 3 is an example of a phase plot with the 1999 observations. I did the same with the ASAS-3 survey (Pojmański 2002) to obtain five ToM for 2001–2004. All these ToM are listed in Table 2.

4. Analysis

I derived the ephemeris for the eclipses of the contact binary and the orbital parameters of the third body the following way:

- Section 5, below: I obtained a preliminary ephemeris for the eclipses by fitting the ToM with a linear function. I then derived an O–C diagram with the difference between the observations and this preliminary ephemeris;

- Section 6, below: I fitted the O–C diagram with the equations from Kepler's laws, obtaining a preliminary determination of the orbital parameters;

- Section 7, below: I corrected the observed ToM with the light-travel times. A new ephemeris for the eclipses was then obtained, and a new O–C diagram was derived, the same way as in Section 5.

I then fitted the new O–C diagram with Kepler's equations, obtaining a new determination of the orbital parameters, the same as in Section 6.

I obtained a final ephemeris for the eclipses (with the light-travel time effect removed) and a final determination of the orbital parameters for the third star iteratively by repeating the above several times.

5. Preliminary determination of the ephemeris for the eclipses (iteration 0)

I made a preliminary determination of the period and origin of eclipses of the contact binary from the times of minima of Table 1 the following way:

- I started from my 2008 observations, using an already published period for the cycle count, determining the ephemeris with a least squares method;
- I included the ToM from 2007 and 2009, obtaining a more accurate ephemeris;
- I continued with more ToM, always checking that there is no cycle ambiguity, obtaining smaller and smaller uncertainties;
- When I used all the data of Table 1, I gave some heavy weight to the lone 1940 measurement (and a weight of 1 to all the others).

The resulting preliminary ephemeris for the secondary minima is then:

$$HJD(E) = 2454644.4323(10) + 0.35825792(10)\,E \tag{1}$$

where the uncertainties also reflect different values of the 1940 weight.

The difference between the observed ToM (of Table 1 and of Table 2) and the above ephemeris is the O–C diagram of Figure 4.

6. Preliminary determination of the parameters of the third body (iteration 0)

The O–C diagram of Figure 4 shows variations with an amplitude of about 50 minutes. This is considered to arise from the light-travel time effect in the ternary system. The period appears to be about 33 years.

The light-travel time effect can be computed from Kepler's laws. When the eclipse minima are observed on Earth, they are delayed by:

$$LTT = \frac{-r\,sin(i)}{c}\sin(\phi+\omega) + \frac{a\,e\,sin(i)}{c}\sin(\omega) \tag{2}$$

where ω is the periastron longitude (from the node line), *a* the semi-major axis, *i* the inclination, *e* the eccentricity, *c* the velocity of light, and:

$$r = \frac{a(1-e^2)}{1+e\,cos(\phi)} \tag{3}$$

$$\phi = 2\,atan\left[\sqrt{\frac{1+e}{1-e}}\;tan\left[\pi\frac{t-t_0}{P} + \frac{\sqrt{1-e^2}}{2(1+e\,cos(\phi))}\,e\,sin(\phi)\right]\right] \quad (4)$$

with t the time, t_0 the time of passage at periastron and P the period.

I fitted the O–C diagram with LTT using a "Monte Carlo" algorithm. For the five parameters to be determined, I considered the ranges of possible values given in Table 3.

The Monte Carlo algorithm works the following way:

- 1,000,000 sets of the five parameters are generated randomly, within their respective ranges;
- the set that gives the best fit to the observations of Table 1 and Table 2 is retained. To determine how good a fit is, the uncertainties on the O–C measurements are used as weights: the larger the uncertainty, the less the measurement is taken into account;
- the above process is repeated ten times so that ten sets of best fitting parameters are obtained;
- the adopted values are the averages of the ten sets and, as the uncertainties, the standard deviations.

The resulting parameters are given in Table 4 and the O–C diagram with the fit is the solid line in Figure 4.

7. Iterative determination of the ephemeris and of the orbital parameters

I used the above determination of the orbital parameters to correct the observed times of minima for the light-travel times. A new ephemeris for the period of the contact binary was then obtained the same way as in Section 5. A new O–C diagram was also derived and a new Kepler's solution was obtained the same way as in Section 6.

The above process was repeated a few times. It converged quickly. It also became independent of the weight given to the 1940 measurement (this can be set to 1). The resulting ephemeris for the secondary eclipses of the contact binary (with the light-travel time effect removed) is:

$$HJD(E) = 2454644.4321(7) + 0.35825789(2)\,E \quad (5)$$

and the orbital parameters of the third body are in Table 5, with the O–C diagram shown in Figures 5 and 6.

8. Discussion

Qian *et al.* (2008) fitted the O–C diagram with a sinusoidal function. Their Figure 2 shows a period of about 35,000 cycles, which looks about the same as the period of 34.8 years I obtained. However, they reported a period half that, 17.1 years, with which my results are not in agreement.

The period *P* is connected to the total mass *M* and to the semi-major axis *a* through:

$$P = \frac{2\,\pi\,a^{1.5}}{\sqrt{GM}} \tag{6}$$

where *G* is the gravitational constant.

According to Zola *et al.* (2004) the mass of the contact binary is: $M_1 + M_2 = 1.480 \pm 0.068 + 0.378 \pm 0.034 = 1.858 \pm 0.102\,M_\odot$.

The mass M_3 of the third star can then be computed as a function of the inclination and the result is shown Figure 7. M_3 is sharply dependent upon the inclination, allowing *i* to be constrained to i = 11.5° with an uncertainty of about 1°.

According to Szalai *et al.* (2007) the mass of the contact binary is $M_1 + M_2 = 1.06 + 0.35 = 1.41\ M_\odot$, and of the third star is $M_3 = 0.90$.

With my parameters, the value of the inclination is in the same range as above.

The semi-major axis is then a = 15 AU, which corresponds to an angular distance of 0.09".

The orbital plane of the eclipsing contact binary is not at all in the orbital plane of the third star. This suggests that the contact binary did not form along with the ternary system. The fairly elongated orbit (e = 0.30) may not favor a common origin either.

References

Bradstreet, D. H., and Steelman, D. P. 2004, BINARY MAKER 3, Contact Software.

Claria, J. J., and Lapasset, E. 1981, *Inf. Bull. Var. Stars*, No. 2035.

D'Angelo, C., van Kerkwijk, M. H., and Ruciński, S. M. 2006, *Astron. J.*, **132**, 650.

Krajci, T. 2006, *Inf. Bull. Var. Stars*, No. 5690.

Lu, W., Ruciński, S. M., and Ogłoza, W. 2001, *Astron. J.*, **122**, 402.

Mamajek, E. E., Meyer, M. R., and Liebert, J. 2002, *Astron. J.*, **124**, 1670.

Mamajek, E. E., Meyer, M. R., and Liebert, J. 2006, *Astron. J.*, **131**, 2360.

Ogłoza, W., Niewiadomski, W., Barnacka, A., Biskup, M., Malek, K., and Sokolowski, M. 2008, *Inf. Bull. Var. Stars*, No. 5843.

Perryman, M. A. C., European Space Agency Space Science Department, and the Hipparcos Science Team 1997, *The Hipparcos and Tycho catalogues*, ESA SP-1200, ESA Publications Division, Noordwijk, The Netherlands.
Pojmański, G. 2002, *Acta Astron.*, **52**, 397.
Qian, S. B., Liao, W. P., Liu, L., Yuan, J. Z., He, J. J., Zhu, L. Y., Dai, Z. B., and Zhang, J. 2008, *New Astron.*, **13**, 98.
Ruciński, S. M., Pribulla, T., and van Kerkwijk, M. H. 2007, *Astron. J.*, **134**, 2353.
Samolyk, G. 2009, *J. Amer. Assoc. Var. Star Obs.*, **37**, 44.
Szalai, T., Kiss, L. L., Mészáros, S., Vinkó, J., and Csizmadia, S. 2007, *Astron. Astrophys.*, **465**, 943.
Woźniak, P. R., *et al.* 2004, *Astron. J.*, **127**, 2436.
Zejda, M., Mikulasek, Z., and Wolf, M. 2006, *Inf. Bull. Var Stars*, No. 4751.
Zola, S., *et al.* 2004, *Acta Astron.*, **54**, 299.

Table 1. VZ Lib times of minima.

Date	*ToM*	*Uncertainty*	*I/II*	*Reference*
1940	2429645.010		I	Tsessevich (1954), reported by Claria and Lapasset (1981)
1980	2444366.7339		II	Claria and Lapasset (1981)
1980	2444408.6509		II	Claria and Lapasset (1981)
1981	2444698.8448		II	Claria and Lapasset (1981)
1981	2444787.5154		I	Claria and Lapasset (1981)
1981	2444788.5901		I	Claria and Lapasset (1981)
1981	2444789.6654		I	Claria and Lapasset (1981)
1981	2444790.5608		II	Claria and Lapasset (1981)
1991	2448500.3370	0.0001	II	Perryman *et al.* (1997)
2003	2452725.4345	0.0001	I	Qian *et al.* (2008)
2003	2452725.6135	0.0002	II	Qian *et al.* (2008)
2003	2452726.5097	0.0001	I	Qian *et al.* (2008)
2003	2452727.4050	0.0002	II	Qian *et al.* (2008)
2003	2452727.4047		II	Zola *et al.* (2004)
2003	2452727.5847	0.0003	I	Qian *et al.* (2008)
2003	2452730.6304	0.0004	II	Qian *et al.* (2008)
2004	2453189.0102		I	Szalai *et al.* (2007)
2005	2453438.8952	0.0003	II	Krajci (2006)
2005	2453450.5387	0.0004	I	Zejda *et al.* (2006)
2005	2453509.8297	0.0006	II	Ogłoza *et al.* (2008)
2005	2453511.6204	0.0010	II	Ogłoza *et al.* (2008)
2005	2453511.7985	0.0021	I	Ogłoza *et al.* (2008)
2005	2453517.7113	0.0013	II	Ogłoza *et al.* (2008)

(Table 1 continued on following page)

Table 1. VZ Lib times of minima, continued.

Date	ToM	Uncertainty	I/II	Reference
2007	2454164.3650	0.0005	II	Qian *et al.* (2008)
2007	2454233.502	0.0015	II	This paper
2007	2454301.3905	0.0020	I	This paper
2008	2454539.6335	0.0005	I	This paper
2008	2454644.4240	0.0010	II	This paper
2008	2454646.3950	0.0003	I	This paper
2008	2454656.4265	0.0015	I	This paper
2008	2454667.3522	0.0001	II	Samolyk (2009)
2009	2454894.6686	0.0010	I	This paper
2009	2454971.5140	0.0010	II	This paper

Table 2. VZ Lib times of minima (averages) from the ROTSE-1 and ASAS-3 surveys.

Date	ToM	Uncertainty	I/II	Survey
1999	2451314.615	0.002	I	ROTSE
2000	2451615.201	0.002	I	ROTSE
2001	2452034.711	0.003	I	ASAS
2002	2452475.012	0.002	I	ASAS
2003	2452773.799	0.002	I	ASAS
2004	2453132.763	0.003	I	ASAS
2005	2453521.475	0.002	I	ASAS

Table 3. VZ Lib ranges of values for the ternary orbital parameters.

Parameter	Range
a *sin*(i) (AU)	-3.5 ± 1.0
e	0.3 ± 0.3
ω(°)	180 ± 180
P (yr)	33 ± 5
t_0 (HJD)	2454900 ± 200

Table 4. VZ Lib first result (iteration 0) for the determination of the ternary orbital parameters.

Parameter (iteration 0)	*Value (iteration 0)*	*Uncertainty*
a *sin*(i) (AU)	3.05	0.03
e	0.305	0.005
ω(°)	90.6	0.5
P (yr)	35.1	0.2
t_0 (HJD)	2454977	15

Table 5. VZ Lib ternary orbital parameters.

Parameter	*Value*	*Uncertainty*
a *sin*(i) (AU)	3.026	0.019
e	0.308	0.007
ω(°)	91.0	0.8
P (yr)	34.78	0.26
t_0 (HJD)	2454979 (27 May 2009)	18

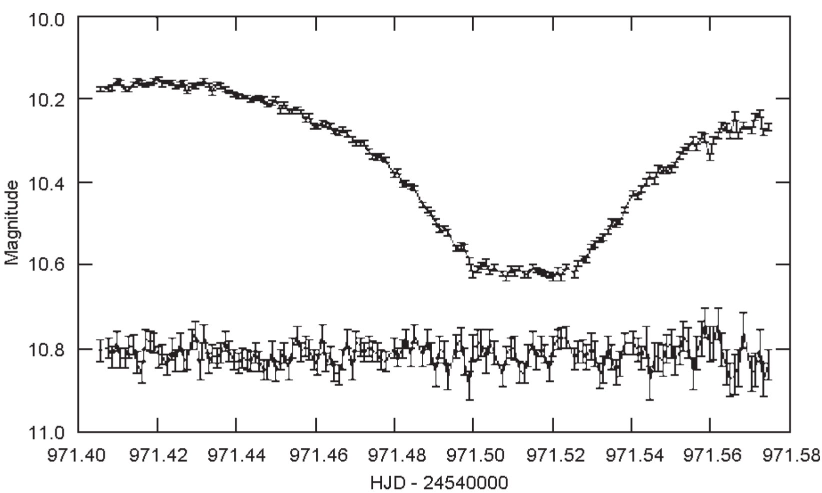

Figure 1. An example of a VZ Lib light curve, from the session of 19 May 2009. The check star (GSC6184-00385) measurements are shifted by –1.8 magnitude. The error bars are ± the 1-sigma statistical uncertainties. The eclipse is a secondary one (II), note the flat bottom.

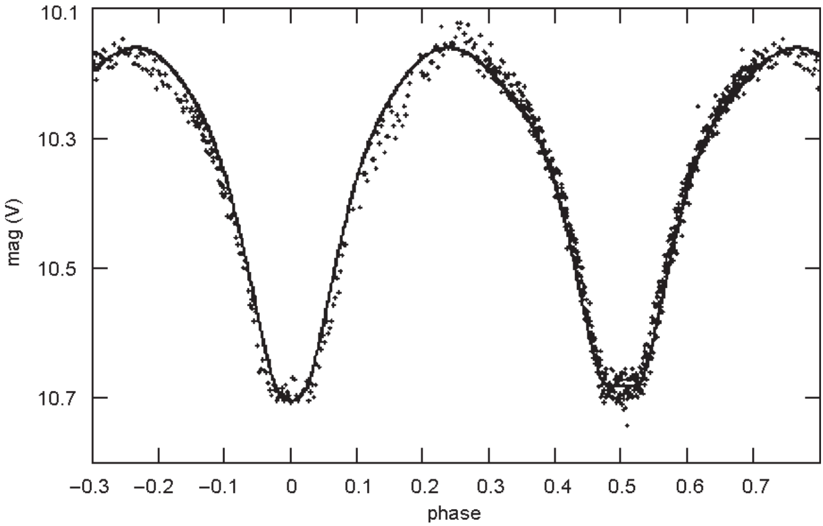

Figure 2. Phase plot of the author's 2008 observations of VZ Lib along with the synthetic light curve. Note the variability at the secondary eclipse, and also in Figure 3.

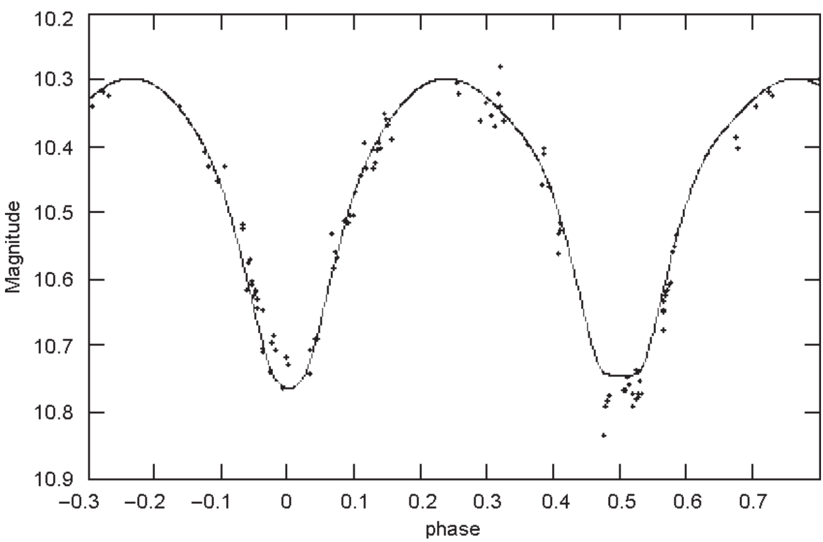

Figure 3. Phase plot of the 1999 ROTSE-1 observations of VZ Lib along with the synthetic light curve.

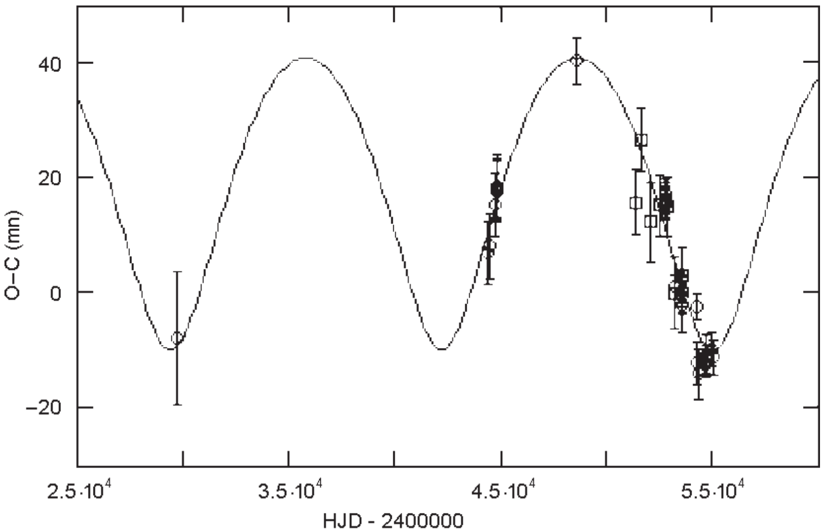

Figure 4. O–C diagram (1940–2009) for VZ Lib from the first result (iteration 0) for the determination of the primary parameters. Circles, individual minima; Squares, average minima from ROTSE-1 and ASAS-3; Solid line, light- travel time calculation.

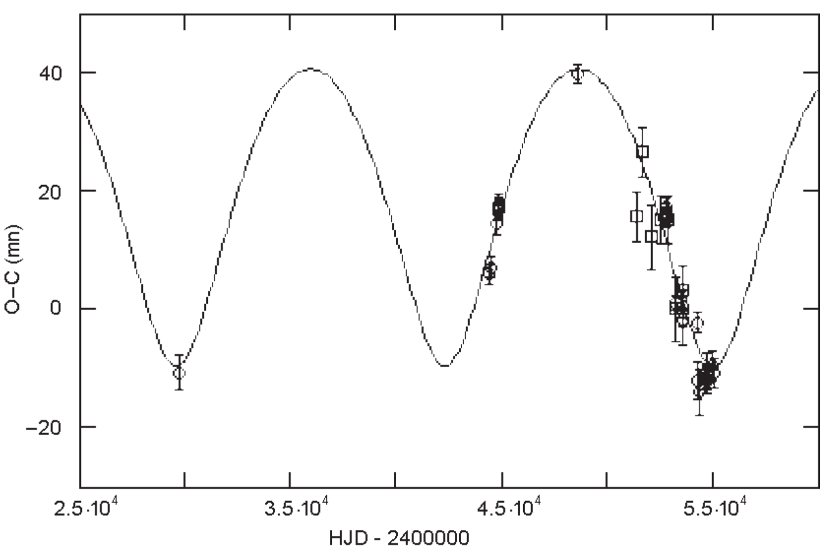

Figure 5. O–C diagram (1940–2009) for VZ Lib with the light-travel time calculation, after several iterations. Note than the error bars are much smaller than in Figure 4 which was for iteration 0.

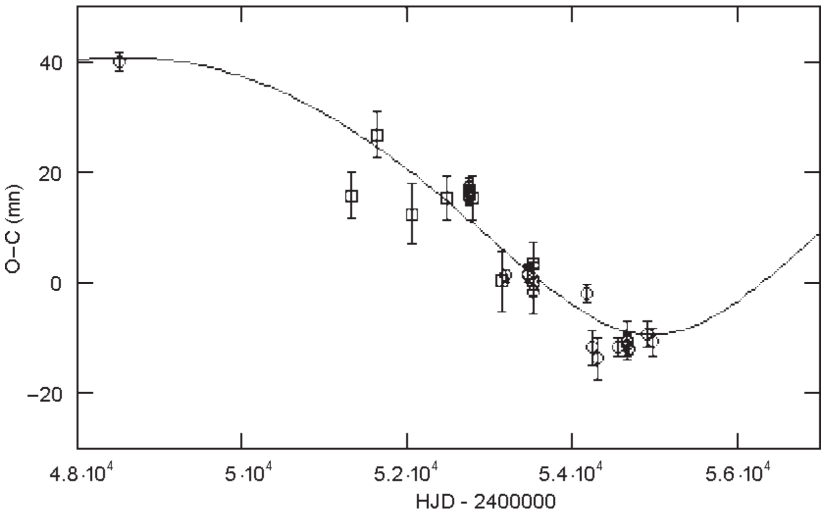

Figure 6. O–C diagram (1991–2009) for VZ Lib. A close-up of Figure 5.

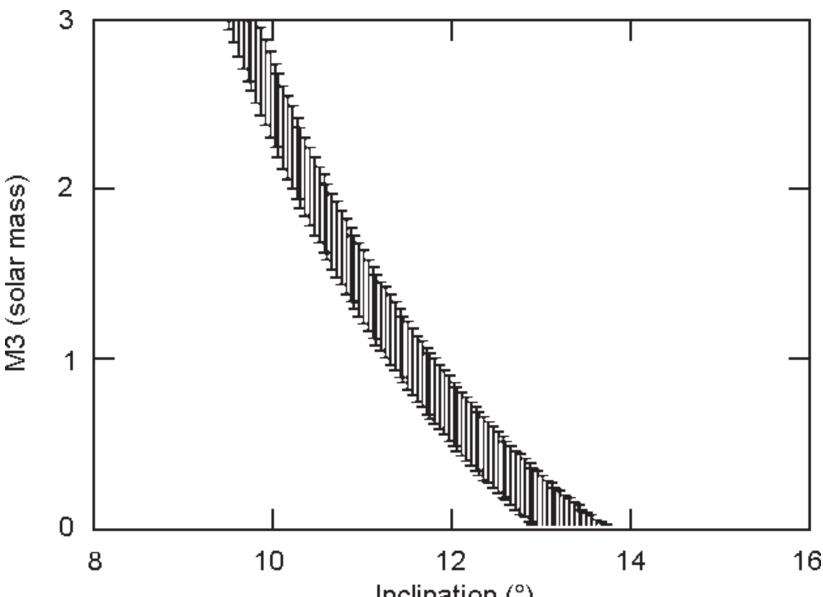

Figure 7. The mass of the third star as a function of the inclination.

A Multi-year Multi-passband CCD Photometric Study of the W UMa Binary EQ Tauri

Kevin B. Alton
UnderOak Observatory, 70 Summit Avenue, Cedar Knolls, NJ 07927

Received June 5, 2009; revised August 7, 2009; accepted September 1, 2009

Abstract A revised ephemeris and updated orbital period for EQ Tau have been determined from newly acquired (2007–2009) CCD-derived photometric data. A Roche-type model based on the Wilson-Devinney code produced simultaneous theoretical fits of light curve data in three passbands by invoking cold spots on the primary component. These new model fits, along with similar light curve data for EQ Tau collected during the previous six seasons (2000–2006), provided a rare opportunity to follow the seasonal appearance of star spots on a W UMa binary system over nine consecutive years. Fixed values for q, $\Omega_{1,2}$, T_1, T_2, and i based upon the mean of eleven separately determined model fits produced for this system are hereafter proposed for future light curve modeling of EQ Tau. With the exception of the 2001 season all other light curves produced since then required a spotted solution to address the flux asymmetry exhibited by this binary system at Max I and Max II. At least one cold spot on the primary appears in seven out of twelve light curves for EQ Tau produced over the last nine years, whereas in six instances two cold spots on the primary star were invoked to improve the model fit. Solutions using a hot spot were less common and involved positioning a single spot on the primary constituent during the 2001–2002, 2002–2003, and 2005–2006 seasons.

1. Introduction

The variability of EQ Tauri was discovered by Tsesevich (1954) but was not rigorously characterized until the first modern orbital period was reported by Whitney (1972). Thereafter largely neglected for over two decades, Benbow and Mutel (1995) produced the first CCD-derived (R) light curve found in the literature. More recently, photoelectric (*UBV*) studies by Pribulla *et al.* (2001) and Vaňko *et al.* (2004) have been published along with more robust multi-color CCD investigations by Yang and Liu (2002), Zola *et al.* (2005), Hrivnak *et al.* (2006), Csizmadia *et al.* (2006b), and Yuan and Qian (2007). A period study of EQ Tau was conducted by Qian and Ma (2001), who comprehensively analyzed times of minimum light over a twenty-three year period from 1973 to 1996.

Similar to the Sun, EQ Tauri is spectral type G2 but due to mutual eclipses its visual magnitude changes from 10.3 to 11 every 0.341349 day. Since the most massive (1.22 $M_\odot$) and hotter primary star is occulted (annular eclipse) by the less massive (0.539 $M_\odot$) but cooler secondary constituent during primary minimum, EQ Tau belongs to the A-type subclass of W UMa binaries (Binnendijk 1984). With an orbital inclination approaching 86°, our view of this system is nearly edge on. This relatively bright variable is easily within the light grasp of a modest aperture telescope coupled with a consumer-grade CCD camera. In the neighborhood, but not part of the Pleiades (~2° southeast), EQ Tau is well positioned for mid-latitude observers in the Northern Hemisphere during the fall and winter months.

Being one of the more frequently studied W UMa binary systems, existing Wilson-Devinney modeling data which cover 2000–2006 combined with new data collected between 2006 and 2009 provides a unique opportunity to refine our understanding of EQ Tau. Significant changes to physical or geometric elements such as effective stellar temperature (T_1 and T_2), Roche potential ($\Omega_{1,2}$), inclination angle (i), and mass ratio ($q = m_2/m_1$) generally occur over millennia. There is a reasonable expectation that values for each of these parameters should have remained fairly constant over the past decade, yet an unrealistically wide range in values is found in the literature (Table 1). Therefore a strategy was developed to fix values for i, $\Omega_{1,2}$, T_1, T_2, and q, so that the latest (2006–2009) epochal variations in light curve morphology could potentially be more accurately modeled, in this case by the addition of putative spot(s).

2. Observations and data reduction

2.1. Photometry

Images of EQ Tau were matched against the standard star fields provided in MPO CANOPUS (version 9.5.0.3; Minor Planet Observer 2003) as described previously for SW Lac (Alton and Terrell 2006). CCD photometric imaging began on December 10, 2006, with the intent of generating light curves over three consecutive years which could be used to: 1) refine the orbital period for EQ Tau; 2) calculate an updated ephemeris; and 3) potentially track the course of starspots known to appear in this binary system. Equipment included a 0.2-m Celestron Nexstar 8 GPS (*f*/6.3) with an SBIG ST-402ME CCD camera mounted at the Cassegrain focus. The field of view (FOV) produced by this configuration was 12.3 × 18.5 arcmin (1.45 arcsec/pixel). Multi-passband imaging was automatically performed with SBIG photometric B, V, and I_c filters (consistent with Bessell standard definition) mounted onto a multi-position wheel. Each exposure was captured (unbinned) over a 20- to 45-second period with thermoelectric cooling regulated to maintain the CCD chip at –5°C. Typical sessions lasted from two to four hours with I_c, V, and B images taken in immediate succession. Computer clock time was updated via the Internet Time Server immediately prior to each session. Image acquisition (raw lights, darks, and flats) was performed using SBIG CCDSOFT 5 (version 5.00.174) while calibration and registration was accomplished with AIP4WIN (version 2.1.10;

Berry and Burnell 2000). Further photometric reduction (circular aperture) with MPO CANOPUS was achieved using two non-varying comparison stars (TYC1260-00575-1, V=10.4, B–V=1.1; and TYC1260-00893-1, V=9.49, B–V=0.74) to ultimately generate light curves for calculating ephemerides and orbital period. Instrumental readings were not reduced to standard magnitudes.

2.2. Light curve analyses

Preliminary light curve fits and final geometric renderings were produced by BINARY MAKER (version 3.0; Bradstreet and Steelman 2002). Light curve modeling was performed using PHOEBE (Prša and Zwitter 2005) and WDWINT (Nelson 2005b), both of which employ the W-D code (Wilson and Devinney 1971; Wilson 1979). PHOEBE is an elegant implementation of the W-D code which provides a very convenient as well as enhanced user interface. Each model fit incorporated individual observations and not binned to normal points. SIGMA was assigned according to the standard deviation measured from the average difference in instrumental magnitude (C_{avg}) for each comparison star. For the B, V, and I_c passbands, variability was typically ±0.03, ±0.01, and ±0.01, respectively.

3. Results and discussion

3.1. Ensemble photometry

A representative exposure (20 seconds) taken in V-band showing EQ Tau along with two comparison stars from the Tycho 2 catalog is reproduced in Figure 1. Prior to accepting processed results from each session, comparison stars were tested for variability over the observation period. A typical example is shown for a dataset in V acquired on February 18, 2008 (Figure 2). Collectively, C_{avg} in I_c, V, or B passband did not exhibit a pattern or trend that would otherwise suggest variability beyond experimental error.

3.2. Folded light curve and ephemeris

A total of 2,123 individual photometric readings in B, 2,134 in V, and 2,144 in I_c were combined within each passband to produce three seasonal light curves (2007, 2008, and 2009) that spanned 778 days of data collection. These observations included forty-two new times of minima (ToM) which were captured between December 10, 2006, and January 4, 2009 (Table 2). CANOPUS provided a period solution for the folded datasets using Fourier analysis. The time of minimum for the first primary epoch was estimated by CANOPUS using the Hertzsprung method as detailed by Henden and Kaitchuck (1990). The linear ephemeris equation (1) for the Heliocentric Primary Minimum (HPM) was initially determined to be:

$$\mathrm{HPM} = 2454520.5788 + 0.341349(2)\,\mathrm{E} \qquad (1)$$

and in excellent accordance with previously published orbital periods (d) for EQ Tau. A periodogram (Figure 3), produced using PERANSO (version 2.31; Vanmunster 2005) by applying periodic orthogonals (Schwarzenberg-Czerny 1996) to fit observations and analysis of variance (ANOVA) to evaluate fit quality, reaffirmed the period determination. ToM values (Table 2) were estimated by the program MINIMA (version 24d; Nelson 2005a) using the simple mean from a suite of six different methods including: parabolic fit, tracing paper, bisecting chords, Kwee and van Woerden (1956), Fourier fit, and sliding integrations (Ghedini 1981). These new minima along with values from Pribulla and Vanko (2002), Yang and Liu (2002), Yuan and Qian (2007), Hrivnak *et al.* (2006), Alton (2006), and additional observations published (*IBVS, AAVSO, VSOLJ,* as given in the reference list) between 2001 and 2008 or readings otherwise posted on the B.R.N.O. Project website

(http://var.astro.cz/ocgate/ocgate.php?star=EQ+Tau&lang=en)

were used to calculate residual values based upon the GCVS reference epoch (Kholopov *et al.* 1985) defined by the ephemeris (2):

$$\mathrm{HPM} = 2440213.3250 + 0.341348\,\mathrm{E} \tag{2}$$

Two separate regression analyses were performed due to the curvilinear nature of the O–C residuals observed for at least a decade. A revised equation (3) based upon a linear least squares fit (Figure 4) of near term (O–C)1 data from October 2, 2005, to January 4, 2009 was calculated from:

$$\mathrm{O–C} = a + b\mathrm{E} \tag{3}$$

where:

$a = –4.0414 \times 10^{–2} \pm 2.0806 \times 10^{–3}$
$b = 3.4355 \times 10^{–7} \pm 5.0322 \times 10^{–8}$

$$\mathrm{HPM} = 2440213.2846\,(21) + 0.341349\,(1)\,\mathrm{E} \tag{4}$$

Expanding the analysis to include a notably rich ($n > 150$) set of photometrically-derived ToM data from the past nine years revealed a parabolic relationship (Figure 5) between residuals $(\mathrm{O–C})_1$ and HJD that can be fit by the quadratic expression (5):

$$\mathrm{O–C} = a + b\mathrm{E} + c\mathrm{E}^2 \tag{5}$$

where:

$a = 9.5316 \times 10^{–2} \pm 1.5271 \times 10^{–2}$
$b = –6.3369 \times 10^{–6} \pm 7.9365 \times 10^{–7}$
$c = 8.2080 \times 10^{–11} \pm 1.0265 \times 10^{–11}$

which leads to the following ephemeris (6):

$$\mathrm{HPM} = 2440213.4207\,(153) + 0.341321\,(1)\,\mathrm{E} + 8.21(103) \times 10^{–11}\,\mathrm{E}^2 \tag{6}$$

From the fall of 2000 and on consecutive years through 2009, EQ Tau has apparently experienced a very slow orbital period increase as defined by equation (7):

$$dP/dt = 2 \times (8.21 \times 10^{-11})(1/0.341321)(86400)(365.25) \quad (7)$$
$$= 0.01518 \text{ sec/yr}$$

Interestingly, Qian and Ma (2001) reported a negative parabolic fit in previous years (1973–1997), which corresponded to a secular decrease in the orbital period (dP/dt = –0.016 sec/yr). Unfortunately there is a paucity of published observations for EQ Tau between 1997 and 2000 so that the transition between positive and negative orbital period rate changes was not captured. Nonetheless, this fluctuation in periodicity is not uncommon behavior for W UMa type variables, as discussed by Dryomova and Svechnikov (2006). Therein it is suggested that according to thermal relaxation oscillation (TRO) theory, thermal oscillations begin to temporarily disrupt the contact phase when the mass ratio (q) approaches a value of 0.45. The cycle of contact breakup and restoration due to the inability to simultaneously achieve thermal and dynamic equilibrium could potentially explain the succession of increasing and decreasing orbital periods often observed with W UMa binaries like EQ Tau.

Folded light curves in B, V, and I_c, show that both minima are separated by ~0.5 phase and are consistent with a circular orbit (Figure 6). As has been reported by a number of investigators including Yang and Liu (2002) and Pribulla and Vaňko (2002), the so-called O'Connell effect was also observed in all new light curves described herein. This asymmetry, common to many light curves from overcontact binaries, exhibited its greatest effect in the I_c band, where in all cases Max I > Max II. One plausible explanation for this intrinsic variability involves the presence of starspot(s) on one or more binary components and is examined further in section 3.3.1.

3.3. Light curve synthesis

The Roche model derived from the seminal Wilson and Devinney (1971) paper has been widely applied to produce simulated light curve solutions which closely fit changes in flux arising from eclipsing star systems. Collectively, synchronous rotation, no third light (l3 = 0), and circular orbits (e = 0) were defined as constants within PHOEBE using the "overcontact binary not in thermal contact" model. Bolometric albedo ($A_{1,2}$ = 0.5) and gravity darkening coefficients ($g_{1,2}$ = 0.32) for cooler stars with convective envelopes were according to Ruciński (1969) and Lucy (1967), respectively. Logarithmic limb darkening coefficients (x_1, x_2, y_1, y_2) for both stars were interpolated within PHOEBE according to Van Hamme (1993) after any change in T_{eff}. The mean effective temperature of star 1 (the star eclipsed at primary minimum) was set equal to 5800K based on its spectral type (G2). Radial velocity measurements previously performed on EQ Tau (Ruciński *et al.* 2001) provided a spectroscopically determined value for the mass ratio (q = 0.442) which helped constrain the many possible solutions.

Once an approximate fit was obtained, differential corrections (DC) were applied simultaneously to photometric data in all filters. Standard errors for the present study (Table 1) are those calculated by WDWINT (Nelson 2005b).

3.3.1. Unspotted and spotted models

Since immediate visual feedback from each synthetic light curve iteration is possible in PHOEBE, this application proved to be particularly adept at rapidly reaching a convergent solution. As a starting point for an unspotted solution, the *V*-band values for q, $\Omega_{1,2}$, T_1, T_2, and i reported by Alton (2006) were used. For each epoch, $A_{1,2}$, $g_{1,2}$, $x_{1,2}$, and T_1 were fixed, whereas $\Omega_{1,2}$, T_2, q, and i were iteratively adjusted using DC to achieve a minimum simultaneous residual fit of *B*, *V*, and I_c photometric observations. As was the case with all new light curves described herein, the unspotted W-D model error [Σ(O–C)^2], where O–C is the residual between the observed and synthetic light curve, was unacceptable due to the poor coverage of the light curve especially during Max I and Min II. This is visually obvious in a representative example taken from photometric data (I_c) collected in early 2009 (Figure 7).

The excess flux during Max I suggested starspot solution(s) for the 2007–2009 epochs. Yang and Liu (2002) were the first to reproduce the asymmetrical shape of EQ Tau light curves by employing the geometrical and physical elements (A_S, Θ, ψ, and r_S) of hot and dark starspots on each stellar component. The asymmetry observed at Max I for EQ Tau may arise from a number of possibilities, including: 1) cold starspot(s) on either component facing the observer to decrease the depth of Max II, or 2) hot starspot(s) on either star responsible for an increase in flux during Max I. It is clear from the recent literature, which covers five consecutive years (2000–2006) of light curves for EQ Tau, that both cold and hot starspots have been successfully used to minimize the residual fit of the Roche model (Table 1). Since seasonal variations in light curves from W UMa binary systems are well documented, data from each new epoch (2007, 2008, and 2009) were modeled independently but using the same seed values (*V*-band) for q, $\Omega_{1,2}$, T_1, T_2, and i initially reported by Alton (2006). Newly fit values for q, T_2, and i were averaged with literature values reported between 2000 and 2004 (Table 1) and thereafter, along with T_1 (5800K), entered afresh as fixed values. In all three cases (2007, 2008, and 2009), DC iterations of A_S, Θ, ψ, and r_S yielded a best fit which supported placement of two cold starspots on the primary constituent (Figure 8). An additional cold spot was positioned on the secondary star to improve the model fit to the 2008 light curves. Synthetic light curves superimposed upon *B*, *V*, and I_c passband data are illustrated in Figure 9 (2007), Figure 10 (2008), and Figure 11 (2009). Using PHOEBE, an improved fit of the 2005–2006 light curves (*V* and *R*) previously produced by this author (Alton 2006) was obtained by adding a cold spot to the primary star. Interestingly, this would appear to be the only epoch over the past nine years in which Max II > Max I. However, as previously noted (Alton 2006), the large gap in *R*-band data around Max II (Figure 12) does leave some doubt about the robustness of the model fit.

With the exception of the 2001 light curves generated by Vaňko *et al.* (2004), all other light curves produced since 2000 required a spotted solution to address the flux asymmetry exhibited by this binary system at Max I and Max II. Even in this case the authors suggested the possibility of cool spot(s) but refrained from introducing any spot during modeling due to the poor quality and photometric coverage at Max I. At least one cold spot on the primary has figured prominently in the simulated W-D solution in seven out of twelve light curves for EQ Tau produced since 2000. In six instances—2000, 2004 (two different solutions), 2007, 2008, and 2009—two cold spots on the primary star were invoked to improve the model fit. Solutions using a hot spot were less common and involved positioning a single spot on the primary constituent during the 2001–2002, 2002–2003, and 2005–2006 seasons.

4. Conclusions

Filtered (B, V, and I_c) CCD-based photometric readings have lead to forty-two new times of minima and the construction of light curves between 2007 and 2009 which were used to revise the orbital period for EQ Tau and calculate an updated ephemeris. A positive parabolic relationship between O–C residuals and cycle number continues to suggest a secular rate increase in dP/dt which started over a decade ago. Fixed values for q, $\Omega_{1,2}$, T_1, T_2, and i were calculated from the mean of eleven independently determined model fits produced for this system over nine consecutive years. A Roche-type model invoking cold spots primarily on the more massive constituent produced simultaneous theoretical fits of light curve data in three passbands between 2006 and 2009 that largely account for the asymmetrical flux intensity at maximum light. This result is not unexpected since cold spots on the primary star are featured in the simulated models for seven of twelve light curves produced since 2000.

5. Acknowledgements

The many constructive comments suggested by the referee are greatly appreciated. Special thanks are due to the NASA Astrophysics Data System hosted by the Computation Facility at the Harvard-Smithsonian Center for Astrophysics without which this research effort would not be possible. This investigation has also made use of the SIMBAD database, operated at CDS, Strasbourg, France, and the B.R.N.O. Project database generously maintained by the Czech Astronomical Society.

References

Agerer, F., and Hübscher, J. 2002, *Inf. Bull. Var. Stars*, No. 5296.
Agerer, F., and Hübscher, J. 2003, *Inf. Bull. Var. Stars*, No. 5484.
Alton, K. 2006, *Open European J. Var. Stars*, **39**, 1.
Alton, K. B., and Terrell, D. 2006, *J. Amer. Assoc. Var. Star Obs.*, **34**, 188.
Baldwin, M. E., and Samolyk, G. 2002, *Observed Minima Timings of Eclipsing Binaries No. 7*, AAVSO, Cambridge, MA.
Baldwin, M. E., and Samolyk, G. 2005, *Observed Minima Timings of Eclipsing Binaries No. 10*, AAVSO, Cambridge, MA.
Baldwin, M. E., and Samolyk, G. 2007, *Observed Minima Timings of Eclipsing Binaries No. 12*, AAVSO, Cambridge, MA.
Benbow, W. R., and Mutel, R. L. 1995, *Inf. Bull. Var. Stars*, No. 4187.
Berry, R., and Burnell, J. 2000, "Astronomical Image Processing Software," version 2.1.10, provided with *The Handbook of Astronomical Image Processing*, WIllmann-Bell, Richmond, VA.
Binnendijk, L. 1984, *Publ. Astron. Soc. Pacific*, **96**, 646.
Bíró, I. B., *et al.* 2007, *Inf. Bull. Var. Stars*, No. 5753.
Bradstreet, D. H., and Steelman, D. P. 2002, *Bull. Amer. Astron. Soc.*, **34**, 1224.
Borkovits, T., Bíró, I. B., Csizmadia, S., Patkós, L., Hegedüs, T., Pál, A. Kóspál, Á., and Klagyivik, P. 2004, *Inf. Bull. Var. Stars*, No. 5579.
Cook, J. M., Divoky, M., Hofstrand, A., Lamb, J., and Quarderer, N. 2005, *Inf. Bull. Var. Stars*, No. 5636.
Csizmadia, Sz., Klagyivik, P., Borkovits, T., Patkós, L., Kelemen, J., Marschalkó, G., and Marton, G. 2006a, *Inf. Bull. Var. Stars*, No. 5736.
Csizmadia, Sz., Kővári, Z., and Klagyivik, P. 2006b, *Astrophys. Space Sci.*, **304**, 355.
Csizmadia, Sz., Zhou, A. Y., Könyves, V., Varga, Z., and Sándor, Zs. 2002, *Inf. Bull. Var. Stars*, No. 5230.
Diethelm, R. 2003, *Inf. Bull. Var. Stars*, No. 5438.
Dogru, S. S., Dogru, D., and Dönmez, A. 2007, *Inf. Bull. Var. Stars*, No. 5795.
Dryomova, G. N., and Svechnikov, M. A. 2006, *Astrophys.*, **49**, 358.
Ghedini, S. 1981, *Mem. Soc. Astron. Italiana*, **52**, 633.
Henden, A. A., and Kaitchuck, R. H. 1990, *Astronomical Photometry: A Text and Handbook for the Advanced Amateur and Professional Astronomer*, Willmann-Bell, Richmond.
Hrivnak, B. J., Lu, W., Eaton, J., and Kenning, D. 2006, *Astron. J.*, **132**, 960.
Hübscher, J. 2005, *Inf. Bull. Var. Stars*, No. 5643.
Hübscher, J., Paschke, A., and Walter, F. 2005, *Inf. Bull. Var. Stars*, No. 5657.
Hübscher, J., Paschke, A., and Walter, F. 2006, *Inf. Bull. Var. Stars*, No. 5731.
Hübscher, J., and Walter, F. 2007, *Inf. Bull. Var. Stars*, No. 5761.
Kholopov, P. N., *et al.* 1985, *General Catalogue of Variable Stars*, 4th ed., Moscow.
Krajci, T. 2005, *Inf. Bull. Var. Stars*, No. 5592.

Kwee, K. K., and van Woerden, H. 1956, *Bull. Astron. Inst. Netherlands*, **12**, 327.
Lucy, L. B. 1967, *Z. Astrophys.*, **65**, 89.
Minor Planet Observer 2003, MPO Software Suite, BDW Publishing, Colorado Springs (http://www.minorplanetobserver.com).
Müyesseroglu, Z., Törün, E., Özdemir, T., Gürol, B., Özavci, I., Tunç, T., and Kaya, F. 2003, *Inf. Bull. Var. Stars*, No. 5463.
Nagai, K. 2004, *VSOLJ Variable Star Bulletin*, No. 42.
Nagai, K. 2009, *VSOLJ Variable Star Bulletin*, No. 48.
Nelson, R. H. 2001, *Inf. Bull. Var. Stars*, No. 5040.
Nelson, R. H. 2003, *Inf. Bull. Var. Stars*, No. 5371.
Nelson, R. H. 2004, *Inf. Bull. Var. Stars*, No. 5493.
Nelson, R. H. 2005a, MINIMA astronomy software, URL:http://members.shaw.ca/bob.nelson/software1.htm.
Nelson, R. H. 2005b, WDWINT (version 5.4e) astronomy software, URL: http://members.shaw.ca/bob.nelson/software1.htm.
Nelson, R. H. 2008, *Inf. Bull. Var. Stars*, No. 5820.
Parimucha, Š., *et al.* 2007, *Inf. Bull. Var. Stars*, No. 5777.
Pribulla, T., and Vaňko, M. 2002, *Contrib. Astron. Obs. Skalnaté Pleso*, **32**, 79.
Pribulla, T., Vaňko, M., Parimucha, Š., and Chochol, D. 2001, *Inf. Bull. Var. Stars*, No. 5056.
Pribulla, T., *et al.* 2005, *Inf. Bull. Var. Stars*, No. 5668.
Prša, A., and Zwitter, T. 2005, *Astrophys. J.*, **628**, 426.
Qian, S., and Ma, Y. 2001, *Pub. Astron. Soc. Pacific*, **113**, 754.
Ruciński, S. M. 1969, *Acta Astron.*, **19**, 245.
Ruciński, S. M., Lu, W., Mochnacki, S. W., Ogloza, W., and Stachowski, G. 2001, *Astron. J.*, **122**, 1974.
Šarounová, L., and Wolf, M. 2005, *Inf. Bull. Var. Stars*, No. 5594.
Schwarzenberg-Czerny, A. 1996, *Astrophys. J., Lett. Ed.*, **460**, L107.
Tsesevich, V. P. 1954, *Izv. Astron. Obs. Odessa*, **4**, No. 3.
Van Hamme, W. 1993, *Astron. J.*, **106**, 2096.
Vaňko, M., Parimucha, Š., Pribulla, T., and Chochol, D. 2004, *Baltic Astron.*, **13**, 151.
Vanmunster, T. 2005, PERANSO period analysis software, www.peranso.com
Whitney, B. S. 1972, *Inf. Bull. Var. Stars*, No. 633.
Wilson, R. E. 1979, *Astrophys. J.*, **234**, 1054.
Wilson, R. E., and Devinney, E. J. 1971, *Astrophys. J.*, **166**, 605.
Yang, Y., and Liu, Q. 2002, *Astron. J.*, **124**, 3358.
Yuan, J., and Qian, S. 2007, *Mon. Not. Roy. Astron. Soc.*, **381**, 602.
Zola, S., *et al.* 2005, *Acta Astron.*, **55**, 389.

Table 1. Comparison of light curve parameters and geometric elements determined for EQ Tau between 2000 and 2009.

Parameter	*Yuan and Qian (2007) 2000*	*Pribulla and Vaňko (2002) 2001*	*Yang and Liu (2002) 2001 D2*	*Yang and Liu (2002) 2001 H1*	*Hrivnak et al. (2006) 2001–2002*	*Hrivnak et al. (2006) 2002–2003*
T_1 (K)	5800	5860	5800	5800	5800	5800
T_2 (K)	5754 (5)	5851 (8)	5735 (4)	5722 (5)	5721 (7)	5721 (7)
q (m_2/m_1)	0.442 (3)	0.442 (7)	0.4457 (11)	0.4347 (15)	0.445 (6)	0.445 (6)
$\Omega_{1,2}$	2.7316 (27)	2.7303 (29)	2.7192 (17)	2.7161 (20)	2.7250 (20)	2.7250 (20)
$i°$	85.21 (38)	86.59 (69)	84.32 (45)	83.67 (13)	84.7 (2)	84.7 (2)
f (% overcontact)	11.57 (99)	12.0 (1.3)	18.8	12.1	16 (1)	16 (1)
$A_{S1a} = T_{S1}/T_2$	0.64 (6)		0.80 (3)	1.10 (4)	1.10	1.10
Θ_{S1a} (spot colatitude)	14.1° (2.4)		95.8° (6)	103.2° (9)	90°	90°
ψ_{S1a} (spot longitude)	96.8° (2.3)		261.8° (6)	260.9° (8)	257.70 (63)	269.20° (32)
r_{S1a} (angular radius)	30.5° (3.5)		18.6° (1)	14.2° (2)	11.1 (10)	10.8° (4)
$A_{S1b} = T_{S2}/T_2$	0.60 (6)					
Θ_{S1b} (spot colatitude)	165.8° (6.5)					
ψ_{S1b} (spot longitude)	252° (3.2)					
r_{S1b} (angular radius)	38.3° (2.8)					

(Table 1 continued on following page)

Table 1. Comparison of light curve parameters and geometric elements determined for EQ Tau between 2000 and 2009, continued.

Parameter	*Csizmadia et al. (2006b) 2004*	*Yuan and Qian (2007) 2004*	*Alton (2006) 2005–2006*	*Present Study 2006–2007*	*Present Study 2007–2008*	*Present Study 2008–2009*
T_1 (K)	NR	5800	5800	5800	5800	5800
T_2 (K)	NR	5754 (5)	5753 (38)	5753 (38)	5753 (38)	5753 (38)
q (m_2/m_1)	NR	0.442 (3)	0.4406 (56)	0.4406 (56)	0.4406 (56)	0.4406 (56)
$\Omega_{1,2}$	NR	2.7316 (27)	2.7226 (29)	2.7226 (29)	2.7226 (29)	2.7226 (29)
$i°$	NR	85.21 (38)	85.6 (13)	85.6 (13)	85.6 (13)	85.6 (13)
f (% overcontact)	NR	11.57 (99)	13.96	13.96	13.96	13.96
$A_{S1a} = T_{S1}/T_2$	0.72	0.94 (3)	1.23 (1)	0.878 (8)	0.85 (1)	0.767 (7)
Θ_{S1a} (spot colatitude)	0	34.6° (4.4)	94.2° (16)	112° (3)	94° (2)	86.3° (23)
ψ_{S1a} (spot longitude)	270	96.4° (9.9)	1.23° (38)	130° (3)	175.7° (11)	63.0° (10)
r_{S1a} (angular radius)	15	48.6° (7.8)	15.1° (2)	10.74° (21)	11.4° (6)	13.26° (9)
$A_{S1b} = T_{S2}/T_2$	0.95	0.93 (0.11)	0.818 (8)	0.663 (96)	0.761 (44)	0.585 (2)
Θ_{S1b} (spot colatitude)	0	135.8° (31.5)	103.7° (39)	105.3° (19)	89.4° (98)	29.4° (21)
ψ_{S1b} (spot longitude)	180	288.8° (6.4)	281.5° (30)	186.7° (25)	56° (1)	170.6° (12)
r_{S1b} (angular radius)	10	21.3° (9.5)	13.4° (2)	7.1° (4)	15.5° (1)	17.6° (6)
$A_{S2a} = T_{S1}/T_2$					0.685 (40)	
Θ_{S2a} (spot colatitude)					118° (7)	
ψ_{S2a} (spot longitude)					127.7° (38)	
r_{S2a} (angular radius)					13.9° (4)	

Note: $A_{1,2} = 0.5$; $g_{1,2} = 0.32$; NR = not reported. Values in parenthesis represent the standard error in the rightmost digit(s).

Table 2. Journal of new light curve minima captured from EQ Tauri between December 10, 2006, and January 4, 2009.

Observed Time of Minima (HJD-2400000.0)	*UT Date*	*Passband*	*No. of Observations*	*Type of Minima*
54079.5565 ± 0.0001	10 Dec 2006	V	132[a]	I
54079.5563 ± 0.0002	10 Dec 2006	B	135	I
54079.5566 ± 0.0003	10 Dec 2006	I_c	133	I
54089.6267 ± 0.0001	20 Dec 2006	V	154	II
54089.6269 ± 0.0002	20 Dec 2006	B	153	II
54089.6262 ± 0.0001	20 Dec 2006	I_c	151	II
54103.6221 ± 0.0001	3 Jan 2007	I_c	154	II
54103.6220 ± 0.0001	3 Jan 2007	V	152	II
54103.6221 ± 0.0002	3 Jan 2007	B	156	II
54111.6437 ± 0.0001	11 Jan 2007	I_c	171	I
54111.6437 ± 0.0001	11 Jan 2007	V	164	I
54111.6424 ± 0.0042	11 Jan 2007	B	169	I
54491.5644 ± 0.0002	26 Jan 2008	B	111[b]	I
54491.5646 ± 0.0001	26 Jan 2008	I_c	112	I
54491.5645 ± 0.0001	26 Jan 2008	V	112	I
54499.5844 ± 0.0002	3 Feb 2008	B	99	II
54499.5860 ± 0.0001	3 Feb 2008	I_c	100	II
54499.5861 ± 0.0001	3 Feb 2008	V	99	II
54508.6313 ± 0.0001	12 Feb 2008	B	129	I
54508.6319 ± 0.0001	12 Feb 2008	I_c	131	I
54508.6313 ± 0.0001	12 Feb 2008	V	133	I
54513.5823 ± 0.0003	17 Feb 2008	B	125	II
54513.5819 ± 0.0001	17 Feb 2008	I_c	127	II
54513.5824 ± 0.0002	17 Feb 2008	V	125	II
54520.5791 ± 0.0002	24 Feb 2008	B	74	I
54520.5792 ± 0.0001	24 Feb 2008	I_c	72	I
54520.5791 ± 0.0001	24 Feb 2008	V	77	I
54798.6080 ± 0.0002	28 Nov 2008	B	74[c]	II
54798.6079 ± 0.0001	28 Nov 2008	I_c	75	II
54798.6077 ± 0.0001	28 Nov 2008	V	74	II
54813.6276 ± 0.0002	13 Dec 2008	B	72	II
54813.6273 ± 0.0001	13 Dec 2008	I_c	73	II
54813.6277 ± 0.0002	13 Dec 2008	V	73	II
54823.6968 ± 0.0001	23 Dec 2008	B	78	I
54823.6967 ± 0.0001	23 Dec 2008	I_c	80	I
54823.6964 ± 0.0001	23 Dec 2008	V	80	I

(Table 2 continued on following page)

Table 2. Journal of new light curve minima captured from EQ Tauri between December 10, 2006 and January 4, 2009, continued.

Observed Time of Minima (HJD-2400000.0)	*UT Date*	*Passband*	*No. of Observations*	*Type of Minima*
54830.5234± 0.0001	30 Dec 2008	B	58	I
54830.5238± 0.0002	30 Dec 2008	I_c	58	I
54830.5236± 0.0001	30 Dec 2008	V	57	I
54835.6440± 0.0002	4 Jan 2009	B	111	I
54835.6441± 0.0002	4 Jan 2009	I_c	112	I
54835.6439± 0.0001	4 Jan 2009	V	111	I

a: 2007 folded light curves (10 Dec 06—11 Jan 07).
b: 2008 folded light curves (26 Jan 08—10 Mar 08).
c*: 2009 folded light curves (28 Nov 08—25 Jan 09).*

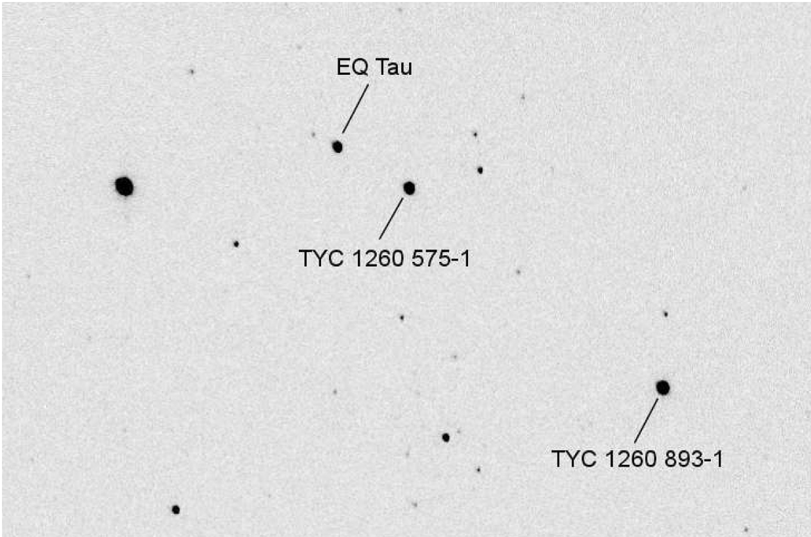

Figure 1. Exposure (20 seconds) in *V*-band taken on December 8, 2006, showing EQ Tau and two comparison stars from the Tycho 2 catalog.

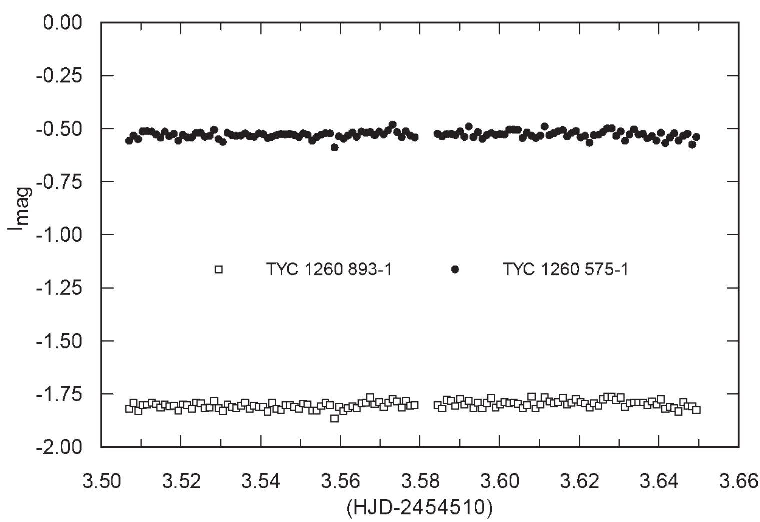

Figure 2. *V*-band instrumental magnitude (Imag) vs time (HJD) for the average magnitude (Cavg) from two comparison stars. Discontinuities in data arise from rejected readings due to the sporadic appearance of clouds.

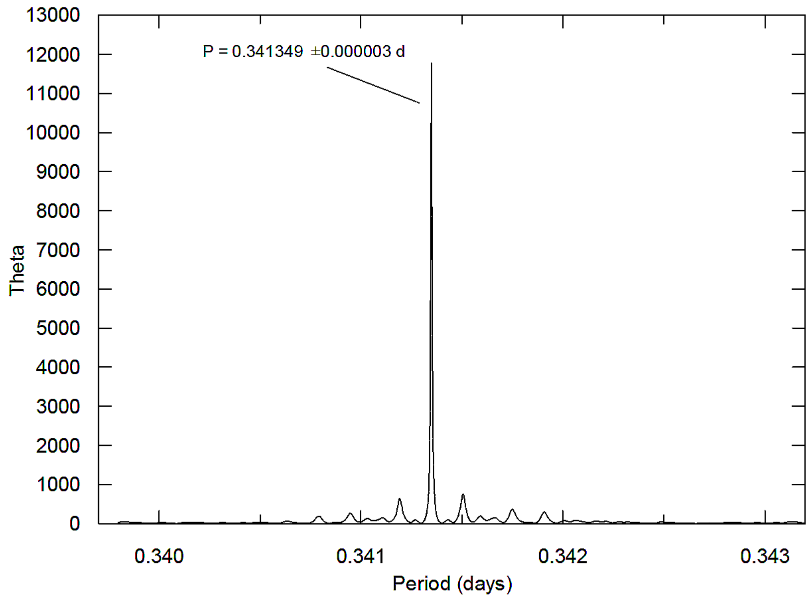

Figure 3. Periodogram for EQ Tau using the Schwarzenberg-Czerny (1996) method to search for periodicity in unevenly sampled observations.

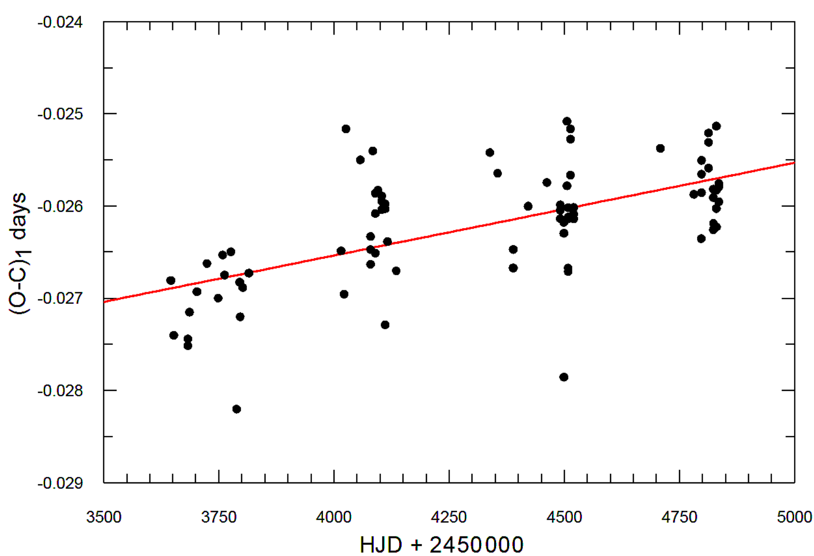

Figure 4. Linear least squares fit of residuals (O–C)1 vs HJD for EQ Tau observed between October 2, 2005, and January 4, 2009.

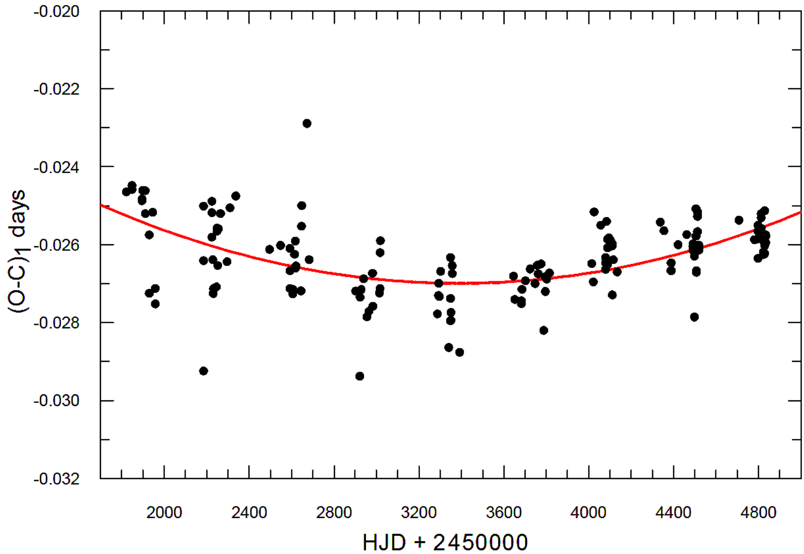

Figure 5. Quadratic least squares fit of residuals (O–C)1 vs HJD for EQ Tau observed between October 5, 2000, and January 4, 2009.

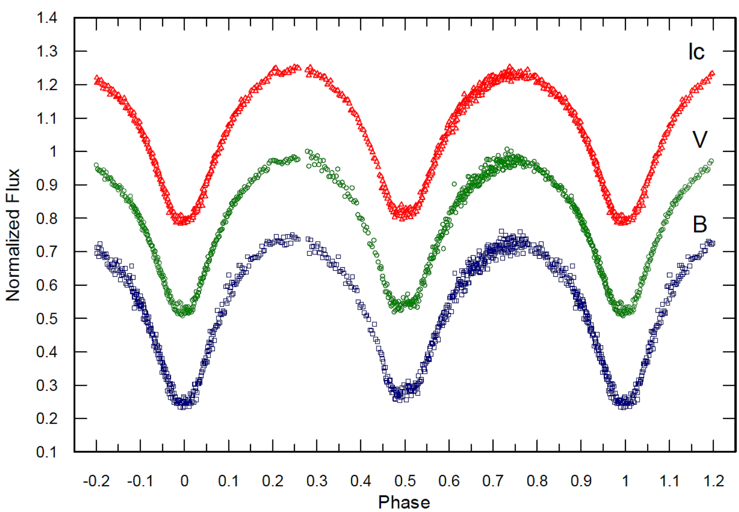

Figure 6. Representative folded CCD-derived light curves for EQ Tau captured in *B*-, *V*-, and *Ic*-passbands (January 26, 2008- March 10, 2008). Light curves are intentionally offset for clarity.

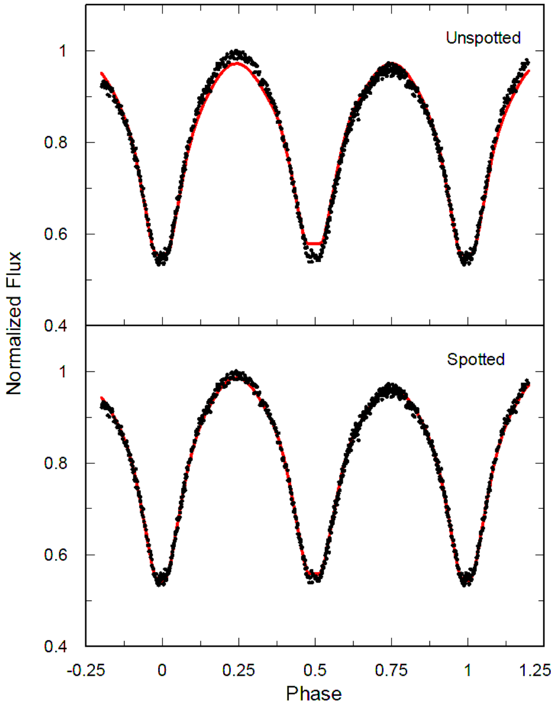

Figure 7. Representative unspotted (top) and spotted (bottom) W-D simulation of light curve for EQ Tau superimposed on CCD observations in *Ic*-passband (2009) from the present study.

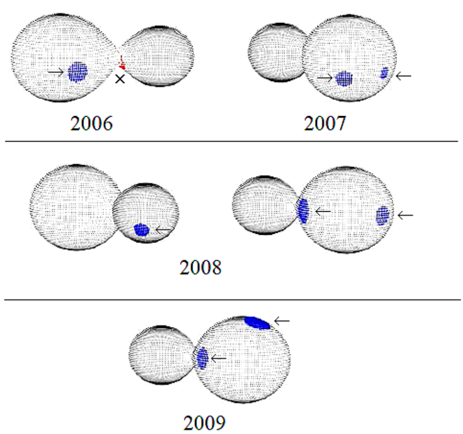

Figure 8. BNINARYMAKER-generated geometric renderings of EQ Tau showing the putative location of starspots from 2006 to 2009. Cold spots are depicted by the arrows while the only hot spot (2006) is marked by the ×.

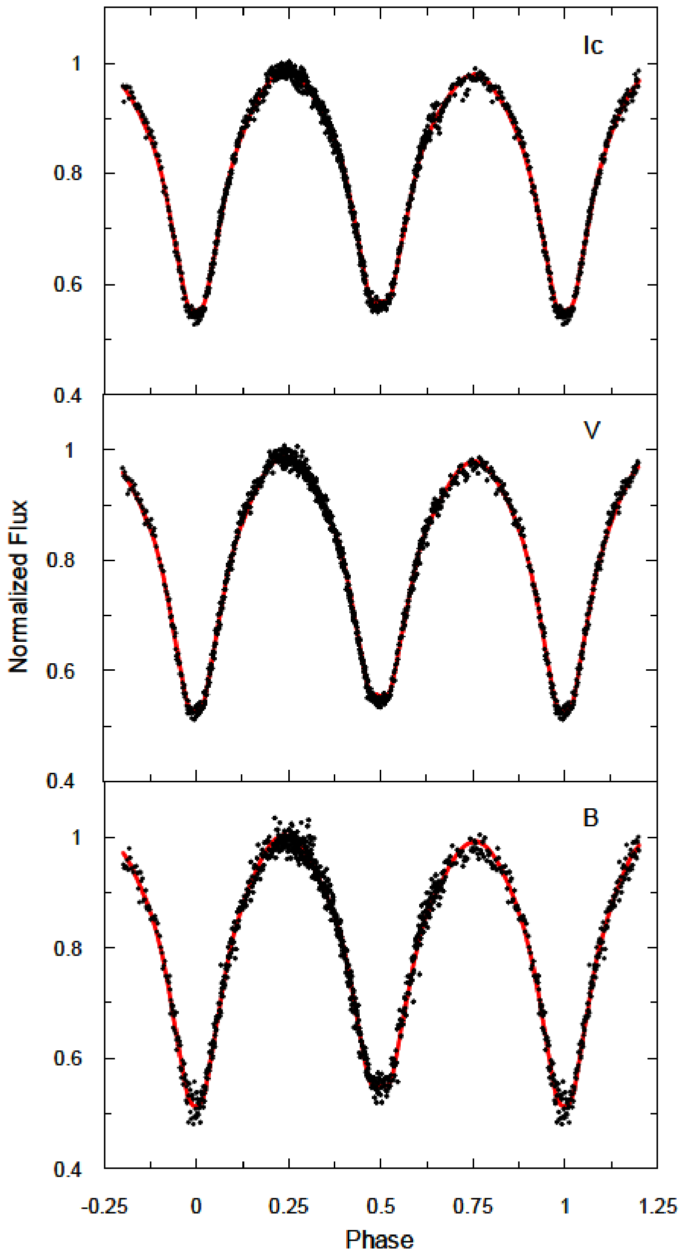

Figure 9. Spotted W-D simulation of 2007 light curves for EQ Tau superimposed on CCD observations in *Ic*- (top), *V*- (middle), and *B*-passbands (bottom) from the present study.

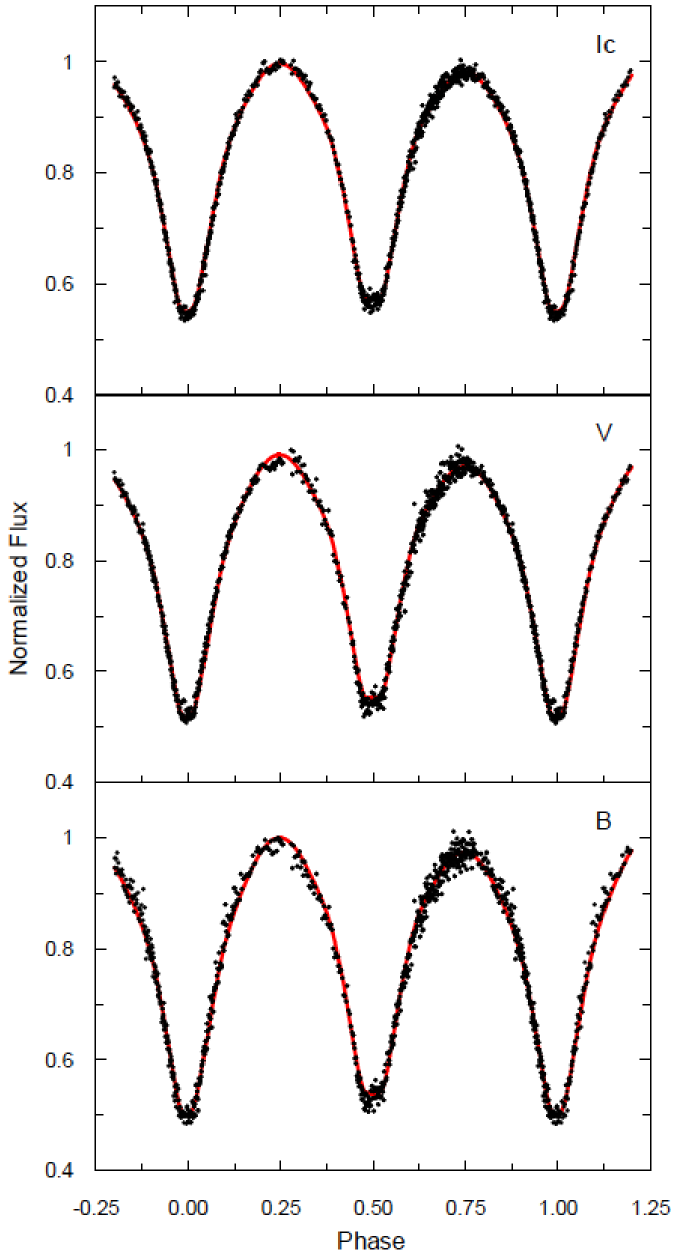

Figure 10. Spotted W-D simulation of 2008 light curves for EQ Tau superimposed on CCD observations in *Ic*- (top), *V*- (middle), and *B*-passbands (bottom) from the present study.

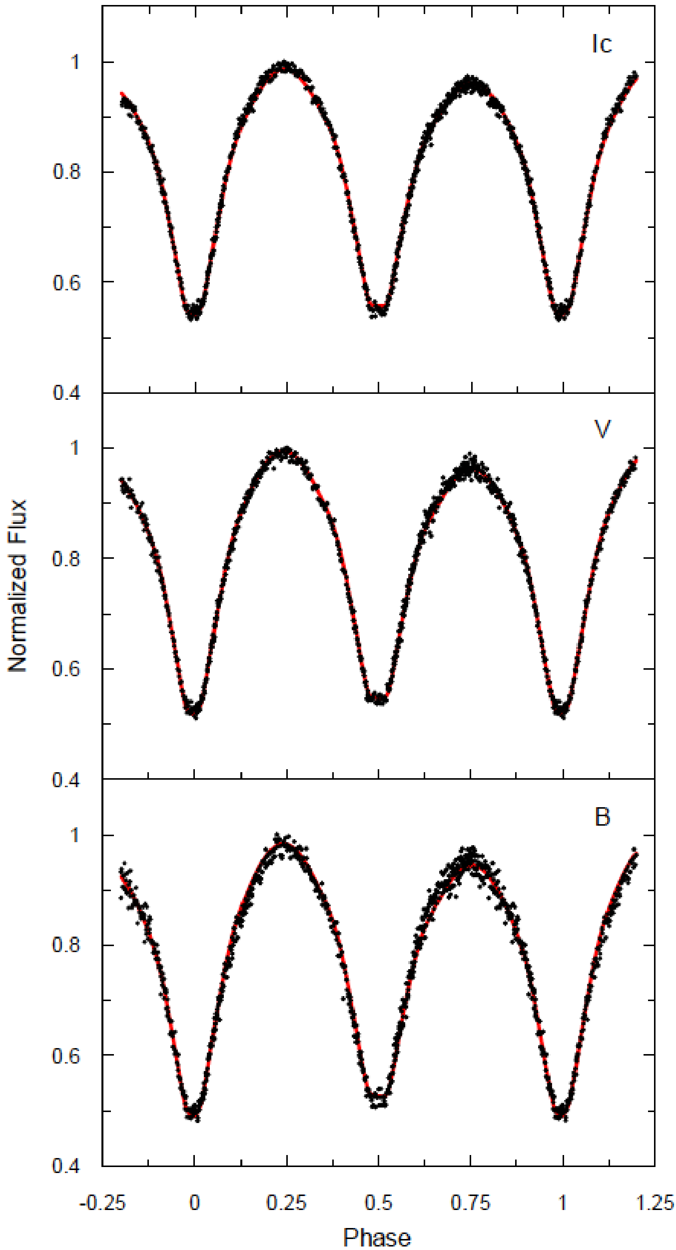

Figure 11. Spotted W-D simulation of 2009 light curves for EQ Tau superimposed on CCD observations in *Ic*- (top), *V*- (middle), and *B*-passbands (bottom) from the present study.

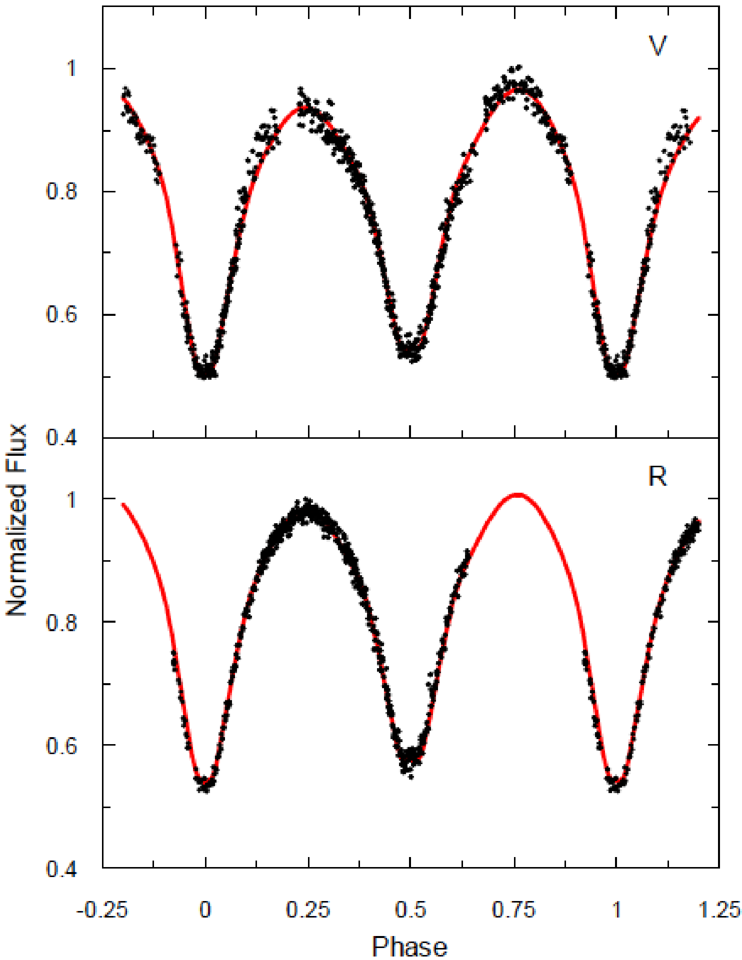

Figure 12. Revised spotted W-D simulation of 2006 light curves for EQ Tau superimposed on CCD observations in *V*- (top) and *R*-passband (bottom) from the present study.

Identifying Previously Uncatalogued Red Variable Stars in the Northern Sky Variability Survey

Martin Nicholson
3 Grovelands, Daventry, Northamptonshire NN11 4DH, England

Received November 30, 2008; revised December 23, 2008, and April 27, 2009; accepted May 26, 2009

Abstract Candidate variable stars in the publicly available data of the Northern Sky Variability Survey (NSVS) were identified by data mining the 2MASS survey for entries that matched the following criteria: Dec. > –20.000, ($J – K$) > 1.2, and J-magnitude < 7.000. A total of 1,233 such stars were identified: 1 type M, 64 type M:, 26 type SR:, and 1,142 type L:, with amplitudes between 0.3 magnitude and 3.4 magnitudes. Only stars not listed in the International Variable Star Index (VSX) at the time of submission or not identified as variable in SIMBAD have been included.

1. Introduction

The Northern Sky Variability Survey (NSVS) was conducted from Los Alamos, New Mexico, and used four unfiltered telephoto lenses equipped with CCD cameras. The entire northern sky was covered with a one-year baseline and up to 500 measurements per object. Some parts of the southern sky, between declinations 0° and –38°, were also covered but with fewer data points. At galactic latitudes |b| < 20° the data quality was reduced due to blending of stars resulting from the 14-arcseconds pixel size.

The pulsating red variable stars forming the subject of this study include Miras (M), semiregular (SR), and slow irregular (L) variables. The Miras and at least some of the SR variables are known to be on the asymptotic giant branch. Both the M and SR category variable stars obey period-luminosity relationships and so can be used as indicators of distance and as targets for studies of galactic kinematics.

A more detailed description of NSVS and a discussion of the importance of the red variable stars forming the subject of this survey was written by Woźniak *et al.* 2004.

It is important to appreciate that the boundaries between these three classes of variable stars are somewhat subjective, particularly so between SR and L variables. In a lot of cases data would need to be collected for many years before a definitive classification could be made.

Mira variables have periods between 80 and 1,000 days and light amplitudes between 2.5 magnitudes and 11 magnitudes in the V band, although infrared amplitudes can be less than 2.5 magnitudes. In situations where the observed amplitude is greater than 1–1.5 magnitudes, but where it is not certain that the full amplitude is greater than 2.5 magnitudes, the symbol M: can be used.

SR variables differ from Miras in having a visual amplitude of less than 2.5 magnitudes and/or a less regular light curve that may be interrupted by irregularities. The period of SR stars varies from 20 to over 2,000 days and the amplitude varies from less than 0.1 magnitude to several magnitudes.

There are four subtypes of semiregular variable stars:

SRa—Late type giants showing persistent periodicity, though both the amplitude and shape of the light curve vary between cycles. SRa stars can be distinguished from Mira type variables by the smaller amplitude.

SRb—Late type giants with poorly defined periodicity that might include spells of little or no variation.

SRc—Late type supergiants with amplitudes of about 1 magnitude.

SRd—Giants and supergiants of spectral classes F, G, and K that sometimes show emission lines in their spectra and with amplitudes in the range of 0.1 to 4.0 magnitudes.

Slow irregular (L) variable stars show little or no evidence of periodicity. Unfortunately, many stars are placed in this category because they have not been studied for long enough to allow accurate analysis of the light curve.

2. Data

Identification and classification of these red variable stars required time-resolved photometry and examination of the resultant light curve.

The one year of NSVS data was examined using the SQL interface available from the Skydot website (http://skydot.lanl.gov/nsvs/nsvs.php). The default settings for the eight extraction and seven photometric correction flags within the NSVS user interface were used except—following the suggestion of Wils, Lloyd, and Bernhard (2006)—the APINCOMPL flag was set and the RADECFLIP flags were unset. The function of the various quality flags are summarized in Table 1.

Wide field images of the type used in this survey are prone to photometric problems such as color-dependent atmospheric extinction and color-independent (gray) extinction due to thin cloud. These issues were minimized using the technique of local photometric corrections.

For each of the 644 fields a template was prepared for all persistent objects including the median object magnitude and the standard deviation of individual magnitudes around the median. By comparing the template results with those obtained from each exposure, photometric problems could be identified and quantified and the necessary corrections applied. This was done individually to each of 100 macro pixels—each of which comprised 200 × 200 detector pixels—each time a field was imaged.

The observed magnitude scatter, as used to generate error bars on the light curves, was based on the work of Wils, Lloyd, and Bernhard (2006) and is presented as Table 2.

In November 2006, when candidate variables were being identified and examined via the NSVS interface, the results were available in two forms. A light curve was generated automatically and the photometry contributing to the light curve was available in tabular form. Unfortunately the plotting of the light curve has been "temporarily unavailable" since early 2008.

The operational characteristics of NSVS created some photometric difficulties. The resolution of the four CCD cameras corresponded to a pixel size of 14.4 arcseconds and this resulted in significant cross-contamination between objects, particularly in crowded fields. The wide spectral response of the unfiltered charge-coupled devices used means that the quoted magnitude figures are most comparable to Cousins *R*-band values.

3. Object selection

The NSVS database contained nearly twenty million light curves so it was important to use selection criteria that would specifically identify red variable stars. Candidates were identified by data mining the Two-Micron All Sky Survey (2MASS, Skrutskie *et al.* 2006) for entries that matched the following criteria: Declination > –20.000, $(J-K) > 1.2$, and *J*-magnitude < 7.000. Stars matching all of these criteria would, respectively, fall within the region of the sky covered by NSVS, would be red in color, and would be bright enough for reliable photometry.

Although the positional accuracy of the 2MASS survey far exceeded that of NSVS there was little difficulty in matching specific NSVS entries to the 2MASS red stars previously identified by their magnitude in two different 2MASS pass bands. This was despite the use of a fairly conservative search radius of 15 arcseconds. In a number of cases one 2MASS entry matched up to two or more NSVS entries and such instances are reported in the results spreadsheet.

The light curves for all candidates were examined by eye to check for clear evidence of variability. Inevitably there was some subjectivity in this decision and a number of factors were taken into account.

Figures 1 and 2 are examples of slightly noisier curves, both showing evidence of a maximum or minimum magnitude being reached. This was taken as strong evidence of genuine variability.

Figure 3 is an example of a light curve where the overall variation in magnitude far exceeded any noise in the data. This, too, was taken as strong evidence of genuine variability.

In some cases almost all the observed amplitude of variation was due to a small number of outlying values. In such cases the variability was regarded as unproven and no further data processing was carried out.

As a further check, the magnitude data for a group of fifteen stars, provisionally identified as variable during the survey, were averaged over a range of dates and the results plotted to see if there was any evidence for a residual trend. If the average magnitude of the fifteen stars showed a consistent pattern of brightening or fading over time, then it would be possible for a star to be identified as variable purely on the basis of this systematic error rather than due to any change in the behavior of the star itself. The gradient of the resulting graph (+0.0007) was not indicative of any residual trend likely to invalidate any previous assessments of variability.

For over half of all the candidate variables examined there was no reliable light curve available from the NSVS archive. This was usually in those parts of the sky where blending of the stellar images was a problem, that is where |b| < 20°. In a small percentage of cases, despite there being enough photometry, there was insufficient evidence of variability. This was usually confined to fainter candidate variable stars where the noise in the data was proportionately greater.

As a final check, only stars not listed in the *Combined General Catalogue of Variable Stars* (Samus *et al.* 2004), *New Catalogue of Suspected Variable Stars and Supplement* (Kazarovets *et al.* 1998), *Red Variables in the NSVS* (Woźniak *et al.* 2004), not identified as variable in SIMBAD, or not identified as variable in the International Variable Star Index (VSX, Watson *et al.* 2007) at the time of original submission to the VSX moderation process have been included in the 1,233 "new discoveries."

4. Periods and amplitudes

The *General Catalogue of Variable Stars* (GCVS) classification scheme for these red variable stars is based only on the amplitude and regularity of the visual variation. Kiss *et al.* (1999) explored the factors that contributed to making an accurate assessment of these two key variables. They concluded that a continuous time-series lasting "a few decades, at least" was required. Providing the time-series is long enough both the period and amplitude determinations were "almost completely independent of the S/N ratio."

The time span of the NSVS results at twelve months was insufficient in the vast majority of cases for a valid estimate to be made of the period of variation. Similarly for these long period variable stars, twelve months of NSVS data is most unlikely to demonstrate the full amplitude of variation in the pass band used by the survey. Red variable stars also have a smaller amplitude in this pass band, most comparable to Cousins *R* band, than in the *V* band used by GCVS in the basis for classification.

The implication of these caveats is that any assignment of variability type in this list should be viewed as highly provisional. Many, particularly longer period, SR: variable stars will have been classified as L: variables due to insufficient data for an estimate of the period, and Mira variable stars will tend to get classified as SR: variables through under-estimation of the amplitude.

Any variable star with an amplitude of greater than 1.5 magnitudes and showing no sign of irregularity within the year of observation was provisionally classified as M:.

Variable stars with amplitudes of less than 1.5 magnitudes or showing clear departures from single-maximum periodicity were provisionally classified as SR: or L:. The distinction between SR: or L:—being based on a visual examination of the light curve—was somewhat subjective, but all stars for which it was possible to calculate a period of variation were automatically classified as SR:.

5. Reliability and completeness

All these new entries that were accepted into the International Variable Star Index (VSX) (http://www.aavso.org/vsx/) were required to go through a moderation process.

In the case of this survey every entry was subject to a clerical and then to an astronomical check by a volunteer moderator. VSX moderators are experienced observers and have usually looked at thousands of light curves in the course of their studies. The clerical check was used to ensure that the associated data files were complete and free from error, that the star was "clearly variable" based on the NSVS data, and that at the time that VSX was checked—November 2006 to January 2007—that the variability of each new entry had not previously been reported. Of course, any remaining errors are the responsibility of the author and not the moderator.

The joint astronomical check was used to inform the decision on the most appropriate classification to allocate to a small number of the candidate variable stars. This usually involved replacing a classification of L: with SR:.

6. Data access and light curves

Figures 1 and 2 illustrate the light curves of two of the higher amplitude variable stars discovered during the course of this project. In both cases a provisional classification of M: seems justified, although the previously mentioned caveats should not be ignored.

Figure 3 illustrates an example of a variable star with a provisional classification of SR, and Figure 6 illustrates a star that, while clearly variable, is difficult to classify.

Figures 4, 5, and 7 illustrate the variety of long period variables covered in this paper. The number of data points, the period covered by the graph, and the observed amplitude of variation all vary significantly.

All data relating to the new discoveries discussed in this paper can be downloaded from http://www.martin-nicholson.info/nsvs.xls. This file will also be archived and made available through the AAVSO ftp site at ftp://ftp.aavso.org/public/datasets/jnichm372.xls. The spreadsheet contains positional information, numerical identifiers (including 2MASS, GSC, Tycho, and IRAS data where available), magnitude data in six pass bands, spectral type, links to the original NSVS data, provisional variability type, period, epoch, and an estimate of the maximum and minimum magnitude of the variable star.

The spectral types quoted in the spreadsheet were obtained by cross referencing the 2MASS positions with the *Catalogue of Stellar Spectral Classifications* (Skiff 2008). These can be accessed via: http://vizier.u-strasbg.fr/viz-bin/VizieR?-source=B/mk.

7. Summary

A search for previously uncatalogued red variable stars in the publicly available data of the Northern Sky Variability Survey (NSVS) yielded a total of 1,233 such stars. These were all passed through the International Variable Star Index moderation process prior to inclusion in the database.

Only stars not listed in the *Combined General Catalogue of Variable Stars* (Samus *et al.* 2004), or in the *New Catalogue of Suspected Variable Stars and Supplement* (Kazarovets *et al.* 1998), or in *Red Variables in the NSVS* (Woźniak *et al.* 2004), or in VSX at the time of submission, or not identified as variable in SIMBAD have been included.

8. Acknowledgements

This publication makes use of data products from the Two Micron All Sky Survey, which is a joint project of the University of Massachusetts and the Infrared Processing and Analysis Center/California Institute of Technology, funded by the National Aeronautics and Space Administration and the National Science Foundation.

This research has made use of the SIMBAD database, operated at Centre de Données astronomiques de Strasbourg (CDS), Strasbourg, France.

Patrick Wils acted as moderator for the VSX online database.

References

Kazarovets, E. V., Samus, N. N., Durlevich, O. V. 1998, *New Catalogue of Suspected Variable Stars and Supplement, http://www.sai.msu.su/groups/cluster/gcvs/gcvs/nsv.*

Kiss, L. L., Szatmáry, K., Cadmus, R. R., Jr., and Mattei, J. A. 1999, *Astron. Astrophys.*, **346**, 542.

Samus, N. N., *et al.* 2004, *Combined General Catalogue of Variable Stars, http://www.sai.msu.su/groups/cluster/gcvs/gcvs.*

Skiff, B. 2008, *Catalogue of Stellar Spectral Classifications,* http://vizier.u-strasbg.fr/viz-bin/VizieR?-source=B/mk.

Skrutskie, M. F., *et al.* 2006, *The Two Micron All Sky Survey, Astron. J.*, **131**, 1163.

Watson, C. L., Henden, A. A., and Price, A. 2007, International Variable Star Index (VSX), http://www.aavso.org/vsx/*, J. Amer. Assoc. Var. Star Obs.*, **35**, 414.

Wils, P., Lloyd, C., and Bernhard, K. 2006, *Mon. Not. Roy. Astron. Soc.*, **368**, 1757.

Woźniak, P. R., Williams, S. J., Vestrand, W. T., and Gupta, V. 2004, *Astron. J.*, **128**, 2965.

Table 1. The NSVS data quality flags and their functions.

Data quality flag used	*Nature of problem*
SATURATED	Object has at least 1 saturated pixel
APINCOMPL	Aperture data incomplete or corrupted
NOCORR	Relative photometry correction could not be calculated
LONPTS	Low number of points in a macropixel
HISCAT	High scatter of magnitude differences in macropixel (> 0.2 mag.)
HICORR	High value of correction (> 0.1 mag.)
HISIGCORR	High scatter of corrections across the map (> 0.1 mag.)

Table 2. NSVS standard deviations as a function of magnitude.

NSVS Magnitude	*Average standard deviation*
9	0.04
10	0.03
11	0.03
12	0.04
13	0.07
14	0.12
15	0.2

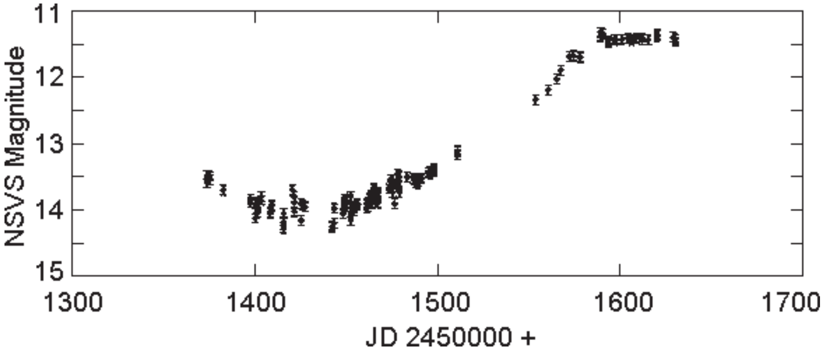

Figure 1. Star 2MASS 03415975+5542172 (#123), variable star type M:, in Camelopardalis.

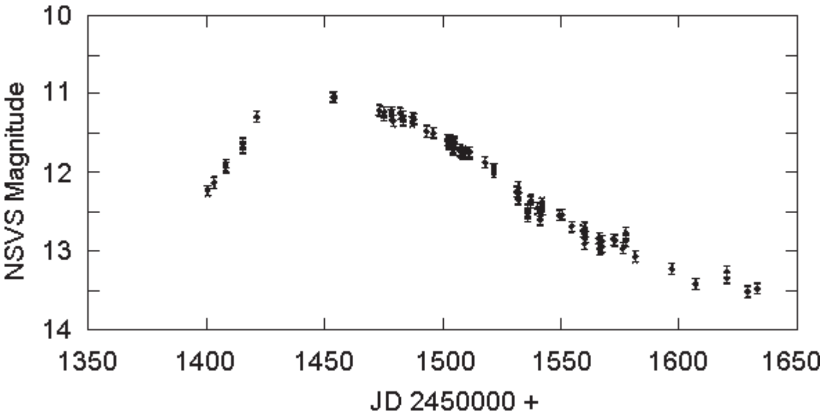

Figure 2. Star 2MASS 05045383+4657167 (#159), variable star type M:, in Auriga.

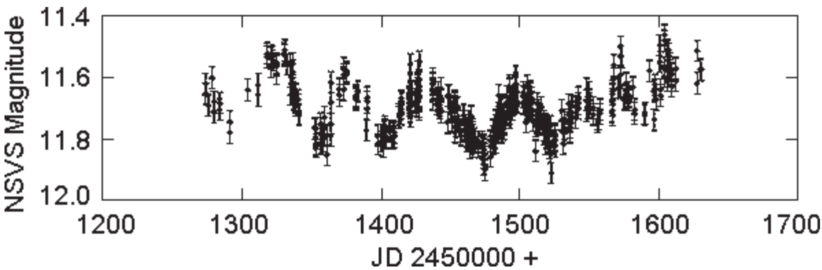

Figure 3. Star 2MASS 23325563+6746211 (#1214), variable star type SR:, in Cepheus.

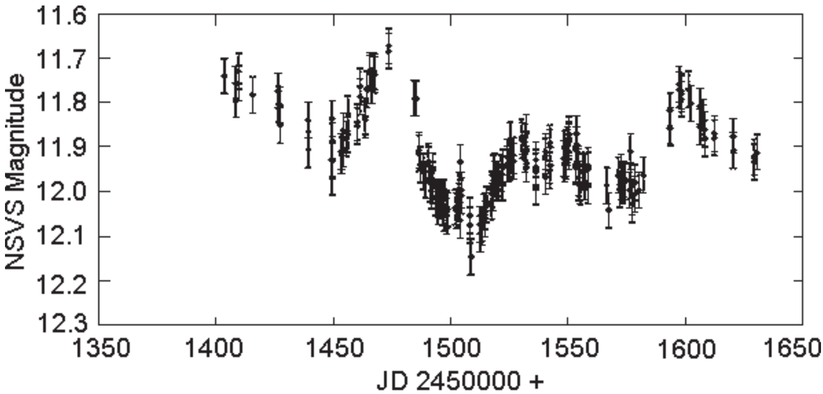

Figure 4. Star 2MASS 05211246+1930271 (#167), variable star type L:, in Taurus.

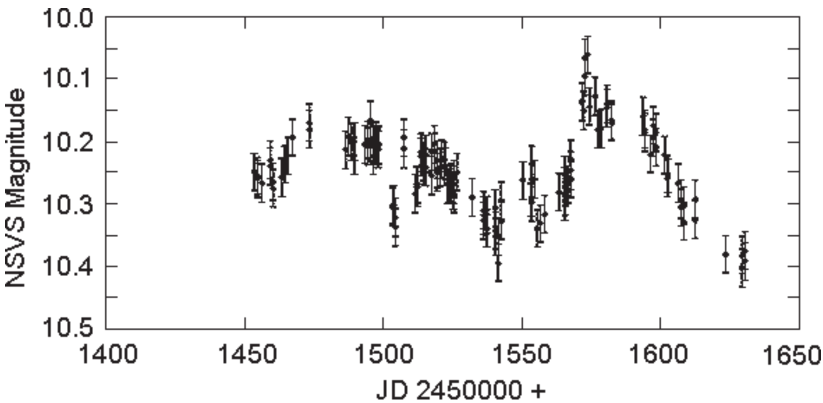

Figure 5. Star 2MASS 05443664+0236418 (#189), variable star type L:, in Orion.

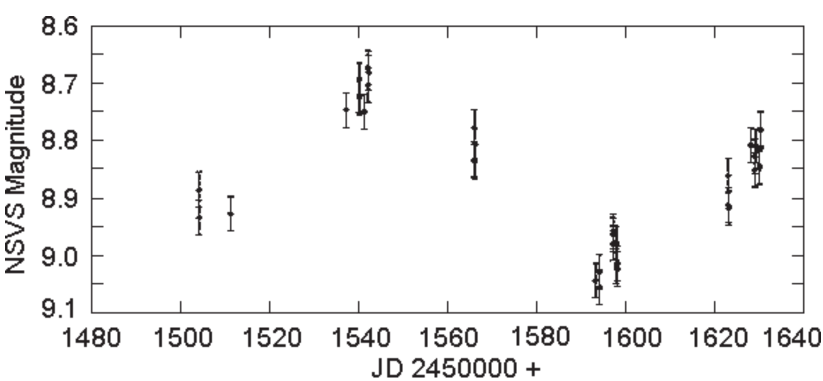

Figure 6. Star 2MASS 07065958+3136173 (#252), variable star type SR:, in Gemini.

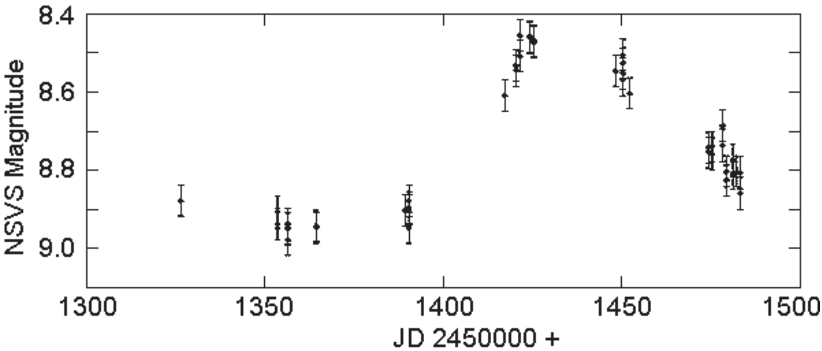

Figure 7. Star 2MASS 17200219-1556114 (#287), variable star type L:, in Serpens.

Figures—User notes:

1) The magnitude figures are most comparable to Cousins R *band values.*

2) The quoted variable star types are based on the classification system used within the General Catalogue of Variable Stars. This can be accessed at: http://www.sai.msu.su/groups/cluster/gcvs/gcvs/iii/vartype.txt

3) The quoted number—for example, #123—corresponds to the entry in the spreadsheet containing the data on each variable star.

4) Figures 1 through 7 include error bars based on the median magnitude of the variable star and the data listed in Table 2.

Searching Beyond the Obscuring Dust Between the Cygnus-Aquila Rifts for Cepheid Tracers of the Galaxy's Spiral Arms

Daniel J. Majaess
David G. Turner
David J. Lane
Saint Mary's University, Halifax, Nova Scotia, Canada

and

The Abbey Ridge Observatory, Stillwater Lake, Nova Scotia, Canada

Received August 13, 2009; revised August 20, 2009; accepted August 25, 2009

Abstract A campaign is described, open to participation by interested AAVSO members, of follow-up observations for newly-discovered Cepheid variables in undersampled and obscured regions of the Galaxy, a primary objective being to use these supergiants to clarify the Galaxy's spiral nature. Preliminary multiband photometric observations are presented for three Cepheids discovered beyond the obscuring dust between the Cygnus and Aquila Rifts ($40° \leq \ell \leq 50°$), a region reputedly tied to a segment of the Sagittarius-Carina arm which appears to cease unexpectedly. The data confirm the existence of exceptional extinction along the line of sight at upwards of $A_V \simeq 6$ magnitudes ($d \simeq 2$ kpc, $\ell \simeq 47°$), however, the noted paucity of optical spiral tracers in the region does not arise solely from incompleteness owing to extinction. A hybrid spiral map of the Galaxy comprised of classical Cepheids, young open clusters and H II regions, and molecular clouds presents a consistent picture of the Milky Way and confirms that the three Cepheids do not populate the main portion of the Sagittarius-Carina arm, which does not emanate locally from this region. The Sagittarius-Carina arm, along with other distinct spiral features, is found to deviate from the canonical logarithmic spiral pattern. Revised parameters are also issued for the Cepheid BY Cas, and it is identified on the spiral map as lying in the foreground to most young associations in Cassiopeia. A Fourier analysis of the light curve of BY Cas implies overtone pulsation, and the Cepheid is probably unassociated with the open cluster NGC 663 since the distances, ages, and radial velocities do not match.

1. Introduction

Classical Cepheid variables and young open clusters trace the Galaxy's spiral features in a consistent fashion (Walraven *et al.* 1958; Bok 1959; Kraft and Schmidt 1963; Tammann 1970; Opolski 1988; Efremov 1997; Berdnikov *et al.* 2006; Majaess *et al.* 2009). Establishing distances for newly discovered classical Cepheids is therefore useful for further studies of the Milky Way's structure.

The All Sky Automated Survey (ASAS, Pojmański 2000), the Northern Sky Variability Survey (NSVS, Woźniak *et al.* 2004), and The Amateur Sky Survey (TASS, Droege *et al.* 2006), have possibly made over 200 detections of new Cepheid variables through their photometric signatures (Akerlof *et al.* 2000; Wils and Greaves 2004; Schmidt *et al.* 2007; Berdnikov *et al.* 2009), a sizeable addition to the Galactic sample (Harris 1985; Berdnikov *et al.* 2000; Samus *et al.* 2009). However, some candidates possess only single passband photometry, which is insufficient for establishing either a distance or color excess through existing relations (Tammann *et al.* 2003; Benedict *et al.* 2007; van Leeuwen *et al.* 2007; Fouqué *et al.* 2007; Laney and Caldwell 2007; Majaess *et al.* 2008a; Turner 2009). The present study outlines a campaign of multiband photometry from the Abbey Ridge Observatory (Lane 2007; Majaess *et al.* 2008b) to establish mean *BV* magnitudes for newly detected classical Cepheids in undersampled regions of the Galaxy. The primary focus lies in long period classical Cepheids between the Cygnus-Aquila Rifts ($40° \leq \ell \leq 50°$, Forbes 1983, 1984, 1985; Dame *et al.* 2001; Straižys *et al.* 2003; Prato *et al.* 2008), the intent being to trace the Sagittarius-Carina arm through the first Galactic quadrant, where it appears to cease unexpectedly (e.g., Georgelin and Georgelin 1976). Long period classical Cepheids are young and massive (e.g., Turner 1996), ideal characteristics for objects used to delineate spiral structure, since they have not had time to travel far from their birthplaces in the arms.

This study also highlights ways in which small telescopes, like those used by most AAVSO members, can contribute to our knowledge of Galactic structure via classical Cepheids. The examples may provide inspiration for enthusiasts to add newly-discovered Cepheid variables to their own observing programs. On the order of a thousand variables are flagged as suspected Cepheids in the ASAS alone, of which a small yet relevant fraction are bona fide Cepheids. Multiband Johnson mean magnitudes for such objects would enable the determination of distances and reddenings through existing relationships (e.g., Majaess *et al.* 2008a; Turner 2009). Establishing reliable photometric parameters for new Cepheids increases the size of the Galactic sample, thereby helping to place stronger constraints on a host of Galactic parameters, including its warp and spiral structure (e.g., Majaess *et al.* 2009).

Precise differential CCD photometry for short period Cepheids is needed for Fourier analysis of their light curves in order to help constrain their pulsation mode (Beaulieu 1995; Welch *et al.* 1995; Beaulieu and Sasselov 1998; Zabolotskikh *et al.* 2005), an important characteristic affecting distance estimates ($\simeq 30\%$). The Cepheid BY Cas is provided as a pertinent example of how small telescope photometry can help. Detailed photometry for the star was obtained to assess its pulsation mode and to examine its possible membership in the open cluster NGC 663, an analysis prompted in part by the study of Usenko *et al.* (2001). Cluster membership is important for the calibration of classical Cepheid distances, reddenings, period-mass relations, and period-age relations (Turner 1996; Turner and Burke 2002; Laney and Caldwell 2007; Fouqué *et al.* 2007; Majaess *et al.* 2008a; Turner 2009). Classical Cepheids like BY Cas are also useful to establish the distance of the Sun above the plane, as well as to deduce the classical Cepheid scale height (Fernie 1968; Majaess *et al.* 2009). BY Cas is also identified on a hybrid spiral map of the Milky Way, which was constructed to assess the locations of the Cepheids surveyed within the broader context of the Galaxy.

2. Cepheid research from the ARO

The Abbey Ridge Observatory (Lane 2007; Majaess *et al.* 2008b) is engaged in a campaign aimed at studying Cepheid variables (Turner 2008; Turner *et al.* 2009b). Light curves for several Cepheids being monitored are presented in Figure 1 as an example of what can be achieved by means of small telescopes (e.g., the ARO). Research consists of monitoring northern hemisphere Cepheids to determine rates of period change, a parameter important for constraining rate of stellar evolution and location within the Cepheid instability strip (Turner *et al.* 2006). Suspected connections between classical Cepheids and open clusters are also being investigated (Turner and Burke 2002; Majaess *et al.* 2008a; Turner 2008), the objective being to establish additional calibrators for distance, reddening, period-mass, and period-age relations (Turner 1996; Turner and Burke 2002; Laney and Caldwell 2007; Majaess *et al.* 2008a; Turner 2009). Precise photometry ($\sigma \simeq 0.01$ magnitude) is being obtained for short period classical Cepheids to discriminate between fundamental mode and overtone pulsators, especially in previously ambiguous cases (e.g., BD Cas, Majaess *et al.* 2008a). A future campaign will aim to establish *VI* photometry for Type II Cepheids in globular clusters (Clement *et al.* 2001; Pritzl *et al.* 2003; Horne 2005; Randall *et al.* 2007; Rabidoux *et al.* 2007; Corwin *et al.* 2008), the primary objective being to test the metallicity dependence in Cepheid distance relations (Majaess *et al.* 2009).

The present study highlights our goal to establish mean *BV* observations for long period classical Cepheids discovered in the obscured and undersampled region between the Cygnus and Aquila Rifts (Figure 2).

3. Observations

All-sky *BV* photometry for our program objects were obtained on several nights, with extinction coefficients derived using techniques outlined by Henden and Kaitchuck (1998) and Warner (2006). The data were standardized to the Johnson system using stars in the open cluster NGC 225 for calibration (Hoag *et al.* 1961). Period analysis of the photometry was carried out in the PERANSO software environment (Vanmunster 2006) using the algorithms

ANOVA (Schwarzenberg-Czerny 1996), FALC (Harris *et al.* 1989), and CLEANEST (Foster 1995).

3.1. Cepheids (40° ≤ ℓ ≤ 50°)

Observations have been obtained for three newly discovered, suspected long period Cepheids from the NSVS (GSC 01050-00485 and GSC 01049-01505, Woźniak *et al.* 2004; Wils and Greaves 2004) and ASAS (GSC 01050-00361, Pojmański 2000). Phased *V*-band light curves for the Cepheids, and BY Cas, are illustrated in Figure 1, with relevant parameters summarized in Table 1.

Distances to the Cepheids were computed from a mean of *BV* and *VJ* reddening-free classical Cepheid distance relations (Majaess *et al.* 2008a), the latter using mean *J*-band magnitudes derived from single epoch 2MASS observations (Cutri *et al.* 2003) following a prescription outlined in Ma jaess *et al.* (2008a) (an alternative procedure can be found in Soszyński *et al.* 2005). Reddenings for the same stars were estimated from a Cepheid *VJ* color excess relation (Majaess *et al.* 2008a). Single epoch 2MASS infrared *J* magnitudes are available for most Cepheids, newly discovered or otherwise. Caution is urged in their use, however, since bright Cepheids ($J \sim 5$ magnitudes) may have saturated infrared magnitudes given their spectral energy distributions. Also, as noted by Majaess *et al.* (2008a), the derivation of mean magnitudes from single epoch observations has several complications, one being that Cepheids undergo changes in pulsation period (Szabados 1977, 1980, 1981; Berdnikov 1994; Berdnikov *et al.* 1997; Glushkova *et al.* 2006; Turner *et al.* 2006), so a significant time lapse between single epoch observations and those of the reference optical light curves can result in correspondingly large phase offsets. Long period Cepheids, in particular, tend to exhibit both random and rapid period changes (Turner and Berdnikov 2004; Turner *et al.* 2006; Berdnikov *et al.* 2007; Turner *et al.* 2009a). A large uncertainty in the periods determined for recently discovered Cepheids is a primary concern.

An additional ten stars from the ASAS are to be monitored as well, with relevant details to appear in a separate study.

3.2. BY Cas

The discovery of variability in BY Cas is attributed to Beljawsky (1931) (Gorynya *et al.* 1994). A Fourier analysis of the new ARO photometry yields an amplitude ratio $R_{21} = 0.069 \pm 0.011$, a value implying overtone pulsation (Welch *et al.* 1995; Beaulieu and Sasselov 1998; Zabolotskikh *et al.* 2005). The distance to BY Cas was computed from a mean of *BV* and *VI* reddening-free classical Cepheid distance relations (Majaess *et al.* 2008a), and the reddening was determined using a Cepheid *VI* color excess relation formulated from the same study. Infrared photometry (I_C) catalogued by Berdnikov *et al.* (2000) was used.

The membership of BY Cas in NGC 663, and thus its inferred distance and pulsation mode, have been questioned previously by Usenko *et al.* (2001). The implied age (t ~ 10^8 yrs, Turner 1996) and resulting distance for the Cepheid (Table 1) are inconsistent with parameters for the cluster NGC 663 (d ≃ 2.8 kpc, t ≃ 2 × 10^7 yrs, Phelps and Janes 1994), a discrepancy also confirmed by recent radial velocity measures of the cluster and Cepheid (Liu *et al.* 1991; Gorynya *et al.* 1994; Mermilliod *et al.* 2008). BY Cas is therefore unlikely to be a member of NGC 663, and its parameters obtained through use of the Cepheid relations are preferred (Table 1).

Lastly, Gorynya *et al.* (1994) argue on the basis of radial velocities that BY Cas is a binary Cepheid (Szabados 2003a).

4. The spiral nature of the Milky Way

Maps of the Milky Way's spiral structure exhibit striking differences (Russeil 2003; Nakanishi and Sofue 2003; Vallée 2005; Benjamin *et al.* 2006; Churchwell *et al.* 2009; Hou *et al.* 2009; Majaess *et al.* 2009). Some 150 years after Alexander (1852) first suggested that the Milky Way was a spiral, there is currently no consensus on the number of arms in our Galaxy. Moreover, the Sagittarius-Carina and Local arm are not well matched by superposed logarithmic spirals (Forbes 1983; Russeil 2003; Majaess *et al.* 2009). That may not be surprising given that an organized and idealistic grand design structure is not a characteristic shared by a sizeable fraction of the universe's spirals, including perhaps the Milky Way. Readers are encouraged to examine images of spiral galaxies observed by HST or catalogued in photographic atlases (Sandage and Bedke 1988) and note that galaxies commonly exhibit arms that branch, merge, twist unexpectedly, and feature a degree of irregularity or flocculence. Furthermore, the possible scenario of the Sun within a spur/Local arm (e.g., Russeil 2003) indicates that such features are likely not unique, and probably exist elsewhere in the Galaxy.

Majaess *et al.* (2009) noted that classical Cepheids (e.g., Berdnikov *et al.* 2000) and young open clusters (Dias *et al.* 2002; Mermilliod and Paunzen 2003) (YOCs) trace spiral features consistently (Figure 3, top and middle). The location of the classical Cepheids studied here have been tagged on the classical Cepheid-YOC map (triangles, Figure 3, middle). BY Cas appears to lie foreground to young associations in Cassiopeia (F, Figure 3, top). The new long period Cepheids occupy an obvious gap in the classical Cepheid-YOC data for Galactic longitudes spanning $\ell \simeq 35° - 50°$ (Forbes 1983, 1984, 1985; Majaess *et al.* 2009). The gap has complicated efforts to track the Sagittarius-Carina arm (A, Figure 3, top) through this region of the first quadrant, which straddles the Cygnus and Aquila Rifts (Figure 2).

The Cepheids studied here indicate that the extinction is exceptional along this line of sight, partly because of a nearby molecular cloud (Forbes 1983, 1984, 1985). The derived reddenings for the Cepheids at $\ell \simeq 47°$ (Table 1), in tandem with a standard ratio of total to selective extinction ($R = A_V / E_{B-V} = 3.06$, Turner 1976), imply extinction amounting to upwards of $A_V \simeq 3$ magnitudes per kiloparsec, in general agreement with previous results (Forbes 1983, 1984, 1985; Straižys *et al.* 2003). A hybrid spiral structure map consisting of classical Cepheids, YOCs and H II regions (Hou *et al.* 2009), and molecular clouds (Hou *et al.* 2009) indicates that the absence of optical spiral tracers in this region is not tied to incompleteness resulting from large extinction (Figure 3, bottom). An alternative delineation of the Sagittarius-Carina arm which deviates from the canonical superposed patterns is again advocated (Forbes 1983; Russeil 2003; Majaess *et al.* 2009). The arm appears to trace along features *A* and *B* (Figure 3, top) and may continue thereafter along $\ell \simeq 35°$ (Figure 3, bottom). The distinct signature of an additional arm possibly connecting to the Sagittarius-Carina arm can be traced through feature *C* (Figure 3, top). An abundance of optical tracers near $\ell \simeq 0°$ may be a junction that branches into the Carina (*A*) and Centaurus (*E*) features (Figure 3, top). More work is needed to thoroughly examine the connections. Classical Cepheids, YOCs and H II regions, and molecular clouds otherwise delineate the Milky Way's spiral features consistently at other Galactic longitudes.

Matching the distribution of classical Cepheids, YOCs and H II regions, and molecular clouds to a standard spiral pattern is rather challenging, especially in consideration of feature *F* (Figure 3), often treated as a major spiral feature (the reputed Perseus arm). No superposition of such a pattern has been made in Figure 3. Lastly, caution is urged because the spiral map displays features which are somewhat reminiscent of the "fingers of God effect" (see chapter 12 of Shu 1982).

5. Summary

Described here is a photometric campaign initiated at the Abbey Ridge Observatory aimed at establishing multiband photometry for new Cepheids. The objective is to determine reddenings and distances for key Cepheid variables in undersampled and heavily obscured regions of the Milky Way so to further elucidate any potential spiral structure. A general framework is outlined for AAVSO members interested in conducting similar research. Preliminary observations and photometric parameters are presented for three classical Cepheids discovered by the NSVS (Woźniak *et al.* 2004; Wils and Greaves 2004) and ASAS (Pojmański 2000) between the Cygnus-Aquila Rifts ($40° \leq \ell \leq 50°$), a region purportedly tied to a segment of the Sagittarius-Carina arm which appears to cease unexpectedly (e.g., Georgelin and Georgelin 1976). Reddenings inferred from the Cepheids confirm exceptional extinction along the line of sight at upwards of $A_V \simeq 6$ magnitudes ($d \simeq 2$ kpc, $\ell \simeq 47°$), however, it is shown by constructing a hybrid spiral map of the Milky Way from classical Cepheids, YOCs and H II regions, and molecular clouds, that the scarcity of optical spiral tracers in the region is not a consequence of incompleteness

owing to extinction. Rather, the hybrid map advocates an alternative delineation for the Sagittarius-Carina arm, and many other distinct features, which are not matched by conventional logarithmic spiral patterns. The three Cepheids surveyed between the Cygnus and Aquila Rifts ($40° \leq \ell \leq 50°$) do not populate the main portion of the Sagittarius-Carina arm.

The spiral tracers produce a consistent illustration of the Milky Way, reaffirming the importance of adopting a multifaceted approach to facilitate an interpretation of the Galaxy's complex structure. Supplementing optical spiral tracers like classical Cepheids with indicators that are less sensitive to extinction (e.g., molecular clouds) provides larger statistics and more confident conclusions.

Revised parameters issued for the Cepheid BY Cas place it mainly foreground to the young associations in Cassiopeia. The Cepheid is argued to be an overtone pulsator based on a Fourier analysis of its light curve. BY Cas is probably unassociated with the open cluster NGC 663, which exhibits a different distance, age, and radial velocitiy.

The future release of the ASAS-3N survey shall provide a statistically valid sample of new Cepheids with multiband *VI* photometry, thereby enabling the distances and reddenings for the variables to be readily determined. Observatories like the ARO and those run by fellow AAVSO members will continue to serve a role, especially in supplementing the faint end of the survey where the photometric zero-point becomes too uncertain. The present study supports a tradition of utilizing small telescopes to conduct pertinent Cepheid research (Percy 1980, 1986; Turner 1998; Turner *et al.* 1999, 2005, 2009b; Szabados 2003b).

6. Acknowledgements

We are indebted to Leonid Berdnikov and Laszlo Szabados, whose comprehensive research on Cepheid variables was invaluable to our analysis, to the authors of Hou *et al.* (2009) for making the relevant data on H II regions and molecular clouds accessible, Michael Sallman (TASS), Grzegorz Pojmański (ASAS), Arne Henden and Michael Saladyga (AAVSO), Alison Doane (HCO), Carolyn Stern Grant (ADS), and the staff at CDS. Reviews and books by Elmegreen (1985), Freedman and Madore (1996), Feast (1999, 2001), Fernie (1976, 2002), Hoffleit (2002), and Szabados (2006) were useful in the preparation of this work.

References

Akerlof, C., *et al.* 2000, *Astron. J.*, **119**, 1901.

Alexander, S. 1852, *Astron. J.*, **2**, 97.

Beaulieu, J. P. 1995, in *Astrophysical Applications of Stellar Pulsation*, eds. R. S. Stobie, and P. A. Whitelock, ASP Conf. Series Vol. 83, 260.

Beaulieu, J. P., and Sasselov, D. D. 1998, in *A Half Century of Stellar Pulsation Interpretation: A Tribute to Arthur N. Cox*, eds. P. A. Bradley and J. A. Guzik, ASP Conf. Series 135, p. 368.

Beljawsky, S. 1931, *Astron. Nachr.*, **243**, 115.

Benedict, G. F. *et al*. 2007, *Astron. J.*, **133**, 1810.

Benjamin, R. A., Churchwell, E., Haffner, M., and GLIMPSE team 2006, *Bull. Amer. Astron. Soc.*, **38**, 1229.

Berdnikov, L. N. 1994, *Astronomy Lett.*, **20**, 232.

Berdnikov, L. N., Dambis, A. K., and Vozyakova, O. V. 2000, *Astron. Astrophys., Suppl. Ser.*, **143**, 211.

Berdnikov, L. N., Efremov, Y. N., Glushkova, E. V., and Turner, D. G. 2006, *Odessa Astron. Publ.*, **18**, 26.

Berdnikov, L. N., Ignatova, V. V., Pastukhova, E. N., and Turner, D. G. 1997, *Astronomy Lett.*, **23**, 177.

Berdnikov, L. N., Kniazev, A. Y., Kravtsov, V. V., Pastukhova, E. N., and Turner, D. G. 2009, *Astronomy Lett.*, **35**, 39.

Berdnikov, L. N., Pastukhova, E. N., Gorynya, N. A., Zharova, A. V., and Turner, D. G. 2007, *Publ. Astron. Soc. Pacific*, **119**, 82.

Bok, B. J. 1959, *Observatory*, **79**, 58.

Churchwell, E., *et al.* 2009, *Publ. Astron. Soc. Pacific*, **121**, 213.

Clement, C. M., *et al.* 2001, *Astron. J.*, **122**, 2587.

Corwin, T. M., Borissova, J., Stetson, P. B., Catelan, M., Smith, H. A., Kurtev, R., and Stephens, A. W. 2008, *Astron. J.*, **135**, 1459.

Cutri, R. M. *et al.* 2003, *The IRSA 2MASS All-Sky Point Source Catalog*, NASA/IPAC Infrared Science Archive, http://irsa.caltech.edu/applications/Gator/

Dame, T. M., Hartmann, D., and Thaddeus, P. 2001, *Astrophys. J.*, **547**, 792.

Dame, T. M., and Thaddeus, P. 1985, *Astrophys. J.*, 297, 751.

Dias, W. S., Alessi, B. S., Moitinho, A., Lépine, J. R. D. 2002, *Astron. Astrophys.*, **389**, 871.

Droege, T. F., Richmond, M. W., Sallman, M. P., Creager, R. P. 2006, *Publ. Astron. Soc. Pacific*, **118**, 1666.

Efremov, Y. N. 1997, *Astronomy Lett.*, **23**, 579.

Elmegreen, D. M. 1985, in *The Milky Way Galaxy*, Proc. 106 Symp. Groningen, Netherlands, May 30–June 3, 1983, Reidel, Dordrecht, 255.

Feast, M. 1999, *Publ. Astron. Soc. Pacific*, **111**, 775.

Feast, M. 2001, arXiv:astro-ph/0110360.

Fernie, J. D.1968, *Astron. J.*, **73**, 995.
Fernie, J. D. 1976, *The Whisper and the Vision—The Voyages of the Astronomers*, Clarke, Irwin, Toronto.
Fernie, J. D. 2002, *Setting sail for the universe: astronomers and their discoveries*, Rutgers University Press, New Brunswick, NJ.
Forbes, D. 1983, *The Distribution of Spiral Structure Tracers in the Region of the Galaxy Between 30 Degrees and 70 Degrees*, Ph.D. Thesis, Univ. Victoria, Canada.
Forbes, D. 1984, *Astron. J.*, **89**, 475.
Forbes, D. 1985, *Astron. J.*, **90**, 301.
Foster, G. 1995, *Astron. J.*, **109**, 1889.
Fouqué, P. *et al.* 2007, *Astron. Astrophys.*, **476**, 73.
Freedman, W. L., and Madore, B. F. 1996, in *Clusters, Lensing, and the Future of the Universe*, eds. V. Trimble and A. Reisenegger, ASP Conf. Proc. 88, 9.
Georgelin, Y. M., and Georgelin, Y. P. 1976, *Astron. Astrophys.*, **49**, 57.
Glushkova, E. V., Berdnikov, L. N., and Turner, D. G. 2006, *Mem. Soc. Astron. Italiana*, **77**, 127 7.
Gorynya, N. A., Samus, N. N., Rastorgouev, A. S. 1994, *Inf. Bull. Var. Stars*, No. 4130, 1.
Harris, A. W. *et al.* 1989, *Icarus*, **77**, 171.
Harris, H. C. 1985, *Astron. J.*, **90**, 756.
Henden, A. A., and Kaitchuck, R. H. 1998, *Astronomical Photometry: A Text and Handbook for the Advanced Amateur and Professional Astronomer*, Willmann-Bell, Richmond.
Hoag, A. A., Johnson, H. L., Iriarte, B., Mitchell, R. I., Hallam, K. L., and Sharpless, S. 1961, *Publ. United States Naval Obs.*, **17**, 343.
Hoffleit, D. 2002, *Misfortunes As Blessings in Disguise: The Story of My Life*, AAVSO, Cambridge, MA.
Horne, J. D. 2005, *J. Amer. Assoc. Var. Star Obs.*, **34**, 61.
Hou, L. G., Han, J. L., and Shi, W. B. 2009, *Astron. Astrophys.*, **499**, 473.
Kraft, R. P., and Schmidt, M. 1963, *Astrophys. J.*, **137**, 249.
Lane, D. J. 2007, "96th Spring Meeting of the AAVSO," http://www.aavso.org/aavso/meetings/spring07present/Lane.ppt.
Laney, C. D., and Caldwell, J. A. R. 2007, *Mon. Not. Roy. Astron. Soc.*, **377**, 147.
Liu, T., Janes, K. A., and Bania, T. M. 1991, *Astron. J.*, **102**, 1103.
Majaess, D. J., Turner, D. G., and Lane, D. J. 2008 (a), *Mon. Not. Roy. Astron. Soc.*, **390**, 1539.
Majaess, D. J., Turner, D. G., and Lane, D. J. 2009, arXiv:0903.4206.
Majaess, D. J., Turner, D. G., Lane, D. J., and Moncrieff, K. E. 2008 (b), *J. Amer. Assoc. Var. Star Obs.*, **36**, 90.
Mermilliod, J.-C., Mayor, M., and Udry, S. 2008, *Astron. Astrophys.*, **485**, 303.
Mermilliod, J.-C., and Paunzen, E. 2003, *Astron. Astrophys.*, **410**, 511.

Nakanishi, H., and Sofue, Y. 2003, *Publ. Astron. Soc. Japan*, **55**, 191.

Opolski, A. 1988, *Acta Astron.*, **38**, 375.

Percy, J. R. 1980, *J. Roy. Astron. Soc. Canada*, **74**, 334.

Percy, J. R. 1986, *The Study of Variable Stars Using Small Telescopes*, Cambridge Univ. P., Cambridge.

Phelps, R. L., and Janes, K. A. 1994, *Astrophys. J., Suppl. Ser.*, **90**, 31.

Pojmański, G. 2000, *Acta Astron.*, **50**, 177.

Prato, L., Rice, E. L., and Dame, T. M. 2008, *Handbook of Star Forming Regions, Volume I: The Northern Sky,* ASP Monograph Publications, Vol. 4., ed. B. Reipurth, 18.

Pritzl, B. J., Smith, H. A., Stetson, P. B., Catelan, M., Sweigart, A. V., Layden, A. C., and Rich, R. M. 2003, *Astron. J.*, **126**, 1381.

Rabidoux, K., *et al.* 2007, *Bull. Amer. Astron. Soc.*, **39**, 845.

Randall, J. M., Rabidoux, K., Smith, H. A., De Lee, N., Pritzl, B., and Osborn, W. 2007, *Bull. Amer. Astron. Soc.*, **38**, 276.

Russeil, D., 2003, *Astron. Astrophys.*, **397**, 133.

Samus, N. N., *et al.* 2009, VizieR Online Data Catalog, 1, 2025.

Sandage, A., and Bedke J. 1988, *Atlas of Galaxies Useful for Measuring the Cosmological Distance Scale*, NASA Special Publ., Vol. 496, Space Telescope Science Institute, Baltimore.

Schmidt, E. G., Langan, S., Rogalla, D., and Thacker-Lynn, L. 2007, *Astron. J.*, **133**, 665.

Schwarzenberg-Czerny, A. 1996, *Astrophys. J.*, **460**, L107.

Shu, F. H. 1982, *A Series of Books in Astronomy*, University Science Books, Mill Valley, CA.

Soszyński, I., Gieren, W., and Pietrzyński, G. 2005, *Publ. Astron. Soc. Pacific*, **117**, 823.

Straižys, V., Černis, K., and Bartašiūtė, S. 2003, *Astron. Astrophys.*, **405**, 585.

Szabados L., 1977, *Commun. Konkoly Obs.*, **70**, 1.

Szabados L., 1980, *Commun. Konkoly Obs.*, **76**, 18.

Szabados L., 1981, *Commun. Konkoly Obs.*, **77**, 1.

Szabados, L. 2003a, *Inf. Bull. Var. Stars*, No. 5394, 1.

Szabados, L. 2003b, in *The Future of Small Telescopes In The New Millennium. Volume III—Science in the Shadows of Giants*, ed. T. D. Oswalt, Astrophys. Space Sci. Library, 289, Kluwer Academic Publishers, Dordrecht, p.207.

Szabados, L. 2006, *Commun. Konkoly Obs.*, **104**, 105.

Tammann, G. A. 1970, in *The Spiral Structure of our Galaxy*, ed. W. Becker and G. T. Kontopoulos, IAU Symp. 38, 236.

Tammann, G. A., Sandage, A., and Reindl, B. 2003, *Astron. Astrophys.*, **404**, 423.

Turner, D. G. 1976, *Astron. J.*, **81**, 97.

Turner, D. G. 1996, *J. Roy. Astron. Soc. Canada*, **90**, 82.

Turner, D. G. 1998, *J. Amer. Assoc. Var. Star Obs.*, **26**, 101.

Turner, D. G. 2008, *J. Amer. Assoc. Var. Star Obs.*, **36**, 140.

Turner D. G. 2009, *Astrophys. Space Sci.,* submitted.

Turner, D. G., Abdel-Sabour Abdel-Latif, M., and Berdnikov, L. N. 2006, *Publ. Astron. Soc. Pacific*, **118**, 410.

Turner, D. G., and Berdnikov, L. N. 2004, *Astron. Astrophys.*, **423**, 335.

Turner, D. G., and Burke, J. F. 2002, *Astron. J.*, **124**, 2931.

Turner, D. G., Forbes, D., Leonard, P. J. T., Abdel-Sabour Abdel-Latif, M., Majaess, D. J., and Berdnikov, L. N. 2009a, arXiv:0905.0834.

Turner, D. G., Horsford, A. J., and MacMillan, J. D. 1999, *J. Amer. Assoc. Var. Star Obs.*, **27**, 5.

Turner, D. G., Majaess, D. J., Lane, D. J., Szabados, L., Kovtyukh, V. V., Usenko, I. A., and Berdnikov, L. N. 2009b, arXiv:0907.2969.

Turner, D. G., Savoy, J., Derrah, J., Abdel-Sabour Abdel-Latif, M., and Berdnikov, L. N. 2005, *Publ. Astron. Soc. Pacific*, **117**, 207.

Usenko, I. A., Kovtyukh, V. V., Klochkova, V. G., Panchuk, V. E., and Yermakov, S. V. 2001, *Astron. Astrophys.*, **367**, 831.

van Leeuwen, F., Feast, M. W., Whitelock, P. A., and Laney, C. D. 2007, *Mon. Not. Roy. Astron. Soc.*, **379**, 723.

Vallée, J. P. 2005, *Astron. J.*, **130**, 569.

Vanmunster, T. 2006, PERANSO period analysis software, CBABelgium.com.

Walraven, T., Muller, A. B., and Oosterhoff, P. T. 1958, *Bull. Astron. Inst. Netherlands*, **14**, 81.

Warner, B. D. 2006, *A Practical Guide to Lightcurve Photometry and Analysis*, Springer, Berlin.

Welch, D. L., *et al.* 1995, in *Astrophysical Applications of Stellar Pulsation: the Interaction between Observation and Theory*, eds. R. S. Stobie and P. A. Whitelock, IAU Coll. 155, ASP Conf. Series Vol. 83, 232.

Wils, P., and Greaves, J. 2004, *Inf. Bull. Var. Stars*, No. 5512, 1.

Woźniak, P. R., *et al.* 2004, *Astron. J.*, **127**, 2436.

Zabolotskikh, M. V., Sachkov, M. E., Berdnikov, L. N., Rastorguev, A. S., and Egorov, I. E., 2005, in *The Three-Dimensional Universe with Gaia*, eds. C. Turun, K. S. O'Flaherty, and M. A. C. Perryman, (ESA SP-576), 723 (http://www.rssd.esa.int/index.php?project=Gaia&page=Gaia_2004_Proceedings).

Table 1. Cepheids observed from the Abbey Ridge Observatory.

Star ID	ℓ (°)	*P* (*days*)	*V*	*B–V*	V_a	B_a	*d* (*kpc*)	E_{B-V}
GSC 01050-00485	47.61	18.25 ± 0.03	14.02	3.02	0.9	1.5	2.0	1.9
GSC 01050-00361	47.56	8.63 ± 0.01	10.44	1.96	0.42	0.62	1.1	1.1
GSC 01049-01505	45.49	20.84 ± 0.03	13.92	2.53:	0.7	1.0:	5.2:	1.4:
BY Cas	129.55	3.2215 ± 0.0006	10.38	—	1.29	—	1.7	0.6

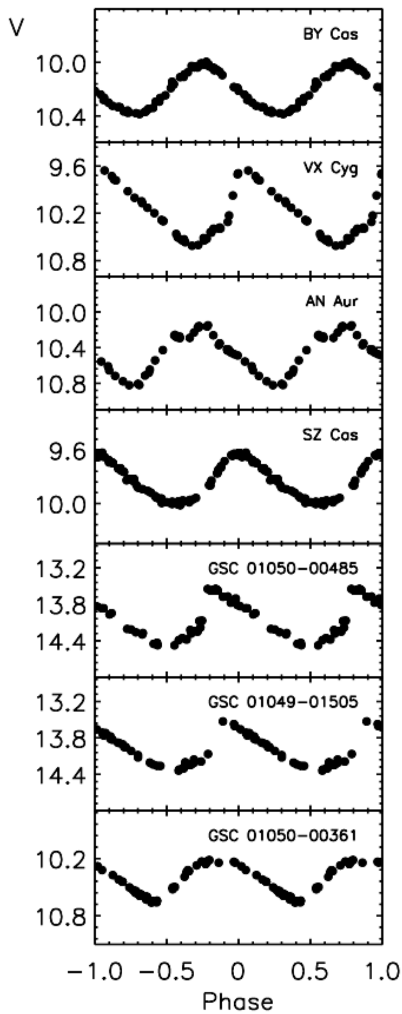

Figure 1. Light curves for several Cepheids being monitored from the Abbey Ridge Observatory.

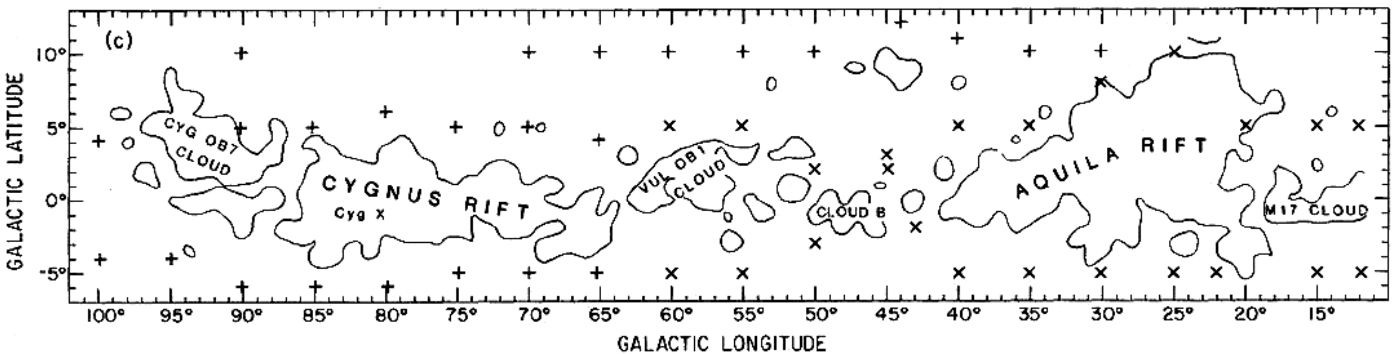

Figure 2. Velocity-integrated CO emission map from the seminal work of Dame and Thaddeus (1985). Much of the region is obscured by molecular clouds, hampering efforts to infer the Galaxy's spiral structure using optical tracers.

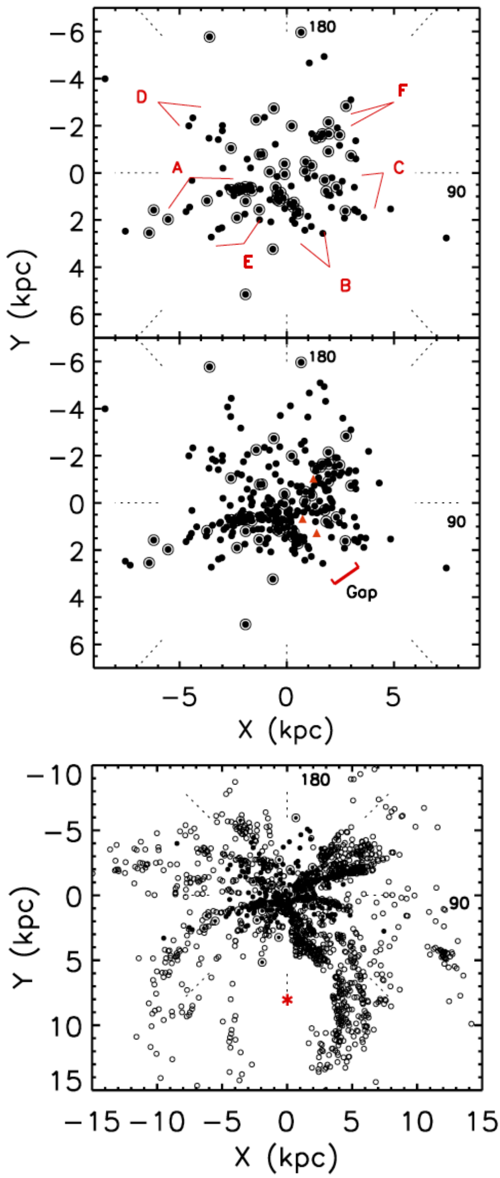

Figure 3. Top and middle: local spiral structure as delineated by classical Cepheid variables (solid points) and young open clusters (YOCs, circled points). See Majaess *et al.* (2009) for details and the corresponding identifiers. Middle: the gap of optical tracers and locations of the Cepheids (triangles) studied here are highlighted. Bottom, the structure of the Milky Way as illustrated by classical Cepheids, YOCs and H II regions, and molecular clouds (see text for details). Galactic center is denoted by an asterisk (Majaess *et al.* 2009).

Abstracts of Papers and Posters Presented at the 97th Annual Meeting of the AAVSO, Held in Nantucket, Massachusetts, October 16–19, 2008

The International Year of Astronomy and Citizen Science

Aaron Price
AAVSO, 49 Bay State Road, Cambridge, MA 02138

Abstract 2009 has been endorsed as the International Year of Astronomy by both the United Nations and the United States Congress. This talk will briefly outline the IYA cornerstone projects and then will go into more detail regarding the AAVSO's role as leading a citizen science project regarding the variable star epsilon Aurigae.

Variable Star Astronomy Education Outreach Initiative

Donna L. Young
The Wright Center for Innovative Science, Tufts University, 4 Colby Street, Medford, MA 02155

Abstract The American Association of Variable Star Observers (AAVSO) published a comprehensive variable star curriculum, *Hands-On Astrophysics, Variable Stars in Science, Math, and Computer Education* in 1997. The curriculum, funded by the National Science Foundation, was developed for a comprehensive audience—amateur astronomers, classroom educators, science fair projects, astronomy clubs, family learning, and anyone interested in learning about variable stars. Some of the activities from the *Hands-On Astrophysics* curriculum have been incorporated into the educational materials for the Chandra X-Ray Observatory's Educational and Public Outreach (EPO) Office. On two occasions, in 2000 and 2001, triggered by alerts from amateur astronomers, Chandra observed the outburst of the dwarf nova SS Cygni. The cooperation of amateur variable star astronomers and Chandra X-Ray scientists provided proof that the collaboration of amateur and professional astronomers is a powerful tool to study cosmic phenomena. Once again, the Chandra and AAVSO have teamed up—this time to promote variable star education. The *Hands-On Astrophysics* curriculum is being re-designed and updated from the original materials to a web-based format and is nearing completion. The new version, re-named Variable Star Astronomy, will provide formal and informal educators, and especially amateur astronomers, educational materials to help promote interest in and knowledge of variable stars.

Update on HST Campaign on Pulsating White Dwarfs in Cataclysmic Variables

Paula Szkody
University of Washington, Department of Astronomy, Box 351580, Seattle, WA 98195

Abstract For the past six years, we have conducted programs on the Hubble Space Telescope, coordinated with ground support from the AAVSO network of observers. These programs have determined temperatures for nine of the dozen known pulsating white dwarfs that exist in cataclysmic variables. Unlike single, non-accreting, white dwarfs, which have a very narrow range of temperatures within their instability strip, the accreting pulsators range from 10,500K to 16,500K with most being near the hot end. In addition, the accreting pulsators are found to stop showing pulsations at times, a phenomenon not seen in the single white dwarfs. The superoutbursts of two of our systems in 2007 complicates the picture further but allows the chance to study the effect of temperature changes on a relatively short timescale.

Forty Years of Mystery: Unraveling BZ UMa

Aaron Price
AAVSO, 49 Bay State Road, Cambridge, MA 02138

Grant Foster
541 Cumberland Avenue, #2, Portland, ME 04101

Abstract The dwarf novae BZ UMa has perplexed astronomers for decades. Activity typical of both UGSU and intermediate polar (IP) dwarf novae have been detected while no expected UGSU type superoutbursts had been detected since the star was discovered in 1968. Finally, the diligence of variable star observers was once again rewarded with a superoutburst in April, 2007. We report on statistical analysis of the 2007 superoutburst and subsequent polarimetry measurements. We integrate all our findings into a proposed description and classification of the system.

120 Years of RZ Dor

James Bedient
1464 Molehu Drive, Honolulu, HI 96818

Abstract Archival data on RZ Dor is examined to update its type and period. Data ranging from pre-1900 Harvard plates through AAVSO visual estimates made during the 1980s and 1990s, to 21st century CCD photometry, is used to confirm its type as Mira and determine an accurate period. The value of multiple independent accessible datasets is confirmed yet again.

The Evolution of R Coronae Borealis Stars

Geoffrey C. Clayton
Louisiana State University, Department of Physics and Astronomy, Baton Rouge, LA 70803

Abstract Among the hydrogen-deficient post-asymptotic giant branch (post-AGB) stars are the R Coronae Borealis (RCB) stars, a small group of carbon-rich supergiants. About fifty RCB stars are known in the Galaxy and the Magellanic Clouds. Their defining characteristics are hydrogen deficiency and unusual variability—RCB stars undergo massive declines of up to 8 magnitudes due to the formation of carbon dust at irregular intervals. Apparently related to the RCB stars are the hydrogen-deficient carbon (HdC) stars. The five known HdC stars are similar to the RCB stars spectroscopically but do not show declines or IR excesses. The evidence for and against the two scenarios that have been proposed for the origin of RCB stars is discussed in the light of recent observational data. These scenarios are, the double degenerate and the final helium-shell flash models. The former involves the merger of a CO- and a He-white dwarf. In the latter, a star evolving into a planetary nebula central star is blown up to supergiant size by a final helium shell flash.

How Do Pulsating Giant Stars Make Dust?

Lee Anne Willson
Iowa State University, Department of Physics and Astronomy, Ames, IA 50011

Abstract Mira variables of spectral types M (more oxygen than carbon), S (carbon ≈ oxygen), and C (more carbon than oxygen) all show signs of dusty winds. Radiative acceleration of the dust is thought to play a crucial role in driving the winds, once the atmosphere has been levitated by the pulsation. However, efforts to model the nucleation and growth of dust grains have encountered a host of difficulties. The process is complex, involving a very large number of reactions of particles (atoms, molecules, clusters, and grains) with each other. The coupling of the grains to the radiation field is also difficult to model with confidence, as it depends on the composition, the size, and the shape of the grains. Common approximations to make the problem tractable have lead to results that contradict observations; for example, they predict that S stars should produce no dust, but some S stars do. Some ideas for solving

this problem come from laboratory studies. There may also be ways to get the right result without so much work by taking advantage of natural feedback evident in the models.

The Chandra Variable Guide Star Catalog

Joy S. Nichols
Harvard-Smithsonian Center for Astrophysics, 60 Garden Street, Cambridge, MA 34, MA 02138

David A. Huenemoerder
Massachusetts Institute of Technology, Kavli Institute, 77 Massachusetts Avenue, NE80-6065, Cambridge, MA 02139

E. Martin
J. Lauer
D. Morgan
Harvard-Smithsonian Center for Astrophysics, 60 Garden Street, Cambridge, MS 34, MA 02138

Arne A. Henden
AAVSO, 49 Bay State Road, Cambridge, MA 02138

Abstract The Chandra X-ray Observatory has observed about 37,000 stars in the wavelength range 4000-9000 Å as guide stars for maintaining pointing control of the satellite. While these guide stars were intended to be non-variable in order to maximize the pointing accuracy, we have found that 673 are variable, generally at the 0.05 magnitude level. The catalog of these variable guide stars includes many types of variable stars, including pulsating stars, detached eclipsing binaries, contact binaries, etc., with spectral types generally in the range A through K. Light curves of these variables are the same length as the X-ray observation performed by Chandra, varying from 1 ksec to 170 ksec. *The Chandra Guide Star Catalog* includes about 300 stars that appear to be newly discovered variables. A description of the instrumentation is included and interesting examples from the catalog are shown and discussed. We introduce a new collaboration between the Chandra Variable Guide Star Team and members of the AAVSO, who will enhance this catalog with expertise in variable star characteristics. For future investigation, we intend to reprocess all available photometry in order to look for long-term variability and lower amplitude fluctuations that may not be apparent in the visual inspection of the existing time series. This work was supported by NASA contract NAS8-37073.

A Microprocessor-based Starfield Simulator

Douglas L. Welch
McMaster University, Physics and Astronomy, 1280 Main Street, W., Hamilton, ON L8S 4M1, Canada

Anthony Tekatch
4 Lawrence Avenue, Grimsby, ON L3M 2L9, Canada

Steve Bickerton
Princeton University, Department of Astrophysical Sciences, Peyton Hall, Princeton, NJ 08544

Abstract We present a microprocessor-based system for reproducing the realtime behavior of stellar time-series, including the effects of selectable degrees scintillation noise. At present, the system has sixty-four white LEDs which are individually programmable. The simulator may be used to investigate measurement and analysis biases since all properties of star (constant and variable) are under the control of the programmer. A live demonstration of the unit will be provided.

Automated Calibration and an Open-source Sky Survey

David W. Hogg
New York University, Department of Physics, 4 Washington Place, New York, NY 10003

Abstract I describe a system that can take any astronomical image (professional, historical, or amateur) and, based on the content of the pixels alone, determine the pointing, rotation, and scale of that image, plus other calibration information (such as date, bandpass, point-spread function, and sensitivity). We are using this system to start an "open-source sky survey" in which we build up time-resolved imaging of the sky, and a physical model of the sources therein, from heterogeneous data from all available sources. This is a great opportunity to start a rich communication channel between professional and amateur astronomers, with data and ideas flowing both ways.

Overview of the DASCH Photometry Pipeline (poster)

Edward J. Los
7 Cheyenne Drive, Nashua, NH 03063

Abstract DASCH is "Digital Access to a Sky Century at Harvard," the effort to digitize approximately 520,000 astronomical plates in the Harvard College Observatory collection. This paper is an overview of the photometry pipeline which has generated over 400 million magnitude measurements from over 3,400 scanned plates.

First Steps Towards a Solar Flare Detector Using the AAVSO Design (poster)

James F. Breitmeyer
Dexter School, 20 Newton Street, Brookline, MA 02445

Abstract Solar flares—ephemeral events often lasting only twenty minutes or so—can be detected indirectly using "sudden ionospheric disturbances," or SIDs. SIDs increase the efficiency of very low-frequency radio waves being reflected by the Earth's ionosphere. During a solar flare, a terrestrial radio station that is normally received as a weak signal can suddenly become much stronger. This characteristic rise in signal strength has been recognized for its correlation with observed solar flares. The AAVSO SID Program offers instructions on its website for construction, tuning, and use of a very low frequency radio receiver appropriate for monitoring solar flares. We have begun building and testing a SID detector, and we look forward to participating in the AAVSO SID Program as solar activity increases in the current new Cycle 24. Our experience may suggest improvements that will make building future SID detectors easier. Besides contributing to the AAVSO database, we are interested to detect solar flares in a timely way for visual observation using a hydrogen-alpha filter. We are also interested in the inevitable, eventual recurrence of "monster" solar flares—for example, the white-light event of 1859 observed by Richard Carrington and the consequent world-wide, violent geomagnetic storm.

Reclaiming the Astronomical and Historical Legacy of Antonia Maury

Kristine Larsen
Central Connecticut State University, Physics and Earth Sciences, 1615 Stanley Street, New Britain, CT 06053

Abstract Antonia Maury is perhaps best known in astronomical history circles as a student of Maria Mitchell's at Vassar and a pioneer in spectral classification at the Harvard College Observatory. Among her other astronomical interests were eclipsing and spectroscopic binaries, especially beta Aurigae (which she discovered) and beta Lyrae, whose peculiar behavior occupied her interest in the later years of her career. This paper will highlight Maury's often overlooked contributions to variable star and binary star astronomy, and strive to put a human face on this brilliant yet enigmatic woman astronomer through personal stories told to the author by Dorrit Hoffleit.

Henrietta Swan Leavitt

Katy Sternberger
Portsmouth Christian Academy, 20 Seaborne Drive, Dover, NH 03820

Abstract Henrietta Swan Leavitt, born in 1868, was a great woman astronomer. Though she is not widely known for her work, she studied Cepheid variable stars and devised a law which states that a star's brightness is directly linked to the length of its period. This launched the quest to discover how to measure the universe.

Abstract of Poster Presented at the 94th Spring Meeting of the AAVSO, Held in Las Cruces, New Mexico, March 25–26, 2005

Outreach at Cornell University's Fuertes Observatory (poster)

Richard C. S. Kinne
Cornell Astronomical Society, 130 E. South St., Groton, NY 13073

Abstract Fuertes Observatory on Cornell University's North Campus in Ithaca, New York, has been rendered useless to research by age and increasing light pollution from a built-up North Campus. However, the Cornell Astronomical Society has adopted the Observatory and has used it to create a growing astronomical outreach program. By creating a popular lecture series and carefully choosing particular astronomical objects to show visitors to the Observatory, the Society is assisting in enhancing popular astronomical education in Ithaca. This poster gives details as to the groups that come to the Observatory, the lecture topics that have been given, and the best astronomical objects that have been shown in light polluted skies.

Abstracts of Papers and Posters Presented at the Joint Meeting of the Society for Astronomical Sciences and the American Association of Variable Star Observers, Held in Big Bear Lake, California, May 19–21, 2009

The AAVSO Wide-Field Photometric Survey

Arne A. Henden
AAVSO, 49 Bay State Road, Cambridge, MA 02138

Abstract The Robert Martin Ayers Sciences Fund has provided funding for a photometric survey of the entire sky. This survey will be conducted in five photometric bands (Johnson *B*, *V*, and Sloan *g'*, *r'*, *i'*) using a pair of ASA N8 astrographs and Apogee U16m 4k × 4k CCD cameras. The survey begins with installation at Dark Ridge Observatory near Weed, NM, to cover the northern declinations. In early 2010, the system will be moved to Chile, where it will survey the southern skies. We estimate the limiting magnitudes of the survey to be between 10th and 17th magnitude, and approximately 100M stars will be in the final catalogue. All intermediate products will be available from the AAVSO web site starting in summer 2009. This paper will present early results from the survey, and discuss the ancillary science that will be performed on non-photometric nights. *[Ed. note: survey formally named the AAVSO Photometric All-Sky Survey (APASS)]*

AAVSO Long Period Variable Section Update

Kate Hutton
969 E. Mountain St., Pasadena, CA 91104

Michael Simonsen
C. E. Scovil Observatory, 2615 S. Summers Road, Imlay City, MI 48444

Abstract The first of the new AAVSO "sections" is the Long Period Variable (LPV) section. This section has decided to "own" Semiregular (SR), irregular (L), and RV Tauri (RV) stars, as well as Miras. There is an LPV Section Wiki, and there has been much discussion on the AAVSO discussion e-mail list regarding the type and number of stars that should be included in the AAVSO LPV Programs. One of our first major tasks is to produce a list of stars to recommend to observers, stars for which the observers can feel that their work will be of value in the present and future age of automated surveys. The core of the list is the AAVSO "legacy stars." The legacy stars will include those stars that have a long and rich history with the AAVSO (more than 15,000

AAVSO observations in fifty-plus years) and those that have been the subject of many scientific publications. The remaining LPV program stars will include those with at least 5,000 observations in the AAVSO International Database, those too bright for most surveys, those that are in fields too crowded for the surveys, plus any that are specifically requested by researchers. The AAVSO Binocular Program will include stars with minima brighter than about 10th magnitude, visible in binoculars for the majority of their cycles.

BL Eri: A Contact Binary System

Lee Snyder
Kings Canyon Observatory, 257 Covertry Drive, Carson City, NV 89703

Abstract BL Eri is a W-type W UMa system with a mass ratio of 0.546 and a contact parameter $f = 0.2$ for the primary star, indicating over-contact, and $f = -0.0008$ for the secondary, indicating near-contact. The system stars have low surface temperature and a short period of 0.42 day. New CCD photometric light curves in *V* and *R* bands and computed parameters solutions using a light curve synthesis program are presented. Prior visual, photographic, and photoelectric observations from February 1978 through October 2004 are analyzed along with this paper data obtained in October 2008. O–C data have been analyzed using a linear ephemeris but were better described by a quadratic ephemeris. The first time radial velocity curves of BL Eri were obtained in 1988 and used to compute the mass ratio of the system along with prior observational data used to compute the physical quantities of the system. The spectral type, orbital period, and angular momentum changes are discussed.

The Addictive Properties of Occultations

John Menke
22500 Old Hundred Road, Barnesville, MD 20838

Abstract Observing asteroid occultations is challenging and rewarding—and is addictive! Techniques are evolving rapidly, with almost monthly contributions to the field. While the predictions of occultations are frequently accurate to a few seconds and a few tens of miles, there are still many challenges of location, weather, equipment, and data analysis that make every observation effort unique. In this paper, we discuss why occultations are useful to observe and how one finds out when/where occultations will occur. We consider the theory of the observation and the pros and cons of the different methods of observing. We also consider other applications of the observing methods used in occultation work.

High Resolution Asteroid Profile by Multi-Chord Occultation Observations

Scott Degenhardt
International Occultation Timing Association (IOTA), 2112 Maple Leaf Trail, Columbia, TN 38401

Abstract For millennia, man has observed celestial objects occulting other bodies and distant stars. We have used these celestial synchronicities to measure the properties of objects. On January 1, 1801, Italian astronomer Giusappe Piazzi discovered the first asteroid that would soon be named Ceres. To date 190,000 of these objects have been catalogued, but only a fraction of these have accurate measurements of their true size and shape. The International Occultation Timing Association (IOTA) currently facilitates the prediction and reduction of asteroidal occultations. By measuring the shadow cast on the earth by an asteroid during a stellar occultation one can directly measure the physical size, shape, and position in space of this body to accuracies orders of magnitudes better than the best ground-based adaptive optics telescope, and can provide verification to 3D inverted reflective light curve prediction models. Recent novel methods developed by IOTA, involving an individual making multiple observations through unattended remote observing stations, have made way for numerous chords of occultation measurement through a single body, yielding high resolution profiles of asteroid bodies. Methodology of how observing stations are deployed will be demonstrated, and results of some of these observations are presented as comparisons to their inverted light curve are shown.

Lightweight Mirror Developments

Russell M. Genet
California Polytechnic State University, Department of Physics, San Luis Obispo, CA 93407

Abstract One goal of the Alt-Az Initiative is the development of transportable 1.5-meter class research telescopes. To this end, several Initiative members are developing lightweight, low cost, primary mirrors. Both multiple and single mirror telescope configurations are being considered. Thin meniscus mirrors are being slumped, and approaches for actively correcting these thin mirrors are being investigated. Sandwich mirrors with glass spacers and others with Foamglas cores are under development. Nanocomposite, polyurethane, and glass replica mirrors, which do not require optical grinding or figuring during production, are being evaluated. Finally, spin-cast polymer mirrors are being explored. Although several of these mirror developments are still

very experimental, and some may only be useful in optically undemanding applications such as on-axis aperture near IR photometry or low resolution spectroscopy, it is our hope that these efforts will enable the development of transportable, low cost, lightweight, 1.5-meter class telescopes.

Optimizing Opto-mechanical Performance Using Simple Tools and Techniques

Tom Krajci
Astrokolkhoz Observatory, P.O. Box 1351, Cloudcroft, NM 88317

Abstract You just purchased a modest setup for your observatory—perhaps a mass produced Schmidt-Cassegrain on a German equatorial mount. However, optically and mechanically it's not performing as well as you would like. What can you do? Some simple assessments and repairs may make all the difference. Assessments can be as easy as visual inspection of various mount components, such as the tripod, where gaps between components reduce stiffness or allow unexpected shifts when loads change. Some assessments are only slightly more involved. Main mirror flop can be evaluated by aligning the main telescope and finder on a bright star and then slewing to various parts of the sky. Pointing differences between the two will be readily apparent if this problem exists. Most mid-level mounts use worm drives, but often excessive spacing between worm and worm gear produces large, and unnecessary, amounts of backlash. Visual inspection of your dovetail mounting system may leave doubts in your mind as to adequate stiffness. Imaging through the entire night may show you that your aluminum tube telescope causes excessive focus shift as temperature drops. Over time, your Schmidt-Cassegrain corrector plate may no longer be securely held by its retaining ring, and the same may apply to the secondary mirror cell. Repairs for these problems are often not difficult if you're mechanically inclined. Gaps in mount components can be eliminated with shims. Combating mirror flop may be the most difficult task. This can involve re-gluing the main mirror and bolting the main mirror cell in a fixed position. Corrector plate and secondary mirror cells can be improved with set screws and shims—implementing sound kinematic principles. Worm gear spacing can often be adjusted with simple tools. This brief paper can't possibly cover all problems and solutions, but it can give you the proper mindset to looking at your system with a critical eye and implementing simple, inexpensive fixes. You may be pleasantly surprised by the improvements.

Enhancements to the Sentinel Fireball Network Video Software

Wayne Watson
James Clerk Maxwell Observatory, 11467 Lothlorien Lane, Nevaca City, CA 95959

Abstract The Sentinel Fireball Network that supports meteor imaging of bright meteors (fireballs) has been in existence for over ten years. Nearly five years ago it moved from gathering meteor data with a camera and VCR video tape to a fisheye lens attached to a hardware device, the Sentinel box, which allowed meteor data to be recorded on a PC operating under real-time Linux. In 2006, that software, SENTUSER, was made available on APPLE, LINUX, and WINDOW operating systems using the PYTHON computer language. It provides basic video and management functionality and a small amount of analytic software capability. This paper describes the new and attractive future features of the software, and, additionally, it reviews some of the research and networks from the past and present using video equipment to collect and analyze fireball data that have applicability to SENTUSER.

Photometry and Light Curves in the Solar System

Jay M. Pasachoff
Williams College, Hopkins Observatory, 33 Lab. Campus Drive, Williamstown, MA 01267

Abstract In a coordination between Williams College and MIT, we have been observing Pluto and Charon as they occult stars, the resulting light curves revealing changes in Pluto's atmosphere and the sizes, shapes, densities, and other aspects of these bodies in the outer solar system. We have seven of our POETS (Portable Occultation, Eclipse, and Transit System) sets of apparatus, mostly for travel to large telescopes in the path of the occultations but two on long-term status in New Mexico at a 2.5-m telescope and in Hawaii on a 3-m telescope, respectively. Each system includes an Andor Technology DV-887 frame-transfer CCD (often used at 10 Hz readout), a GPS for accurate time, and associated computer. During my sabbatical at Caltech, I am associated with Mike Brown's group, and we are observing mutual occultations of Haumea (the second dwarf planet past Eris, which he also discovered) and its moon Namaka, which should establish the size, gravitational fields, and many other aspects of each. We even have an excellent, absolutely calibrated, set of light curves from the ACRIMsat of the light curves showing the total solar irradiance of the sun during transits of Venus and Mercury. Reference: Souza, Steven P., *et al.* 2006, *Publ. Astron. Soc. Pacific*, **118**, 1550.

Sloan-r' Photometry of Comet 17P/Holmes Beyond 3.8 AU: An Observing Methodology for Short-period Comets Far From Perihelion

Richard Miles
Golden Hill Observatory, Stourton Caundle, Dorset DT10 2JP, England

Abstract A photometric method is described for accurately quantifying the brightness of short-period comets far from perihelion. The method utilizes the *Sloan Digital Sky Survey Catalog* (Data Release 7) as a homogeneous source of reference star magnitudes. Results are based on SDSS-r' filtered images taken using 2.0-m aperture telescopes for which the exposure time was adjusted to achieve a constant motion-blur of 2.0 pixels (0.56 arcsec) on the CCD chip. Aperture photometry using circular and tilted elliptical apertures was performed on images, which were stacked to increase signal to noise. Magnitude dependence on "seeing" was determined, and this calibration was used to normalize photometry to constant seeing thereby maximizing photometric accuracy. From observations of Comet 17P/Holmes between 2008 October and 2009 March, a very significant outburst of 17P was found to have occurred on 2009 Jan 4.7 (± 0.5 day). Night-to-night measurements of the brightness of the inner coma (3,000-km radius) exhibited a scatter of only 0.015–0.019 magnitude. No short time-scale (<36 hr) periodicity was found in the fading light curve. From literature data, it was estimated that reflected light from the nucleus contributed 7–11% of the signal within the inner coma, and it is concluded that either the nucleus of 17P must be relatively spherical (projected axial ratio of <1.25), or, if its shape is more typical of other comet nuclei, it has a rotational period in excess of 10 days (assuming the observations were not made with the nucleus "pole-on" to the Earth). Evidence from intermittent activity displayed by the nucleus is indicative of a possible 44-day rotation period.

Spectrashift Exoplanet Transit Search Project: 40,000 Light Curves and Counting

Thomas G. Kaye
Raemor Vista Observatory and Foundation for Scientific Advancement, 7023 Alhambra Drive, Sierra Vista, AZ 85650

David Healy
Junk Bond Observatory, 6929 E. Madera Drive, Sierra Vista, AZ 85650

Abstract Spectrashift has recently branched out from its radial velocity work detecting exoplanets, and has now fully implemented an exoplanet transit search program. Junk Bond Observatory's 0.8-meter fully automated RC telescope has been engaged in this effort full-time since October of 2008. To date the search has examined more than 40,000 light curves. The Spectrashift strategy is to look at fewer but fainter stars, putting this search into the magnitude range the majority of professional searches cannot penetrate. Custom software was developed for the reduction pipeline to handle the volume of data. The software implements artificial intelligence algorithms to sort out the most likely candidates for human inspection at the end of the pipeline. To date the project has come up with several "triple hits" where a transit-like event has happened on three occasions. The Spectrashift team's ultimate goal is to include a network of non-professional telescopes around the world for 24-hour coverage of star fields. It is believed this is the first serious non-professional transit search effort.

ILOX—A Small Visible Imager on the Lunar Surface

Daniel O'Connor
International Lunar Observatory Association, 65-1230 Mamalahoa Highway D 20, Kamuela, HI 96743

Abstract The International Lunar Observatory Association has been invited to provide a piggyback science instrument to fly onboard Odyssey Moon's attempt at the Google Lunar X-Prize. It is likely that the science instrument (ILOX) will be a 10-cm aperture visible imager (300 nm to 700 nm), 1,024 square pixels, with a 2.5 degree field of view. ILOX will have eight filter positions (two polarizers, six color filters) which will allow a variety of measurements to be performed. Total exposure time for ILOX will be < 1 Lunar Day (14 Earth days) from the lunar equator. Limiting magnitude is expected to be 12. We hope to measure the Earth's short wave albedo, characterize the Earth's polarization signature relative to solar phase angle, and possibly map ocean chlorophyll-a with 14 km resolution. We expect to investigate the lunar dust-lofting event associated with the lunar terminator as the terminator approaches ILOX. We will attempt to image a blazar jet in the visible and derive a power spectrum.

Thinking Out Loud: An Optical SETI Campaign Suitable for Amateur Astronomers?

James Edwards
331 Avenue F, Redondo Beach, CA 90277

Abstract To date, there has yet been no confirmed detection of signals transmitted by an extraterrestrial (ET) entity/civilization. Reconsideration

of this problem from the vantage point of amateur astronomy has suggested a logical and reasonable alternative to current professional radio and optical searches. The experiment is suited to the capabilities and strengths unique to the serious amateur having his own well equipped observatory.

The Early History of Photometric Observations of Asteroids Made At Table Mountain Observatory

James W. Young
Jet Propulsion Laboratory, Table Mountain Observatory, P.O. Box 367, Wrightwood, CA 92397

Alan W. Harris
Space Science Institute, 4603 Orange Knoll Avenue, La Canada, CA 91011

Abstract An Ascop S-20 photomultiplier tube mounted in a Mt. Wilson-designed dry-ice cold-box assembly was used with a pulse-counting system to measure the colors, magnitudes, rotational rates, and phase coefficients of over 300 different asteroids between 1978 and 1993. During this time period, nearly one third of all known asteroid rotational rates (~150) were obtained from this effective system. All observations were made with manual telescopic pointing, with data written out long-hand utilizing the 0.6-meter telescope at JPL's Table Mountain Facility. Nearly forty refereed journal (mostly *Icarus*) papers were published containing these results, with yet a few more to come.

What's Next in Asteroid Photometry?

Gary A. Vander Haagen
Stonegate Observatory, 825 Stonegate Road, Ann Arbor, MI 48103

Abstract Our knowledge of an asteroid starts with determination of its position over time using astrometry, calculation of orbital parameters, and collection of time-series photometry data to reveal its light curve, rotational period, and amplitude. Selectively, radar studies are performed by Arecibo and Goldstone to obtain orbital, size, shape, and surface data. Further insight into asteroid populations, general taxonomic class, albedos, estimated diameters, and shape require knowledge of their absolute magnitude (H) and phase slope parameter (G) values. The H-G values are determined through reduced photometric data as the asteroid passes through its opposition or 00 phase angle. Collection of these data is ideally suited to smaller observatories since the time required is considerable and therefore costly for larger facilities. The H-G parameters were determined for 901 Brunsia and 946 Poesia, thereby yielding new insight into their absolute magnitudes, albedos, diameter, and general taxonomic classification.

Slow Rotating Asteroids: A Long Day's Journey Into Night

Brian D. Warner
Palmer Divide Observatory/Space Science Institute, 17995 Bakers Farm Road, Colorado Springs, CO 80908

Abstract While there is no formal definition of a "slow rotator" among asteroids, anything with a period of at least 24 hours can be considered to be at least at the fast end of the group. These objects are of particular interest to those studying the evolution and dynamics of the asteroids within the solar system for several reasons. Most important among them is to generalize theories regarding the Yarkovsky-O'Keefe-Radzievskii-Paddack (YORP) effect, which is the thermal re-radiation of sunlight that can not only affect the orientation of an asteroid's spin axis but its rate of rotation as well. In those cases where the spin rate is decreased, an asteroid can eventually be sent into a state of "tumbling" (NPAR—non-principal axis rotation) that can last for millions of years. However, not all slow rotating asteroids appear to be tumbling. This is not expected and so careful studies of these objects are needed to determine if this is really the case or if the tumbling has reached a condition where the secondary frequency—the precession of the spin axis—has been reduced to near zero. Furthermore, there appears to be an excess of slow rotators among the Near-Earth asteroids (NEA) and inner main-belt populations. Determining whether or not this is true among the broader population of asteroids is also vital to understanding the forces at work among the asteroids.

Extending a Spectroscopic Survey of Main Belt Asteroids With Micro Telescopes: A Proof of Concept Project

Robert Stephens
Goat Mountain Astronomical Research Station, 8300 Utica Avenue, Suite 105, Rancho Cucamonga, CA 91730

Ralph Megna
Goat Mountain Astronomical Research Station, 1201 University Avenue, Suite 206A, Riverside, CA 92507

Abstract In 2002, Schelte J. Bus and Richard P. Binzel proposed a new taxonomy for main belt asteroids based on slope values over segments of the spectral curve; this new classification system has started to gain general acceptance. Their analysis was based on spectrographic data gathered in the late 1980s and early 1990s at Kitt Peak Observatory on research instruments of 2.4 and 1.3 meters in aperture. Most of the original 1,447 asteroids were each observed on a single night. A few, which were observed on multiple nights, exhibited unexplained variations. Spectra and photometric color studies have been done of some asteroids since then, mostly as studies of dynamical families. The authors have undertaken a "proof of concept" project to explore and resolve the technical challenges associated with re-observing some of these asteroids and extending the survey beyond the original targets using small telescopes. Employing a commercially-made 0.36-meter catadioptric telescope and camera/ spectroscope combination, the authors have attempted to reproduce some of the curves from asteroids included in the Bus and Binzel papers. Their work has focused on demonstrating the fidelity and repeatability of a data capture and analysis process on targets of at least 13th magnitude. The authors profile the hardware and software used to conduct the proof of concept project, techniques for data collection and analysis, and review the results of their work to date.

Filling Your Astronomy Program

Pamela Gay
739 St. Louis Street, Edwardsville, IL 62025

Michael Simonsen
C. E. Scovil Observatory, 2615 S. Summers Road, Imlay City, MI 48444

Abstract Every astronomy club has the random month without a speaker and the random blank space in their newsletter that needs just a couple of inches of content. In this talk we present ways to fill your program with content freely provided by the AAVSO via their speakers bureau and writers bureau. These two programs provide libraries of content that can be used to provide presentations or to fill any astronomy not-for-profit publication, respectively. Also, learn how you can help enhance these repositories with your own content.

Spectroscopic Binaries Studies

Olivier Thizy
Shelyak Instruments, Les Roussetts, 38420 Revel, France

Abstract We will introduce some historical background on spectroscopic binaries, amateur high resolution spectroscopy observation, procedure, and processing steps. We will show actual results on three binaries (Mizar, beta Aurigae, and AW UMa) taken with Lhires III Littrow spectrographs and an eShel echelle spectrograph. We will discuss further developments in this field.

Revisiting the O'Connell Effect in Eclipsing Binary Systems

Nicholas J. Wilsey
Matthew M. Beaky
Truman State University, 100 E. Normal, Kirksville, MO 63501

Abstract Many eclipsing binary light curves exhibit a feature known as the O'Connell effect, where the two out-of-eclipse maxima are unequally high. The effect is entirely unexpected, because the two side-by-side configurations of the components should appear equally bright from our line of sight. Several theories have been proposed to explain the effect, including asymmetrically distributed starspots, clouds of circumstellar dust and gas, or a hot spot caused by the impact of a mass-transferring gas stream. Currently, most published models of systems with asymmetric maxima incorporate starspots to rectify their models to fit the observational data. However, the limitations of starspot solutions, as well as other possible explanations for the asymmetry, are rarely discussed. In order to revitalize the study of the O'Connell effect, the astronomy program at Truman State University in Kirksville, Missouri, has initiated a project to construct complete *BVRI* light curves of poorly studied eclipsing binary systems exhibiting the O'Connell effect, including V573 Lyr and UV Mon. We are also exploring methods of applying Fourier analysis to large, all-sky databases to extract correlations that may help to evaluate competing theories for explaining the effect.

Using a Web Cam CCD to Do *V*-Band Photometry

Rev. Paul Temple
508 S. Slate Street, Deming, NM 88030

Abstract With the plethora of cheap web cam-based CCD cameras in the market today, it seemed expedient to find out if they can be used to do photometry. An experiment was planned to determine if it was possible to perform this kind of exacting measurement. Arne Henden (AAVSO) believed it would be possible to do *V*-band photometry to 0.05 magnitude accuracy with a web cam CCD. Using a 6-inch refractor, the heart of M42 was repeatedly imaged. θ^2 Ori and SAO 132322 were the comparison stars and V361 Ori was the target variable. Since the 1/4 HAD CCD chip only allows for a field of 10 × 7 arc minutes using the 6-inch refractor, the number of targets was limited. The RGB on the chip itself provides the filters needed for photometry. The *G* bandpass on the chip ranges from 425 to 650 nm with a peak band pass at 540, *and V* bandpass is 475–645 with a peak at 525. The results indicate that a web cam CCD can be used for *V*-band photometry. With a 10-second calibrated exposure without the Peltier cooling being engaged, the results for the two target stars were ± 0.18

magnitude. θ^2 Ori was 0.18 brighter in *V* than the actual measurement from the Tycho catalog. SAO 132322 was 0.012 magnitude dimmer than the listed Tycho measurement. Then, using SAO 132322 and θ^2 Ori as comparison stars, V361 Ori was estimated at magnitude 7.786. This is in line with visual estimates received before and after this date. With more estimates of known magnitude comparison stars, a correction factor should be estimated and applied to the variable work that will make it more accurate. This correction factor should bring it close to Arne Henden's estimate of 0.05 mag accuracy.

Intrinsic Variability of β Lyrae Observed With a Digital SLR Camera

Donald F. Collins
Anesh Prasai
Warren Wilson College, P.O. Box 9000, Asheville, NC 28815

Abstract We show that a digital SLR (DSLR) camera (Canon XTi) follows a linear response to light exposure when images are saved in raw format. We also demonstrate its usefulness for photometry of bright variable stars such as beta Lyrae (4.2m–3.2m) and other bright variable stars. Mounted on a stationary tripod and fitted with a standard zoom lens set at 55 mm FL at *f*/5.6, this camera obtains reasonably precise photometry (± 0.02m) for bright stars. Imaging bright stars with a telescope and CCD imaging detector is hampered by rapid saturation and the lack of suitable bright comparison stars in the field of view. Subtracting the average brightness for beta Lyrae, we can easily detect the intrinsic variability of beta Lyrae (15%) with a period about 280 days. More such observations are requested to learn more about the period and phase of the intrinsic variability of beta Lyrae.

An Intensive CCD Photometry Campaign to Observe DW Ursae Majoris

David Boyd
British Astronomical Association, Variable Star Section, 5 Silver Lane, West Challow, Wantage, Oxon OX12 9TX, England

Boris Gaensicke
Department of Physics, Warwick University, Coventry, CV4 7AL, England

Abstract We report on a coordinated observing campaign in April and May 2008 to study the eclipsing dwarf nova DW Ursae Majoris. This belongs to the group of SW Sex stars, nova-like variables containing accretion disks which exhibit superhumps in their light curves suggesting that their accretion

disks are elliptical and precessing on time scales of a few days due to tidal interactions with the companion star. It has been suggested that the changing geometry will cause the depth of eclipses to be modulated on the accretion disk precession period. The aim of this campaign was to provide for the first time sufficient continuous photometric coverage of an eclipsing superhumper to test this hypothesis. Twenty-six experienced amateur CCD photometrists in seven countries participated in the project and altogether made almost 55,000 magnitude measurements over a four-week period, keeping DW UMa under observation for more than 50% of the time. The results provide direct measurements of the orbital, superhump, and disk precession periods, confirming unambiguously that the superhump signal is a beat between the orbital and precession periods. They also reveal modulation not only of the eclipse depth but also of the eclipse time of minimum and width on the accretion disk precession period. The project is a good example of cooperation between the amateur and professional communities to address an open research issue.

New Observations of Three Lyra Variables

Jerry D. Horne
3055 Lynview Drive, San Jose, CA 95148

Abstract New *V*-, *B*-, I_c-, and *R*-band photometry is obtained for V480 Lyr, V575 Lyr, and GSC 2118-0402. These new observations, when combined with other published observational data, allowed the determination of multiple period values for each star. From its multi-period behavior and from an examination of other intrinsic parameters, V480 Lyr was determined to be that of an RV Tauri type star, which differs from earlier classifications of the star. The new observational data on the δ Sct variable V575 Lyr confirmed two earlier observed periods of this variable star and identified an additional third period of pulsation. Additionally the precession of the primary period was identified, and new *B–V*, *V–I*, and *V–R* color indices were obtained. New observations of the V575 Lyr field star, GSC 2118-0402, are also examined and analyzed. These observations identified the range of magnitude variation and pulsation periods, which allowed the star to be tentatively classified as a δ Scuti variable.

ε Aurigae, 2009: The Eclipse Begins—Observing Campaign Status

Robert E. Stencel
University of Denver Observatories, Dept. Astronomy and Physics, University of Denver, Denver CO 80208

Jeffrey L. Hopkins
Hopkins Phoenix Observatory, 7812 W. Clayton Drive, Phoenix AZ 85033

Abstract The eclipse of 3rd-magnitude epsilon Aurigae is forecast to begin during August 2009, reaching totality by year's end, based on all six prior eclipse events studied—1982, 1955, 1930, 1902, 1874, and 1847. We have organized a campaign during the past several years in order to raise awareness about this rare opportunity, and to promote reporting of observations of all kinds. We have forty registered participants, seventy-six people signed up for alert notices, plus numerous informal expressions of interest. Categories of observations being reported in *Campaign Newsletters* (eleven since 2006) which include Photometry, Spectroscopy, Polarimetry, Interferometry, and Citizen Science (website: www.hposoft.com/Campaign09.html). In this presentation, we provide a brief update on the optical and near-IR photometry obtained to date. The nature of the short term light variations will be discussed in the context of mapping the eclipse behavior. Spectroscopy benefits from small telescope capabilities now widely available, along with traditional large telescope, higher dispersion work. Examples of each will be presented, along with the research objectives. Polarimetry provided key insights during the last eclipse, and we continue to promote the need for new data using this method. Finally, interferometry has come of age since the last eclipse, and a status report on this powerful method to directly detect the passing dark disk will be provided. Along with these traditional measurements, we will briefly discuss efforts to promote Citizen Science opportunities among the public, in coordination with AAVSO and as part of the International Year of Astronomy, IYA 2009.

ε Aurigae Hydrogen-α Emission Line Variation: The Horn Dance

Jeffrey L. Hopkins
Hopkins Phoenix Observatory, 7812 West Clayton Drive, Phoenix, Arizona 85033

Robert E. Stencel
Astronomy Program, University of Denver, Denver, Colorado 80208

Abstract The Hopkins Phoenix Observatory has been doing high resolution spectroscopy on the 3rd magnitude long period (27.1 year) eclipsing binary star system epsilon Aurigae since August 2008 using a Lhires III spectrograph with a 2,400 line/mm grating mounted on a 12-inch Meade LX200 GPS telescope. Observations have been in both the sodium D-line region of the spectrum and with near continuous observations of the hydrogen alpha region. The out-of-eclipse hydrogen alpha spectrum shows significant night-to-night variation.

While many star systems exhibit a strong hydrogen alpha absorption line, like Be stars, epsilon Aurigae also shows strong blue and red shifted emission components sometimes called wings or horns bracketing the absorption line. Unlike the Be stars, in which the blue and red horns remain relatively constant, the hydrogen alpha horns of epsilon Aurigae seem to be in a wild dance with continuous motion up and down. This paper will discuss techniques and results of recent out-of-eclipse high-resolution spectroscopy of epsilon Aurigae.

The 2009 Eclipse of EE Cephei: An Educational and Collaborative Journey

John Pye
Science, Technology, Engineering, and Mathematics Unit, Maui Community College, 310 Kaahumanu Avenue, Kahului, HI 96732

Lauren Elder
Maui Community College, 310 Kaahumanu Avenue, Kahului, HI 96732

Jeffrey Hopkins
Hopkins Phoenix Observatory, 7812 West Clayton Drive, Phoenix, AZ 85033

Abstract In December 2008, Jeff Hopkins of the Hopkins Phoenix Observatory (HPO) put out a request for assistance in extracting data from images taken by the AAVSO SRO (Sonoita Research Observatory) of EE Cephei, an 11th magnitude (V) long period (5.6 years) eclipsing binary star system that was due to eclipse in January of 2009. The Hopkins Phoenix Observatory originally planned to do *BVRI* CCD photometry of EE Cep for the 2009 eclipse, but equipment and logistical changes at HPO meant the EE Cep project would not be possible. However, in the fall of 2008 Arne Henden of the AAVSO announced the availability of a remote robotic 16-inch telescope (the Sonoita Research Observatory) in southern Arizona for use by members of the AAVSO. Jeff Hopkins contacted Arne Henden and arrangements were made to have the EE Cep star system imaged with *BVRI* filters beginning in November 2008 and running through February 2009. Image files were archived on the AAVSO web site. Soon after his initial request went out, Jeff Hopkins was contacted by John Pye from Maui Community College, who agreed to help with the project by having one of his students, Lauren Elder, examine the image files and extract EE Cep and three comparison stars flux (ADU) counts for each band. The resulting data were then sent to the Hopkins Phoenix Observatory for data reduction and analysis. The project was a successful joint collaboration with forty nights of observations for over 300 *BVRI* data points from 20 November 2008 to 17 February 2009. Light curves for each band as

well as color indices were plotted and eclipse contact points were determined. The data were also contributed to the EE Cep Campaign organized by Cezary Galan at the Centre for Astronomy at Nicolaus Copernicus University in Torun (Poland). Our results are plotted along with those of several dozen other observers from around the world.

The Light Curve of UZ Sagittae

Robert K. Buchheim
Altimira Observatory, 18 Altimira, Coto de Caza, CA 92679

Abstract A complete light curve of the eclipsing binary UZ Sge has been determined in *V* and *R* bands. Four new times of minimum are reported (two for primary eclipse and two for secondary eclipse), which verify other recent O–C observations. The color index changes significantly during both primary eclipse and secondary eclipse, providing some constraints on the stars' temperatures. BINARYMAKER3 software has been used to compare the observed *V* and *R* light curves with two models of this system (with quite different mass ratios of q = 0.14 and q = 0.68, respectively) that have been suggested in the literature.

An Estimate of the Integrated Magnitude of the LCROSS Impact Ejecta Dust Curtain for Exposure Calibration Practice

Kurt A. Fisher
Salt Lake Astronomical Society, Box 26114, Salt Lake City, UT 84126

Abstract The LCROSS-EDUS (Lunar CRater Observation ans Sensing Satellite-Earth departure upper stage) lunar impact will generate a dust ejecta curtain about 10 km × 5 km high according to the NASA-LCROSS Team current best estimate impact model (CBEIM). The dust ejecta curtain could reach 20 km × 20 km. The LCROSS Team has not issued a curtain magnitude estimate for use by amateur imagers. For the limited purpose of pre-event exposure calibration practice, a rough first-order estimate of the LCROSS impact dust ejecta curtain is between 0.3 to 3.5 integrated magnitudes or 5.5 to 6.4 mpsas. This apparent brightness provides a favorable contract index against typical Earthshine (dark limb) irradiance between 12 to 17 mpsas for the dark limb (mean value 15.44 mpsas) but not against Moonshine (bright limb) at 4 to 6 mpsas.

Data Mining Techniques Applied to the GNAT Library Archive (poster)

Erin M. Craine
School of Information Resources and Library Sciences, University of Arizona, 1515 East First Street, Tucson, AZ 85719

Abstract The Global Network of Astronomical Telescopes (GNAT) is in the process of developing a large library of data for its newly discovered variable stars. This revised archive has been recently opened to the public, is largely unexamined, and provides a valuable resource for data mining. The GNAT archive is constantly growing as survey imaging continues; in 2009 the survey imagery is estimated to contain in excess of 150,000 new variable star entries selected from more than about nine million observed stars. The algorithm used for identifying variable stars in these images yields examples of nearly all known classes of such stars. One of the key goals of developing data mining techniques is to be able to narrow down this large volume of data to specific stars of interest. We discuss the nature and content of the GNAT variable star archive, including a discussion of limitations and boundary conditions that affect the data. We present some basic ideas of data mining, examine specific approaches to the GNAT archive, and provide examples of how to extract information related to these variable stars.

Phase Dependent Spectroscopic Monitoring of Cepheid Variable Stars (poster)

Bandon Decker
Matthew M. Beaky
Truman State University, Department of Physics, 100 East Normal Avenue, Kirksville, MO 63501

Abstract Cepheid variables are pulsating yellow giant stars, with a surface temperature somewhat greater than that of the Sun. While Cepheids have been studied photometrically in great detail for many decades, the data on how the spectra of Cepheid variables change over time is relatively scarce. Of special interest is the O I triplet at 7774 Angstroms, because its variation over one cycle is related to the motion of unionized oxygen in the atmosphere of the star as it pulsates. Three classical Cepheid variables, FF Aquilae, T Vulpeculae, and SU Cygni were observed spectroscopically on fifteen nights at the Truman State University Observatory using a SBIG Self-Guiding Spectrograph and a 35-cm Meade LX200GPS telescope. Low resolution (5 Angstroms/pixel) were obtained from 3800 to 9500 Angstroms, as well as higher resolution spectra (1 Angstrom/pixel) from 7400 to 8150 Angstroms. For all three stars,

the spectra clearly revealed the change in surface temperature as a function of phase. Further analysis of the spectroscopic data enabled us to create plots of the equivalent width of the O I triplet as a function of phase for FF Aql.

Searching for Chaos in the Mira Variable Star U Cygni (poster)

Amanda Tougas
Matthew M. Beaky
Truman State University, Department of Physics, 100 East Normal Avenue, Kirksville, MO 63501

Abstract Mira variable stars are pulsating red giant stars whose light curves often exhibit seemingly random variations in amplitude and period from cycle to cycle. One possibility is that the long-term variations in Mira variable light curves are due to a simple linear combination of two or more pulsation modes. For some pulsating red giant stars, however, a multi-periodic solution has been shown to be insufficient, and a nonlinear analysis is required for complete description of the light curve behavior. The application of chaos theory to the light curves of pulsating variable stars remains relatively unexplored, however. In this project we investigated U Cygni, a pulsating Mira-type variable star with a period of approximately 463 days. Over 100 years of U Cyg visual photometric data were obtained from the American Association of Variable Star Observers. A Fourier analysis was conducted on the data and an O–C diagram was created to explore the limitations of standard linear time series analysis. Next, a nonlinear analysis using the TISEAN software package was conducted to search for chaotic behavior in the light curve of U Cyg. From the nonlinear analysis, we obtained phase space projections, determined the maximum Lyapunov exponent, and created a synthetic light curve to represent the U Cyg data. The results provide evidence for the presence of chaotic behavior in the light curve of U Cyg.

Time Delay Integration: A Wide-Field Survey Technique (poster)

Robert La Pointe
Mill Creek Observatory, P.O. Box 155, Forest Falls, CA 92339

E. Hill
L. Leimer
K. McMillian
A. Miller
A. Prindle

Orange Lutheran High School, AP Physics C—Research Project, 2222 North Santiago Boulevard, Orange, CA 92867

Abstract The Advanced Placement Physics class of Orange Lutheran High School has conducted a survey-imaging project using a Time Delay Integration (TDI) technique. TDI enables very wide-field images to be collected in the form of long strips of the sky. A series of five consecutive nights were captured, calibrated, and compared to reveal possible transient phenomena such as supernovae, asteroids, and other events that have a noticeable change over 24-hour intervals.

Quantifying "Irregularity" in Pulsating Red Giants (poster)

John R. Percy
Samantha Esteves
Alfred Lin
Christopher Menezes
Sophia Wu
University of Toronto, Department of Astronomy, 50 St. George Street, Toronto, ON M5S 3H4, Canada

Abstract Hundreds of red giant variables are classified as type L, which the *General Catalogue of Variable Stars* defines as "slow irregular variables of late spectral type...which show no evidence of periodicity, or any periodicity present is very poorly defined." Self-correlation is a simple form of time-series analysis which determines the cycle-to-cycle behavior of the star, averaged over all the data; even for stars with no periodicity, it provides a "profile" of the variability, including the average "characteristic time scale" (Percy and Mohammed 2004, *J. Amer. Assoc. Var. Star Obs.*, **32**, 9, and references therein). We have applied this method to AAVSO visual observations of several dozen L-type variables, and found a range of behavior: despite their irregularity, most have at least one pulsation period; some also have "long secondary periods" whose cause is unknown. For all of them, we have determined a period, or an equivalent "characteristic time scale." There seems to be a continuous spectrum of behavior in pulsating red giants, from periodic to irregular. Co-authors SE, AL, CM, and SW were participants in the University of Toronto Mentorship Program which enables outstanding senior high school students to work on research projects at the university. This program will be described briefly. *[Ed. note: this paper appears in full in this issue of the* Journal*, beginning on page 71.]*

Over-Contact Binary GR Tauri (poster)

Lee Snyder
Kings Canyon Observatory, 257 Covertry Drive, Carson City, NV 89703

Abstract New times of minima and ephemerides are presented on the over-contact system GR Tauri. An observed minus calculated (O–C) time of minimum chart was constructed, and, based on statistical analysis, the orbital period of the system is found to be decreasing with a rate of dP/dE = 3.33^{-4} seconds/year^{-1} since 1931. Both components are filling their respective critical Roche lobes with fillouts f = 0.11 and 0.95. The light curve displays the O'Connell effect, which is discussed on the assumption mass is going from the primary to the secondary creating a hot spot. The thermal relaxation oscillations (TRO, Lucy and Wilson 1979), theory is discussed as an explanation.

Photometry of Variable Stars Using a Lensless Schmidt Camera (poster)

Jeff Horne
11 Cannes, Irvine, CA 92614

Abstract This paper describes the design and use of a lensless Schmidt camera (LSC) as a more cost effective alternative to more expensive telescope types. The lensless Schmidt design uses a short focal length spherical primary mirror and an aperture stop placed at the radius of curvature of that mirror. This results in an optical system without coma or astigmatism and a wide field of view. However, the LSC does have residual spherical aberration which enlarges the size of the stars being imaged by a CCD. The amount of spherical aberration tolerable in measuring stellar magnitudes and the physical length of the camera determine the possible focal ratio and aperture combinations for LSC designs. An LSC was built by the author and used to obtain data on several variable stars. Photometric *V* data plots for V Boo, χ Cyg, and U Cyg are provided as examples of the data than can be captured with this type of instrument.

Index to Volume 37

Author

Subject

PHOTOMETRY, CCD

PHOTOMETRY, PHOTOELECTRIC

PHOTOMETRY, PHOTOGRAPHIC

Recent Minima of 154 Eclipsing Binary Stars

Gerard Samolyk
P.O. Box 20939, Greenfield, WI 53220

Received October 26, 2009; accepted October 26, 2009

In the paper "Recent Minima of 154 Eclipsing Binary Stars" by Gerard Samolyk (*JAAVSO*, 2009, **37**, 44–51), there are three errors to be corrected in Table 1:

page 48: for the second occurrence of "V704 Cyg" read "V1034 Cyg"

page 49: for "UZ Eri" read "UX Eri" (twice).

NOTES